



# Metabolic status is a key factor influencing proteomic changes in ewe granulosa cells induced by chronic BPS exposure

Marie-Emilie Lebachelier de la Riviere, Ophélie Téteau, Coline Mahé, Olivier Lasserre, Alice Desmarchais, Svetlana Uzbekova, Pascal Papillier, Daniel Tomas, Valérie Labas, Virginie Maillard, et al.

## ► To cite this version:

Marie-Emilie Lebachelier de la Riviere, Ophélie Téteau, Coline Mahé, Olivier Lasserre, Alice Desmarchais, et al.. Metabolic status is a key factor influencing proteomic changes in ewe granulosa cells induced by chronic BPS exposure. *BMC Genomics*, 2024, 25 (1), pp.1095. 10.1186/s12864-024-11034-2 . hal-04790961

HAL Id: hal-04790961

<https://hal.inrae.fr/hal-04790961v1>

Submitted on 19 Nov 2024

**HAL** is a multi-disciplinary open access archive for the deposit and dissemination of scientific research documents, whether they are published or not. The documents may come from teaching and research institutions in France or abroad, or from public or private research centers.

L'archive ouverte pluridisciplinaire **HAL**, est destinée au dépôt et à la diffusion de documents scientifiques de niveau recherche, publiés ou non, émanant des établissements d'enseignement et de recherche français ou étrangers, des laboratoires publics ou privés.



Distributed under a Creative Commons Attribution - NonCommercial - NoDerivatives 4.0 International License

RESEARCH

Open Access



# Metabolic status is a key factor influencing proteomic changes in ewe granulosa cells induced by chronic BPS exposure

Marie-Emilie Lebachelier de la Riviere<sup>1†</sup>, Ophélie Téteau<sup>1†</sup>, Coline Mahé<sup>1</sup>, Olivier Lasserre<sup>2</sup>, Alice Desmarchais<sup>1</sup>, Svetlana Uzbeckova<sup>1</sup>, Pascal Papillier<sup>1</sup>, Daniel Tomas<sup>1,3</sup>, Valérie Labas<sup>1,3</sup>, Virginie Maillard<sup>1</sup>, Marie Saint-Dizier<sup>1</sup>, Aurélien Binet<sup>4,5</sup> and Sébastien Elis<sup>1\*</sup>

## Abstract

**Background** Bisphenol S (BPS) is the main substitute for bisphenol A (BPA), a well-known plasticiser and endocrine disruptor. BPS disrupts ovarian function in several species. Moreover, a few studies have reported that the effects of BPS might be modulated by the metabolic status, and none have characterised the granulosa cell (GC) proteome after chronic BPS exposure.

**Objectives** This study aimed to decipher the mechanisms of action of chronic BPS exposure on the proteome of ewe GCs while considering the interaction between a deliberate contrasted metabolism and reproductive function.

**Methods** Forty ewes were split into two groups with contrasted diets: restricted (R,  $n=20$ ) and well-fed (WF,  $n=20$ ). The R and WF ewes were subdivided according to the dose of BPS administered through the diet (0–50 µg/kg/day), forming four groups: R0, R50, WF0 and WF50. After 3-month BPS daily exposure, GCs were recovered during the pre-ovulatory stage and proteins were analysed by nano-liquid chromatography coupled with tandem mass spectrometry.

**Results** Chronic exposure to BPS affected the GC proteome differently according to the ewe metabolic status. Fifty-nine out of 958 quantified proteins were differentially abundant between groups and are mainly involved in carbohydrate and lipid pathways. Unsupervised hierarchical clustering of differentially abundant proteins (DAPs) identified four clusters of 34, 6, 5 and 14 proteins according to the BPS exposure and diet interaction. Pairwise comparisons between groups also revealed a strong effect of BPS exposure and diet interaction. Functional analysis of DAPs highlighted that BPS upregulated β-glucuronidase (GUSB;  $p=0.002$ ), a protein especially able to deconjugate bisphenol glucuronides (BP-g). Moreover, among unexposed ewes, GUSB was detected only in well-fed ewes.

**Discussion** Conjugation of glucuronides inhibits the oestrogenic activity of bisphenols. Upregulation of GUSB in ewes dosed with BPS would prolong the oestrogenic effects of BPS by deconjugating BP-g into free BPS. In addition,

<sup>†</sup>Marie-Emilie Lebachelier de la Riviere and Ophélie Téteau contributed equally to this work.

\*Correspondence:  
Sébastien Elis  
sebastien.elis@inrae.fr

Full list of author information is available at the end of the article



© The Author(s) 2024. **Open Access** This article is licensed under a Creative Commons Attribution-NonCommercial-NoDerivatives 4.0 International License, which permits any non-commercial use, sharing, distribution and reproduction in any medium or format, as long as you give appropriate credit to the original author(s) and the source, provide a link to the Creative Commons licence, and indicate if you modified the licensed material. You do not have permission under this licence to share adapted material derived from this article or parts of it. The images or other third party material in this article are included in the article's Creative Commons licence, unless indicated otherwise in a credit line to the material. If material is not included in the article's Creative Commons licence and your intended use is not permitted by statutory regulation or exceeds the permitted use, you will need to obtain permission directly from the copyright holder. To view a copy of this licence, visit <http://creativecommons.org/licenses/by-nc-nd/4.0/>.

literature has reported an up-regulation of GUSB in people suffering from obesity. Therefore, people suffering from obesity could be subjected to prolonged and aggravated exposure to BPS. These data highlighted the deleterious effects of BPS and its interaction with metabolic status.

**Keywords** Bisphenol S, Diet, Metabolic status, Adiposity, Granulosa cells, Protein, Proteomic, Ewes, Ovary

## Introduction

Bisphenol A (BPA), one of the most widely produced plasticisers throughout the world [1], is recognised as an endocrine disruptor [2]. Several studies have highlighted the harmful effects of BPA on human health, particularly on female reproduction through alterations in steroidogenesis (oestradiol, progesterone, etc.), ovarian diseases (polycystic ovary syndrome), unfavourable pregnancy outcomes and reduced fertility [3–5]. The main route of exposure is oral ingestion, due to the transfer of bisphenol molecules from food packaging to its contents, given that BPA is widely used in the food industry. The most important detoxification reaction for bisphenols is the conjugation reaction with glucuronic acid, which promotes urine excretion of these molecules [6]. Given its status as an endocrine disruptor, BPA has been banned in the food industry in Canada, Belgium and France [2, 7] and replaced by its structural analogues, in particular bisphenol S (BPS) [8]. BPS has been detected in human fluids, such as urine [9], follicular fluid [10–12] and serum [12, 13]. BPS is known as an oestrogen mimetic that can modulate steroidogenesis by binding to oestrogen receptors [14, 15]; moreover, it has been reported to exhibit an androgenic effect, although these results are controversial [16, 17]. Granulosa cells (GCs) are somatic cells surrounding the oocyte in the ovarian follicle; they are involved in follicle growth and steroidogenesis, enabling oocyte maturation. There is also a dialogue between these cells and the oocyte, which is essential for ovulation [18]. Several in vitro studies in different mammalian species have demonstrated BPS-induced disruption of oestradiol and/or progesterone secretion in GCs, although these effects varied according to the dose and duration of BPS exposure [10, 11, 19–22]. The deleterious effects of BPS on health, in particular reproductive function and/or metabolic disorders, are sometimes even worse than those of BPA [23].

In female mammals, reproduction requires adaptations to energy metabolism [24]. Indeed, an insufficient body fat mass leads to a loss of cyclicity and, conversely, overweight or obesity can lead to complications such as an increased risk of miscarriage, impaired cumulus-oocyte complex development and impaired early embryonic development [25]. A higher body mass index (BMI) can also be associated with alterations in the follicular fluid composition, with increased follicular insulin, glucose and lactate concentrations [26], and obesity exerts effects on sex hormone secretion and metabolism, resulting

in changes in the bioavailability of both oestrogens and androgens [27].

BPA has been associated with obesity in humans [28, 29] and promotes adipogenesis [30] and lipid accumulation by impacting lipid and glucose metabolism via the peroxisome proliferator-activated receptor gamma (PPAR $\gamma$ ) receptor signalling pathway [4]. Therefore, bisphenols are able to modulate energy metabolism, which adversely affects female reproduction and cellular functions. For example, bisphenols are able to impair steroidogenesis of cumulus cells, granulosa cells and/or theca cells in several species including bovine [19, 31], rodent [32], ovine [22] and human [11]. BPS also altered ewe oocyte developmental capacity by inducing a decrease in oocyte maturation rate, in embryo cleavage rate and in blastocyst rate in ovine [33]. Finally, the negative effect of BPS may be exacerbated by the metabolic status. Indeed, oestradiol increased in the follicular fluid of only well-fed animals while there was no effect in animals on a restricted diet [34]. Therefore, excess in diet can contribute to impaired reproduction. Similarly, an interaction between chronic exposure to BPS and the metabolic status has been reported to affect the efficiency of in vitro embryo production negatively, whereas BPS or diet alone had no effect in ewes receiving contrasted diets (restricted or well fed) [35].

The aim of this study was to investigate the mechanisms of action of chronic BPS exposure, according to the metabolic status of the animal, on ewe GCs by proteomic analysis to consider the interaction between metabolism and ovarian follicular function. Forty ewes were fed contrasted diets and exposed or unexposed to oral BPS for at least 3 months. The GCs were collected at the pre-ovulatory stage of the cycle; protein was extracted, pooled and analysed by nano-liquid chromatography coupled to tandem mass spectrometry (nanoLC-MS/MS).

## Results

### Validation of the diet model and detection of BPS and its metabolite in the follicular fluid of exposed ewes

Ewe body weight (BW) and body condition score (BCS) differed significantly between the WF and R groups (Table 1) [34]. The mean BW and BCS of restricted ewes were lower than well-fed ewes, with a mean difference of 11 kg in BW ( $52.6 \pm 1.2$  kg vs.  $63.5 \pm 1.2$  kg in restricted and well-fed ewes, respectively,  $p < 0.001$ ) and almost 1 BCS point ( $2.05 \pm 0.07$  vs.  $2.88 \pm 0.05$  in restricted and well-fed ewes, respectively,  $p < 0.001$ ). Despite

**Table 1** Zootechnical parameters of ewes chronically exposed or not to BPS

	Mean ± SEM				p-value		
	R0	R50	WF0	WF50	Diet effect	BPS effect	Diet × BPS effect
Body weight (kg)	53.2 ± 2.1 <sup>a</sup>	51.9 ± 1.4 <sup>a</sup>	64.0 ± 1.7 <sup>b</sup>	62.9 ± 1.7 <sup>b</sup>	<0.001	0.511	1.000
Body condition score	2.02 ± 0.12 <sup>a</sup>	2.08 ± 0.08 <sup>a</sup>	2.78 ± 0.08 <sup>b</sup>	2.98 ± 0.06 <sup>b</sup>	<0.001	0.136	0.387
Plasma glucose (mg/L)	638 ± 29.6	674 ± 35.6	731 ± 57.9	822 ± 81.5	0.039	0.260	0.661
Plasma NEFA ( $\mu\text{mol/L}$ )	173 ± 48.3	164 ± 23.8	326 ± 57.9	276 ± 93.1	0.035	0.611	0.761
Plasma BPS (nM)	0.29 ± 0.29 <sup>a</sup>	2.95 ± 0.8 <sup>b</sup>	0.12 ± 0.12 <sup>a</sup>	2.14 ± 0.36 <sup>b</sup>	0.294	<0.001	0.506
Plasma BPS-g (nM)	0.03 ± 0.02 <sup>a</sup>	201 ± 15.7 <sup>b</sup>	0.38 ± 0.38 <sup>a</sup>	188 ± 11.5 <sup>b</sup>	0.510	<0.001	0.491

A body condition score is graded from 1 to 5, 2 corresponding to a slim ewe and 4 corresponding to a fat ewe. Tukey post-hoc tests are indicated by letters and values with different letters are significantly different ( $p < 0.05$ ). Two-way ANOVA p-values are presented for the effects of diet, dietary exposure to BPS and the interaction of these effects. Bold text indicates significant differences ( $p < 0.05$ )

overfeeding (165% of their maintenance energy requirements), well-fed ewes were not overweighted (BCS=2.88 instead of 4 for typical overweighted animals); however, the plasma glucose and non-esterified fatty acids (NEFA) concentrations were increased compared with the restricted ewes (glucose: 778±50 vs. 657±23 mg/L,  $p=0.039$ ; NEFA: 301±54 vs. 168±26  $\mu\text{mol/L}$ ,  $p=0.035$ ). Ewes in the R50 and WF50 groups were exposed to BPS for an average of 5.4±0.1 months (range: 3.6–7.9 months) before sample collection. BPS and its glucuronon-conjugate BPS glucuronide (BPS-g), a marker of internal BPS exposure, were detected in the plasma of all exposed ewes at the time of slaughter (i.e. 24 h on average after the last exposure; Table 1), with no difference regarding diet effect. BPS-g was detected in 3 among 20 unexposed ewes at a significantly lower level compared to BPS exposed ewes ( $p < 0.001$ ).

#### Proteins identified in ewe granulosa cells (GCs)

A total of 958 proteins were identified by at least two unique peptides in GCs (Supplementary Table S1). Among these proteins, 641 proteins were common to all conditions (Fig. 1). There were 2 specific proteins identified that were common to the R0 and WF0 groups, 20 specific proteins common to the R50 and WF50 groups, 17 specific proteins common to the R0 and R50 groups and 9 specific proteins common to the WF0 and WF50 groups. The most abundant proteins among the 641 common proteins are mainly circulating/blood proteins (serum albumin, fibrinogen alpha chain, fibrinogen beta chain, fibrinogen gamma chain, immunoglobulin and haemoglobin) and structural proteins (histones and heat shock protein family A member 5; Supplementary Table S1). The 958 proteins identified in GCs are involved in metabolism, the processing of genetic or environmental information and the cellular organisation system (see Fig. 2).

Venn diagram showing the overlap between the different conditions (diet × BPS exposure) and histogram showing the number of proteins identified in each condition. R0 – restricted diet, no BPS, R50 – restricted diet and 50  $\mu\text{g/kg/day}$  BPS exposure, WF0 – well fed diet,

no BPS, WF50 – well fed diet and 50  $\mu\text{g/kg/day}$  BPS exposure.

Proteomaps were generated using the KEGG (Kyoto Encyclopedia of Genes and Genomes) Pathway gene classification. Functional categories and proteins are represented by polygons. The polygon areas illustrate the normalised abundance of proteins in each condition. Functions and related proteins are organised into common regions and coded using similar colours. R0 – restricted diet, no BPS, R50 – restricted diet and 50  $\mu\text{g/kg/day}$  BPS exposure, WF0 – well feed diet, no BPS, WF50 – well feed diet and 50  $\mu\text{g/kg/day}$  BPS exposure.

#### Global analysis of DAPs in GCs from restricted or well-fed ewes exposed or not exposed to BPS

To assess more specifically the impact of BPS exposure and of contrasting diets on protein abundance, PCA of the 59 DAPs (ANOVA and chi-square  $p \leq 0.05$ ; Supplementary Table S2) of the 16 GCs samples was performed (Fig. 3). The PCA explained 57% of the variance of the data (Dim1 at 37.9%, light and dark blue and Dim2 at 19.2%, turquoise and green). WF0 did not correlate well in this PCA with the horizontal or vertical axis as it was close to the center of the PCA. On the contrary, R0 (dark blue) was negatively correlated to the horizontal axis while R50 (light blue) is mainly positively correlated to the vertical axis. WF50 was positively correlated to the horizontal axis and negatively correlated to the vertical axis. There was therefore a clear discrimination between these 3 groups (R0, R50 and WF50) as they do not correlate with the same axis. Therefore, the difference between unexposed ewes or ewes exposed to BPS might be greater in the restricted groups. The heatmap representation shows the differences in significant DAPs after ANOVA and chi-square test (Fig. 4). Unsupervised hierarchical clustering identified four DAP clusters (C1–C4): C1 (green) comprises 34 proteins (including FHIT, GUSB, VAPB and TTR) that were more abundant in BPS-exposed ewes (WF50 and R50) and WF0 than in R0. C2 (orange) comprises 6 proteins (including AKR7A2, FDFT1, HSDL1 and TNPO2) that were more abundant in BPS-exposed (WF50 and R50) than unexposed ewes.

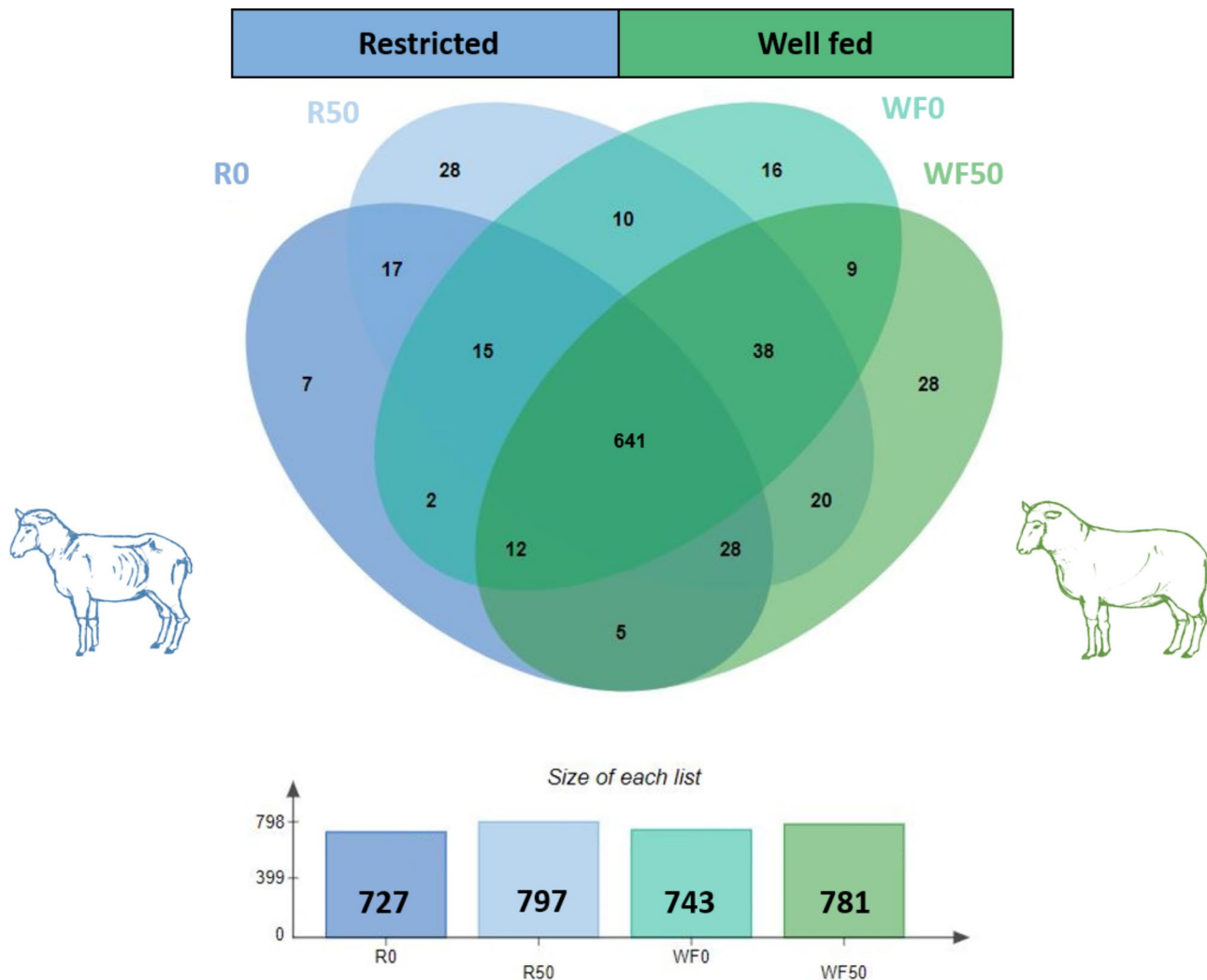


**Fig. 1** Comparative analysis of proteins identified in ewes Granulosa Cells (GCs)

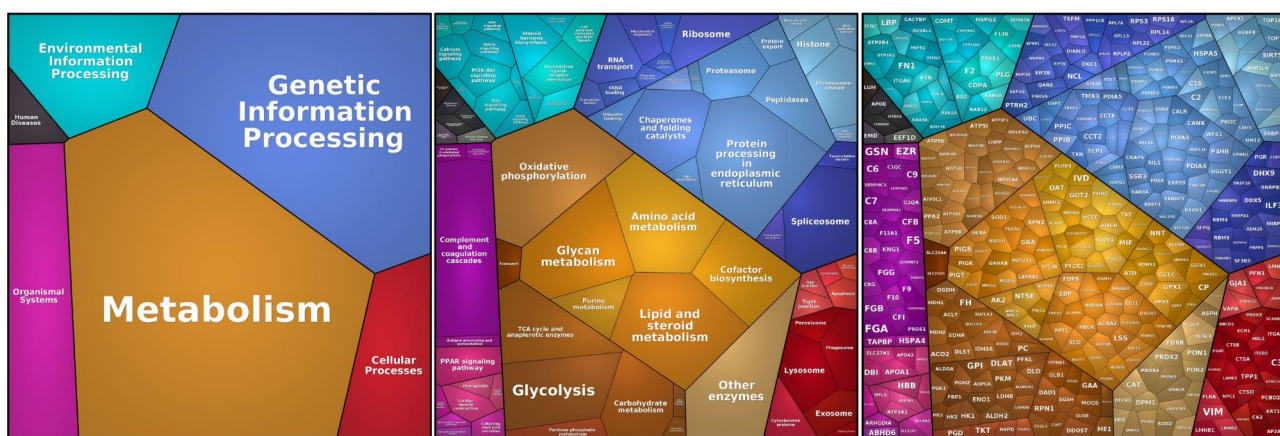


**Fig. 2** Proteomaps analysis of the 958 quantified proteins in ovine GCs

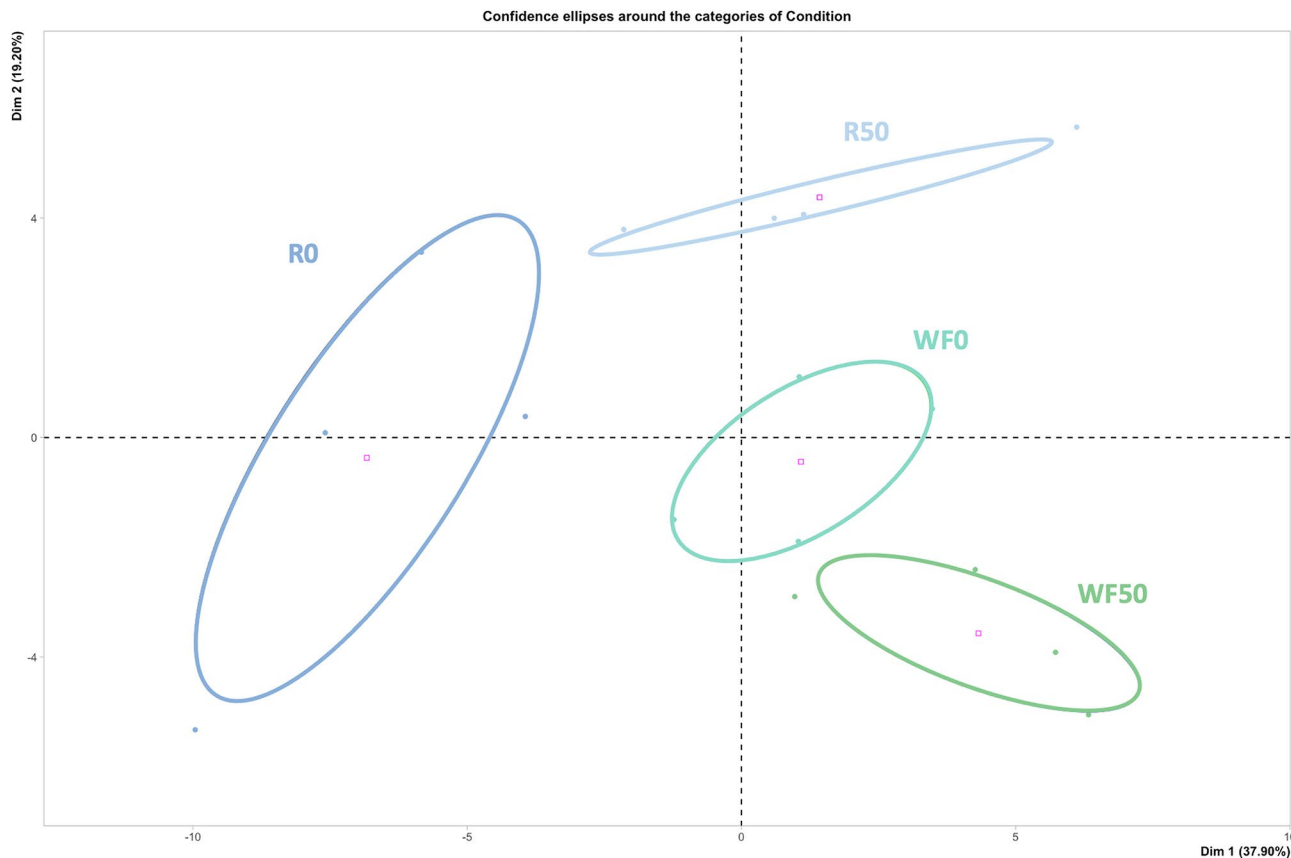


**Fig. 3** Principal component analysis of the 59 differentially abundant proteins according to the diet and BPS exposure

C3 (blue) comprises 5 proteins (including DCD, APOA1, CLEC3B and AMBP) that were more abundant in WF50 than in the three other conditions. Finally, C4 (pink) includes 14 proteins (including TST, NCSTN, SLC27A1 and PRKCSH) that were less abundant in the WF50 group compared with the three other groups (Table 2 and Supplementary Table S2).

Principal component analysis of the 59 DAPs (ANOVA  $p \leq 0.05$ ) showing a separation of the 16 GCs samples between diet (light and dark blue: restricted (R); turquoise and green: well-fed (WF)) and BPS exposure (0–50 µg/kg/day). Each point represents a biological sample with a different diet, exposed or not to BPS (see legends for corresponding colour). The square in each confidence ellipse indicates the mean of the data for a given region. The percentage on each axis (dimension) represents the total variance of data (horizontal axis, dimension 1 and vertical axis, dimension 2). Ellipses represent the 95% interval of confidence for each group.

Each line corresponds to a DAP (ANOVA or Chi-square  $p \leq 0.05$ ). For a given protein, blue lines represent lower abundance, white lines represent median abundance, while red lines represent higher abundance values relative to the other conditions. Four groups of proteins were identified by unsupervised hierarchical clustering

(multicoloured vertical bars on the left). Orange bars indicate groups with higher abundance in ewes exposed to BPS. Green bars indicate a group with lower abundance in R0, blue bars indicate groups with higher abundance in ewes WF50 while pink bars indicate a group with lower abundance in WF50. The proximity between proteins is illustrated by the hierarchical tree at the left side. R0 – restricted diet, no BPS, R50 – restricted diet and 50 µg/kg/day BPS exposure, WF0 – well feed diet, no BPS, WF50 – well feed diet and 50 µg/kg/day BPS exposure.

#### Pairwise comparisons of proteins in GCs from ewes exposed or not exposed to BPS and presenting contrasted metabolic status

Pairwise comparisons were performed on the lists of the 958 quantified proteins ( $t$ -test  $p \leq 0.05$  and  $FC \geq 2$  or  $\leq 0.5$ ; chi-square test  $p \leq 0.05$ ; Supplementary Table S2). Figure 5 shows the distribution and overlap of DAPs between the comparisons. The different comparisons showed relatively similar number of DAPs (34 for R0 vs. R50, 26 for WF0 vs. WF50, 37 for RO vs. WF0, and 48 for R50 vs. WF50). Most of the DAPs were specific to each comparison and there was no DAP shared among all the comparisons.

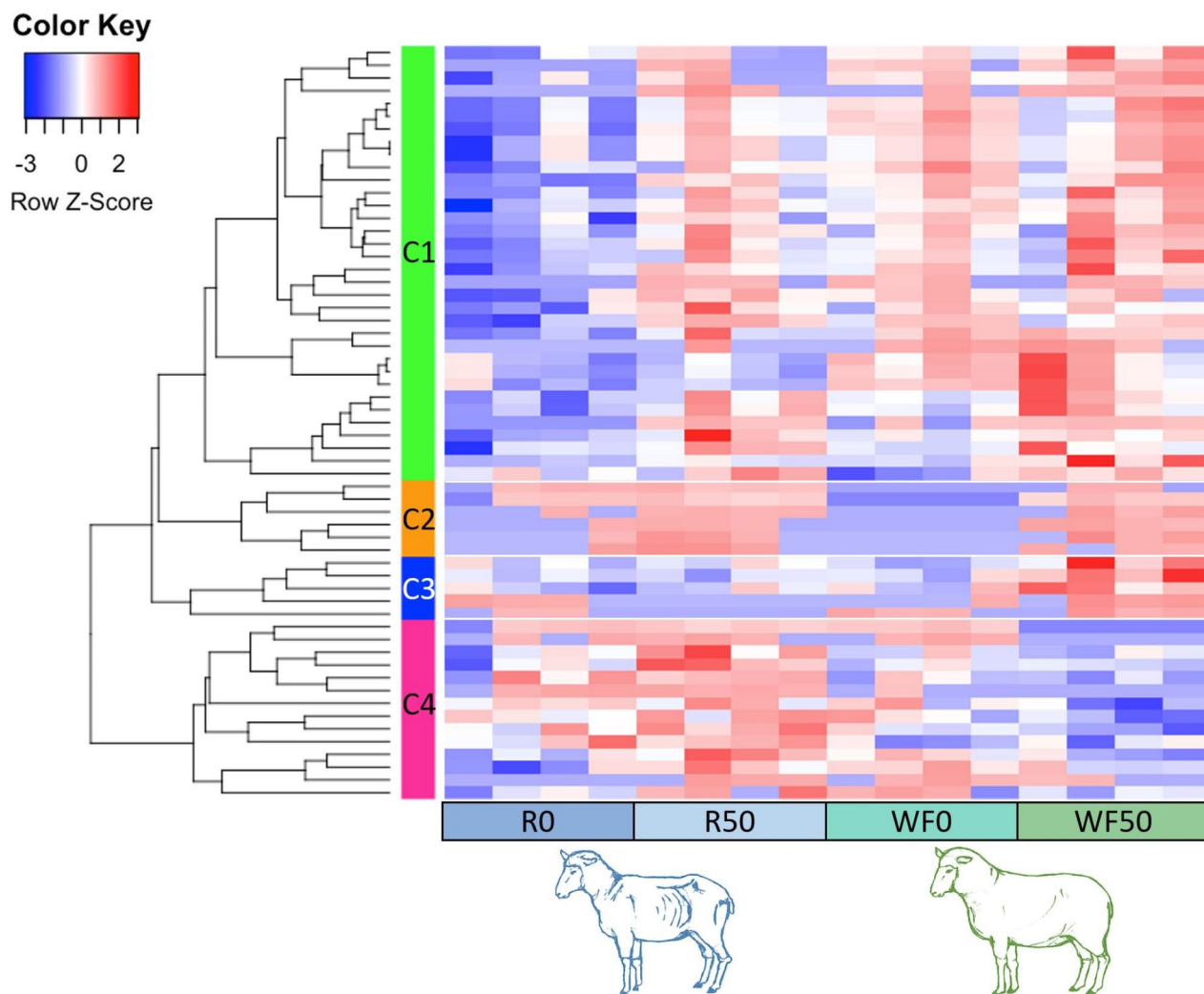


**Fig. 4** Heatmap and hierarchical clustering of the 59 differentially abundant proteins according to the diet and BPS exposure

The gene symbols for the DAPs were used for GO enrichment analysis of biological processes with Metascape (Supplementary Figure S1). The R50 vs. WF50 comparison highlighted a higher number of enriched biological processes compared with the other comparisons (Supplementary Figure S1D). The functional enrichments of DAPs for R0 vs. R50 is related to metabolism and detoxification (carbohydrate metabolic process and cellular detoxification) and proper functioning of the cells (intracellular protein transport, intracellular chemical homeostasis, organic anion transport, negative regulation of amide metabolic process and of cell development; Supplementary Figure S1A). The functional enrichments of DAPs for WF0 vs. WF50 is related to cells and organism balance and development (protein localisation to nucleus, negative regulation of cellular component organisation and of the immune effector process, positive regulation of cell migration, chordate embryonic development, and protein maturation) or in metabolism

(alcohol and carbohydrate metabolic process; Supplementary Figure S1B). The functional enrichment of DAPs for R0 vs. WF0 is related to oxidative stress (response to reactive oxygen species) and proper cell functioning (endoplasmic reticulum membrane organisation, electron transport chain, cellular homeostasis, regulation of vesicle-mediated transport; Supplementary Figure S1C). Finally, the functional enrichment of DAPs for R50 vs. WF50 is related to metabolism (generation of precursor metabolite and energy, carbohydrate derivative biosynthetic and metabolic process and lipid modification), the immune response (regulation of leucocyte migration and defence response to bacterium) and proper cell functioning (positive regulation of substrate adhesion-dependent cell spreading, small molecule biosynthetic process, mitochondrial transmembrane transport, maintenance of location, regulation of establishment of protein localisation, homeostasis of the number of cells, response to hypoxia and negative regulation of cell adhesion).

**Table 2** Examples of main differential proteins in each cluster of the heatmap

Heatmap cluster	Protein name	Gene symbol	Accession number	Molecular weight	Test	p-value (ANOVA or Chi-square)	Mean quantitative value (detection rate %) in R0	Mean quantitative value (detection rate %) in R50	Mean quantitative value (detection rate %) in WF0	Mean quantitative value (detection rate %) in WF50
C1	bis(5'-adenosyl)-triphosphatase isoform X1 beta-glucuronidase	<i>FHTT</i> <i>GUSB</i>	XP_011952467.2 XP_027817734.1	17 kDa 74 kDa	Chi-square Chi-square	0.0117 0.0019	N.D. (0%) N.D. (0%)	6.5 (50%) 6.88 (100%)	5.76 (75%) 6.18 (50%)	7.3 (100%) 6.6 (100%)
	vesicle-associated membrane protein-associated protein B/C	<i>VAPB</i>	XP_017913111.1	27 kDa	ANOVA	0.00037	6.56	7.49	7.57	7.7
	transthyretin precursor	<i>TTR</i>	NP_001009800.1	16 kDa	ANOVA	0.0028	8.33	8.55	8.58	9.17
C2	aflatoxin B1 aldehyde reductase member 2	<i>AKR7A2</i>	XP_027821430.1	41 kDa	Chi-square	0.0070	6.76 (75%)	7.03 (100%)	N.D. (0%)	7.21 (100%)
	inactive hydroxysteroid dehydrogenase-like protein 1	<i>HSD11</i>	NP_00102341.1	37 kDa	Chi-square	0.00270	6.17 (25%)	6.21 (100%)	N.D. (0%)	6.76 (75%)
	squalene synthase isoform X2	<i>FDFT1</i>	XP_004004500.1	48 kDa	Chi-square	0.012	6.56 (75%)	6.63 (100%)	N.D. (0%)	6.59 (50%)
C3	transportin-2 isoform X4	<i>TNPO2</i>	XP_027825368.1	103 kDa	Chi-square	0.003	6.32 (25%)	6.44 (75%)	N.D. (0%)	6.82 (100%)
	dermcidin isoform 1 preproprotein	<i>DCD</i>	NP_444513.1	11 kDa	Chi-square	0.046	5.47 (50%)	N.D. (0%)	5.94 (75%)	6.41 (75%)
	apolipoprotein A-I	<i>APOA1</i>	XP_011950887.2	30 kDa	ANOVA	0.0019	9.17	9.14	9.33	9.87
C4	tetranectin precursor	<i>CLEC3B</i>	NP_001039677.1	22 kDa	ANOVA	0.022	7.07	7.13	6.97	7.47
	protein AMBP isoform X2	<i>AMBP</i>	XP_005684386.1	39 kDa	ANOVA	0.033	6.97	7.07	7.14	7.53
	thiosulfate sulfurtransferase	<i>TST</i>	XP_014950344.2	33 kDa	Chi-square	0.0027	6.99 (75%)	6.91 (100%)	5.87 (25%)	N.D. (0%)
C4	nicastrin isoform X2	<i>NCSTN</i>	XP_012039753.2	67 kDa	Chi-square	0.028	6.58 (50%)	6.8 (75%)	6.68 (75%)	N.D. (0%)
	long-chain fatty acid transport protein 1	<i>SLC27A1</i>	XP_027825247.1	71 kDa	ANOVA	0.0066	6.6	7.16	6.59	6.52
	glucosidase 2 subunit beta	<i>PRKCSH</i>	XP_027825495.1	60 kDa	ANOVA	0.023	7.22	7.94	7.91	7.53

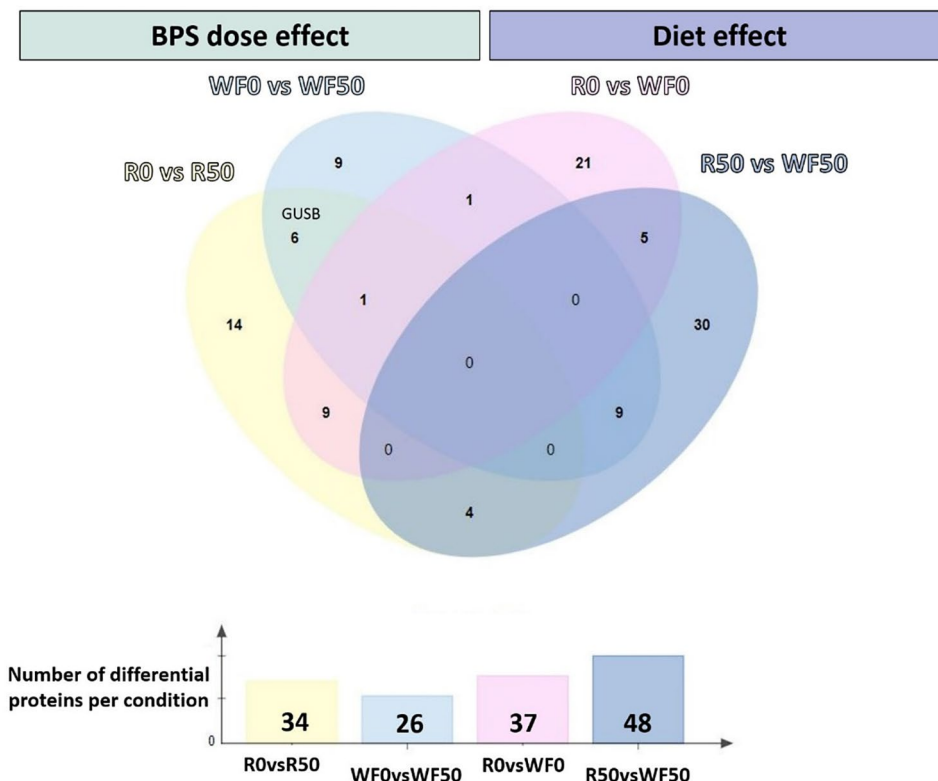


**Fig. 5** Comparative analysis of differentially abundant proteins identified in ewes Granulosa Cells

To decipher the impact of BPS, proteomaps of the DAPs for the R0 vs. R50 and WF0 vs. WF50 comparisons were generated by using the KEGG pathways database (Fig. 6A and B). One of the common functions between both comparisons is carbohydrate metabolism, including the  $\beta$ -glucuronidase (GUSB), which is present in both proteomaps. This protein was detected in all BPS-exposed ewes (the R50 and WF50 conditions), whereas it was not quantified in the R0 samples and was detected in 50% of the WF0 samples (Supplementary Table S3). Another common protein, nucleoprotein translocated promoter region (TPR)—which is involved in the processing of genetic information, more specifically in RNA transport—is also found in both proteomaps (Fig. 6A and B). This protein was more detected in R50 and WF50 (75% detection rate) compared with R0 (25% detection rate) and WF0 (0% detection rate; Supplementary Table S3). The diet effect, visualised as R0 vs. WF0 and R50 vs. WF50, showed proteins that are mainly involved in lipid and glycan metabolism, oxidative phosphorylation and purine and amino acid metabolism, including proteins like thiosulfate sulfurtransferase (TST), farnesyl-diphosphate farnesyltransferase 1 (FDFT1) and bis(5'-adenosyl)-triphosphatase (FHIT). Both TST and FDFT1 were detected more frequently in restricted than well-fed ewes (Fig. 6C and D). TST was detected in 75% and 100% of R0 and R50 samples, respectively, whereas it was detected

in 25% and 0% of WF0 and WF50 samples, respectively. Similarly, FDFT1 was detected in 75% and 100% of R0 and R50 samples, respectively, whereas it was detected in 0% and 50% of WF0 and WF50, respectively. On the contrary, FHIT was detected in 0% and 50% of R0 and R50 samples, respectively, whereas it was detected in 75% and 100% of WF0 and WF50, respectively, and was therefore found more often in well-fed ewes than in restricted ewes. Interestingly, proteins involved in oxidative stress were found in the R0 vs. R50 proteomaps, namely glutathione peroxidase 7 (GPX7), and in the R0 vs. WF0 proteomaps, namely NADH dehydrogenase 1 alpha subcomplex subunit 7 (NDUFA7). GPX7 was more abundant in R50 compared with R0 (FC=15.6) and NDUFA7 was more abundant in WF0 compared with R0 (FC=5.6; Supplementary Table S2). Lipopolysaccharide (LPS)-binding protein (LBP), a protein involved in the NF- $\kappa$ B signalling pathway; nicastrin (NCSTN), a protein involved in the Notch signalling pathway; and apolipoprotein A1 (APOA1), a protein involved in the PPAR signalling pathway, were also found in the WF0 vs. WF50 and R50 vs. WF50 proteomaps. LBP was less abundant in WF0 compared with WF50 (FC=0.34), and less abundant in R50 compared with WF50 (FC=0.06). NCSTN was detected more frequently in WF0 (75%) compared with WF50 (undetected), and more frequently detected in R50 (75%) compared with WF50 (undetected). APOA1 was more

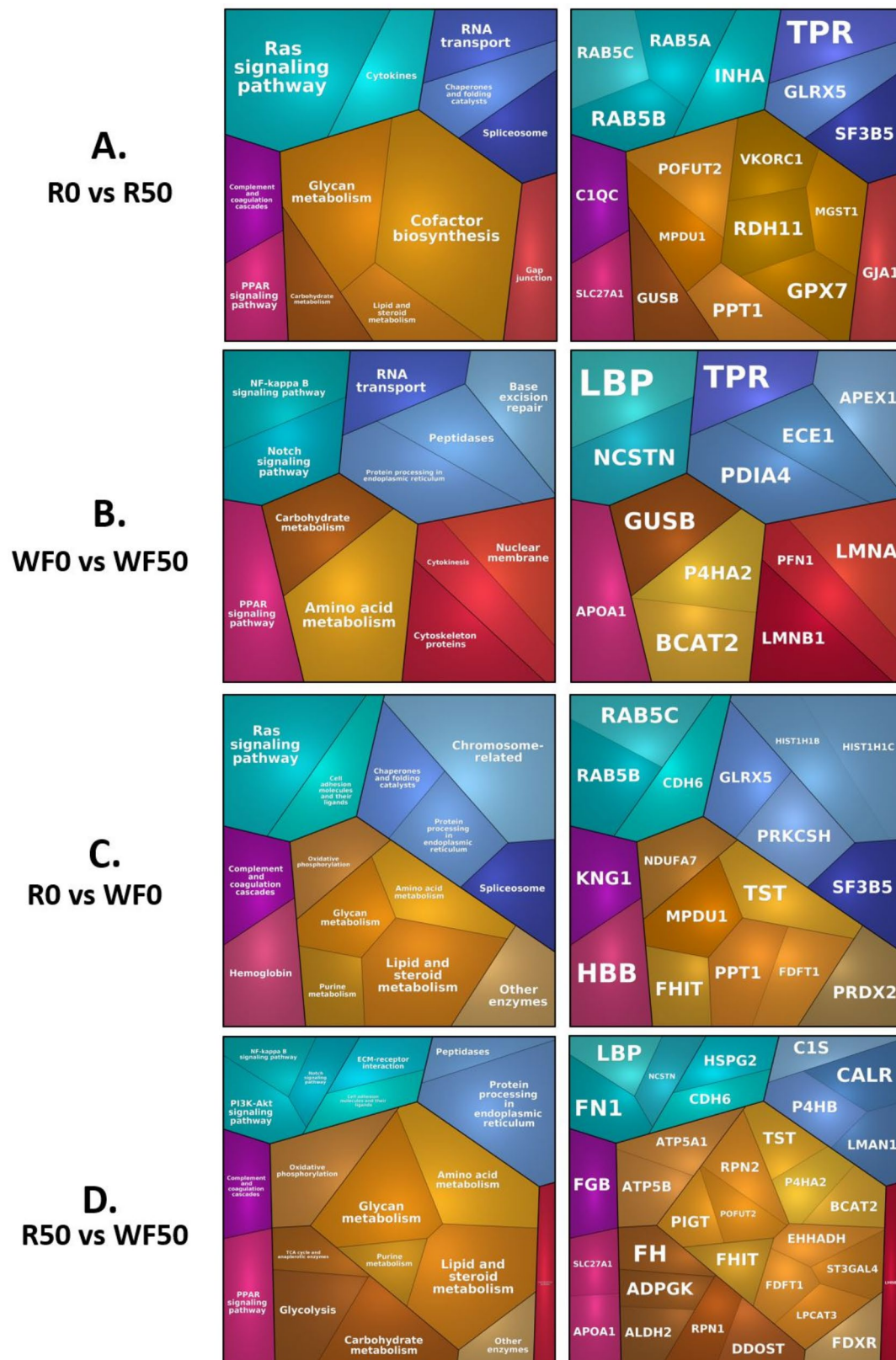


**Fig. 6** Proteomaps of differentially abundant proteins in R0 vs. R50 (**A**) and WF0 vs. WF50 (**B**), R0 vs. WF0 (**C**) and R50 vs. WF50 (**D**)

abundant in WF50 compared with WF0 ( $FC=2.35$ ) and R50 ( $FC=2.48$ ). Lastly, ras-related protein Rab-5B (RAB5B) and ras-related protein Rab-5 C (RAB5C), involved in protein transport, were found in the R0 vs. R50 and R0 vs. WF0 proteomaps. They were more abundant in R50 ( $FC=2.45$  and  $3.10$ , respectively) and WF0 ( $FC=3.23$  and  $3.84$ , respectively) compared with R0.

Venn diagram shows the overlap of the DAPs from the pairwise comparisons ( $p\text{-value } t\text{-test} \leq 0.05$  and fold change ratio  $\text{Log}_2(\text{FC}) \geq 1$  or  $\leq -1$ ; feed  $\times$  BPS exposure) and histogram representing the number of proteins identified in each condition.

Protein maps were generated using the KEGG (Kyoto Encyclopedia of Genes and Genomes) Pathway gene classification. Proteomaps were created from the average of the quantification values of the overabundant or most detected DAPs in each pairwise comparison with a  $\text{Log}_2(\text{FC}) \geq 1$  or  $\leq -1$  minimum. In the left column, functional categories are represented by polygons, and in the right column, proteins are represented by the same polygons. The polygons illustrate the normalised abundance of proteins in each condition. Functions and related proteins are organised into common regions and coded using similar colours.

## Discussion

This study aimed to characterise the effects of chronic BPS exposure on the proteome of ewe GCs, considering the interaction between metabolism status and reproductive function. Even though some deleterious impacts of BPS on GCs have already been reported *in vitro* [10, 11, 19–22], this is the first study to characterise the GC proteome after chronic BPS exposure. Furthermore, this study compared the BPS effects on the GC proteome in ewes with a contrasted metabolic status. These results have highlighted the interaction between metabolism and BPS exposure by identifying specific proteins in each comparison. In addition, proteins related to the BPS effect were also identified, in particular GUSB, which was significantly overexpressed in the GCs of BPS-exposed compared with non-exposed ewes. Because GUSB is able to remove the glucuronide conjugate from bisphenol molecules and thus to restore the oestrogenic activity of bisphenols, it could worsen the effects of this exposure.

### BPS – metabolism interaction

Chronic BPS exposure of adult ewes affected the GC proteome; and its effects varied depending on the metabolic status of the ewes. Most of the DAPs and predicted pathways and functions were specific to one comparison. According to the Venn diagram, only 5 common proteins were identified between the R0 vs. WF0 and R50 vs. WF50 comparisons (diet effect). On the contrary, 21 proteins were identified specifically for the R0 vs. WF0

condition and 30 for the R50 vs. WF50 condition. Therefore, most of the proteins corresponding to the diet effect (21 and 30 proteins) differ depending on the BPS exposure. Similarly, for the BPS effect, 6 proteins common to the R0 vs. R50 and WF0 vs. WF50 comparisons (BPS effect) were identified. On the contrary, 14 proteins were identified specifically for the R0 vs. R50 comparison and 9 for the WF0 vs. WF50 comparison, again suggesting that the 14 and 9 proteins differ depending on diet. This highlighted the interaction between the BPS effect and metabolic status. In addition, the interaction between BPS exposure and the metabolic status was also highlighted by the unexpected common DAPs shared between pairwise comparisons mixing BPS and diet effects. Indeed, there were 9 common DAPs between the R0 vs. R50 (BPS effect) and R0 vs. WF0 (diet effect) comparisons, and 9 common DAPs between the WF0 vs. WF50 (BPS effect) and R50 vs. WF50 (diet effect) comparisons. These results strengthen our hypothesis that the effects of BPS differed according to body condition, which is in line with the analyses previously performed on these same ewes as part of the same study [34, 35]. This interaction might be specific to ovarian cell functioning as it was not reported when studying oviduct proteome in the same ewes, the diet effect being the main effect observed [36]. Modulation of the BPS effect by the metabolic status has already been highlighted regarding the oestradiol content in the preovulatory follicular fluids from the same follicles that provided the GCs for the present proteomic analysis [34]. Indeed, after BPS exposure, the oestradiol level increased in well-fed ewes, while it did not change in restricted ewes [34]. Moreover, *in vitro* embryo production with oocytes punctured during the previous oestrous cycles of the same ewes showed that, even though there was no BPS effect on the embryo parameters, there was a BPS  $\times$  diet interaction, suggesting that the BPS effect differs according to the metabolic status [35]. Other studies on the effects of synthetic chemicals such as BPA, phthalates and microplastics have also shown the importance of considering the metabolic status when studying exposure to environmental pollutants. In rodents, exposure to BPA through intragastric gavage or oral administration combined with a high-fat diet (particularly butter) led to transgenerational dysfunction of the entire reproductive system, including an altered oestrous cycle and disrupted spermatogenesis in rats compared with a low-fat diet or a high-fat olive oil diet [37, 38]. Moreover, a study on di(2-ethylhexyl) phthalate (DEHP) oral exposure, at a dose considered safe in the environment, combined with a high-fat diet in pregnant mice suggested a negative effect on the development of placental vascularisation and foetal growth compared to a regular diet [39]. Similarly, in rats the combination of a high-fat diet and DEHP exposure had joint effects on lipid metabolism [40]. Another

study showed that oral exposure of pregnant mice to a perfluorooctanesulfonic acid (PFOA) and per- and poly-fluoroalkyl substances (PFAS) mixture (PFOA/perfluorooctane sulfonate (PFOS)/perfluorohexanesulfonate (PFHxS)), combined with high-fat diet, could influence the effect of PFAS on the liver of their offspring, and could render them more sensitive to the perinatal effects of PFAS [41].

APOA1 is the main component of high-density lipoprotein and plays an important role in reverse transport of cholesterol [42], which is the precursor molecule for steroidogenesis. LBP is involved in the immune response to LPS by promoting an inflammatory response through the initiation of an inflammatory cytokine cascade which mediates the elimination of LPS [43]. Both proteins are involved in anti-inflammatory or immune functions [44, 45]. Even though the balance between both molecules is not clearly stated in the literature, LBP is increased in exacerbated lipid metabolism environment [46] while APOA1 is reduced [47], which is consistent with the present study with APOA1 being increased when LBP is decreased and vice versa. In contrast to APOA1, LBP was overabundant in R50 and WF0 compared with WF50 (FC=16.22 and 2.93, respectively), which is not consistent with the literature. Indeed, a high-fat and high-carbohydrate meal has been reported to increase the human plasma LBP concentration [48], but this phenomenon did not occur in the present study since LBP protein was overabundant in R ewes compared with WF ewes when exposed to BPS. This could be explained by the fact that LBP reduces circulating LPS levels especially through the nuclear factor kappa-light-chain-enhancer of activated B cells (NF- $\kappa$ B) pathway [43, 48]. Indeed, activation of NF- $\kappa$ B by LPS treatment (leading to an increase in LBP) significantly reduced APOA1 in HepG2 cells in vitro, while NF- $\kappa$ B inhibition in mice increased plasma APOA1 in vivo [49, 50]. This balance between APOA1 and LBP is involved in both diet and BPS exposure effect, as both APOA1 and LBP were found in WF0 vs. WF50 and R50 vs. WF50 comparison. Furthermore, it has been reported that BPS activates NF- $\kappa$ B [51] and BPA inhibits APOA1 [52] in mouse hepatocytes, which is opposite compared with the present study. NF- $\kappa$ B inhibition increases plasma APOA1 through activation of Peroxisome Proliferator-activated Receptor  $\alpha$  [50]. In fact, our results suggested that BPS exposure and WF diet upregulate APOA1 and downregulate LBP protein. These results could be due to the activation of the NF- $\kappa$ B pathway by the interaction of metabolism and BPS exposure, leading to a decrease in LBP and an increase in APOA1. The mechanism through which BPS affects NF- $\kappa$ B pathway requires further investigation. This study has highlighted that the metabolic status should be considered when studying the effects of environmental factors so that their

potential effects in subgroups of the population are not underestimated.

### Metabolism effect

PCA showed a clear discrimination of DAPs according to the metabolic status. There were only 5 common proteins between the R0 vs. WF0 and R50 vs. WF50 comparisons: TST, FHIT and FDFT1, which are involved in metabolism, and CDH6 and DCD, which are involved in cell function. FHIT had a significantly higher detection rate in the GCs of well-fed ewes compared with restricted ewes. This finding is in line with papers establishing a link between the *FHIT* gene in humans and BMI and waist circumference, and that it is correlated with adiposity in adulthood [53, 54]. FDFT1, also known as squalene synthase (SQS), is the first specific enzyme in cholesterol biosynthesis. FDFT1 was detected more frequently in GCs of restricted ewes. FDFT1 hepatic messenger RNA (mRNA) levels are regulated by the cholesterol status [55]. In fact, FDFT1 enzyme activity and protein and mRNA levels can decrease dramatically in response to cholesterol overabundance and increase sharply in response to cholesterol deprivation in both animals and cultured hepatic cells [55]. FHIT and FDFT1 were detected in most BPS-exposed ewes (regardless of the diet) but much less frequently or not at all in the unexposed ewes. These findings highlight the potential involvement of BPS in adiposity and/or lipid metabolism. Indeed, in vitro and in vivo studies showed that BPS could promote obesogenic effect and metabolic disorders [56], and promote adipogenesis in human preadipocytes [57]. Although our experiment was not designed to observe obesogenic effects, additional studies should include such parameters.

In addition, the basic protein profile of GCs is very metabolically oriented as shown by the proteomaps. After several months of restricted feeding, basic requirements have likely been reduced to a minimum due to the energy deficit. This is in line with the lower NEFA level in R0 ewes, indicating that these ewes, contrary to the beginning of the diet restriction, did not have the body reserve to compensate for the lower energy intake relative to the energy requirement. The metabolic functions involved in the R50 vs. WF50 comparison include lipid, carbohydrate and energy metabolism, and most of the proteins involved in these functions were overabundant or detected more frequently in R50 compared with WF50, including ATP5A1 and ATP5B involved in adenosine triphosphate (ATP) production, as a means to compensate for the low energy intake [58, 59]. Similarly, in a previous study of bovine GCs, the authors found that most DAPs (259 total DAPs among 3,409 identified proteins) from the dominant vs. subordinated follicle comparison are also involved in metabolic pathways, according to KEGG

pathway analysis [60]. Therefore, metabolism, including lipid metabolism, is expected to be crucial for the correct maturation of oocytes. Modulations of lipid metabolism could also impair the ability of GCs to perform their functions as previously reported in bovine GCs [61]. A comparative study of the fatty acid composition of oocyte lipids in cattle and sheep showed that these two ruminant species are close in terms of lipid metabolism [62]. Lipid metabolism is therefore likely crucial in ovine GCs and oocytes too.

Oxidative stress proteins such as GPX7 and NDUFA7, both involved in regulating the redox status, were overabundant in the R50 and WF0 ewes compared with R0 ewes, respectively. This suggests that the R0 condition led to an inhibition of the antioxidant response. Under-nourishment in pregnant ewes alters the expression of the glutathione peroxidase genes in the blood and liver of the mother and in the foetus at the end of gestation [63]. Additional data are required to compare pregnant and non-pregnant ewes and to investigate the link between oxidative stress and food restriction.

#### BPS effect

BPS had a moderate effect in terms of the number of DAPs in the GCs proteome. These changes are relevant when considering the results of the embryo production and steroidome study of the same ewes [34, 35]. In fact, BPS alone only results in a moderate number of DAPs, and the interaction between BPS exposure and diet produced more DAPs. Nevertheless, the *in vivo* model is still more sensitive compared with *in vitro* experiments. Indeed, after chronic daily *in vivo* oral exposure to 50 µg/kg/day BPS, corresponding to a follicular fluid concentration of 200 nM BPS (measured as BPS-g) on average, there were changes in oestradiol secretion in the follicular fluid [34]. However, there were no differences in steroidogenesis after acute exposure up to 1 µM BPS *in vitro* in the same species [22]. It is interesting to note that the most outstanding functions in the proteomaps corresponding to the BPS effects are related to energy, glycan, carbohydrate, amino acid, lipid and steroid metabolism; the processing of genetic information, including RNA transport; and cellular processes. Studies on human cohorts have shown that exposure to BPS could be associated with elevated BMI and waist circumference, based on median urinary concentrations [56], and therefore related to changes in energy metabolism. In addition, significant disturbances in lipid and glucose metabolism, as well as an increase in fat accumulation due to BPS, were reported in the preadipocytic 3T3-L1 cell lines *in vitro* [30]. Indeed, BPS is a potent chemical responsible for the hyperglycaemic response and also alters many metabolites by hampering various biological pathways. A metabolomic pathway analysis revealed an alteration in

glycolysis or gluconeogenesis pathway upon BPS exposure in rats [64]. The possible mechanisms of action are attributed to oestrogenic or androgenic activities, favouring alterations in the genetic expression of markers linked to adipogenesis and inducing oxidative stress and an inflammatory state [56]. Of note, BPS binds to oestrogen but not to androgen receptors [17].

There were six common DAPs when comparing BPS-exposed ewes to their respective unexposed controls (R50 vs. R0 or WF50 vs. WF0) including GUSB, involved in metabolism, and HSDL1, TNPO2 and TPR, involved in the proper functioning of the cell. GUSB degrades glycosaminoglycans and participates in the degradation of polysaccharides that contain glucuronide residues [65]. GUSB helps to deconjugate various potential toxins, hormones, and various drugs in the body and is also involved in hydrolysis of glucuronides of endo- and xenobiotics in humans. GUSB has already been reported to hydrolyse conjugated BPA into free BPA as it passes through the placental barrier [66]. While BPS-g is unable to bind to oestrogen receptors [6, 67], it is still able to exert effects on cells [68], and sometimes the effect is even worse compared with free BPA [69]. Therefore, the higher abundance of GUSB in the GCs from BPS-exposed ewes suggested that metabolised BPS-g could be deconjugated into free BPS in the follicular compartment, leading to prolonged intracellular exposure to free BPS and to prolonged oestrogenic effects. Such a conversion cycle of bisphenol has not previously been described at ovarian level. Exposure to BPS likely worsens this potential effect at the ovarian level. In the present study, GUSB was not upregulated in WF50 ewes compared with R50 ewes. Nevertheless, GUSB activity in serum and plasma has been associated with higher BMI in humans [70–72]. It is important to note that in some of those studies, the BMI is closer to overweight than to obesity (i.e. it does not exceed 26.5 kg/m<sup>2</sup>) [70, 72]. In another study of menopausal and premenopausal women, GUSB activity was also positively correlated with fat mass but not with lean mass and therefore with individual adiposity [73] which is consistent with our results. Indeed, even if GUSB is not upregulated in WF0 compared to R0, it was detected in half of the samples in WF0 samples while it was never detected in the R0 sample. GUSB was therefore found in well-fed ewes, whether exposed to BPS or not, unlike in restricted ewes. It could thus be assumed that R0 corresponded to the condition exhibiting the lowest expression. As mentioned before, despite their diet, the WF50 ewes could not be considered obese (their mean BCS was 2.88). It is possible that a further increase in GUSB could be observed in obese individuals exposed to BPS, which would exacerbate exposure to free BPS in this population and, consequently, overfeeding would exacerbate the negative effects of BPS exposure. Additional studies

should assess this hypothesis because its confirmation would suggest a higher sensitivity of women with obesity to bisphenol exposure.

### Limitations of the study

One of the limitations of this study is that GCs were collected with follicular fluid, which is a plasma ultrafiltrate. Therefore, blood proteins were very abundant and could potentially have masked the signal of less abundant proteins, resulting in fewer quantified proteins. In addition, serum albumin was not depleted before analysis to avoid eliminating potential albumin-binding proteins. Another limitation of this study is that the two diets used in this study were either abnormally restrictive or abnormally excessive, so neither group of ewes received 100% of their dietary requirements. Furthermore, as mentioned above, well-fed ewes with a mean BCS of 2.88 cannot be considered as obese [74], despite their elevated plasma NEFA and glucose levels. Consequently, the hypotheses put forward should be interpreted with caution and additional tests should be carried out on animals with a BCS of 4. It is difficult to discuss whether an obese phenotype would worsen the BPS effects. Nevertheless, given these limits, our data suggest that the effects of BPS exposure could vary depending on the metabolic status of the ewes and the involved energy metabolism.

### Conclusion

Chronic exposure of adult ewes to BPS affected the GC protein content, and this effect was modulated by the metabolic status of the animals. A total of 958 proteins were quantified and 59 were differentially abundant in the four experimental groups. In addition, various functional pathways were affected, mainly energy metabolism pathways. GUSB was identified in the GC proteome of BPS-exposed animals. Moreover, among unexposed ewes, GUSB was detected only in well-fed ewes. GUSB could increase BPS exposure by deconjugating BPS-g into free BPS. This protein might worsen or prolong the exposure of these cells to free BPS, therefore prolonging oestrogenic effects that might be even further worsened in people with adiposity. It is difficult to discuss whether the well-fed phenotype worsens the BPS effects, as there are only few studies examining the interaction between BPS exposure and adiposity in vivo and there is no diet group corresponding to normal feeding. Here, leads are suggested but require deeper investigation. Nevertheless, the data showed, in WF ewes exposed to BPS, an alteration in in vitro embryo production, in GC steroidogenesis with increased levels of oestradiol in the follicular fluid [34, 35] and in GC proteomics, in particular GUSB abundance. All these data suggested a potentially higher sensitivity to the effects of BPS in adipose individuals. These results and those of previous studies highlight

the deleterious effect of BPS and its interaction with the metabolic status, indicating that its use in food packaging should be regulated.

## Materials and methods

### Ethics

All experimental procedures were conducted in accordance with the European Directive 2010/63/EU on the protection of animals used for scientific purposes and approved by the French Ministry of Nation Education, Higher Education, Research and Innovation after ethical assessment by the local ethics committee *Comité d'Ethique en Expérimentation Animale Val de Loire* (CEEA VdL) and INRAE consented to use the animals in this experimental protocol (protocols registered under APAFIS numbers 13965-2018042008519239v2 and 14014-2018030717477406v2).

### Experimental design

A total of 40 primiparous Ile-de-France ewes (average age 2.5 years) were housed in a sheepfold from 2018 to 2019. The experimental design was described previously [34]. Briefly, the ewes were divided into two groups with contrasting diets: restricted (R, n=20) and well-fed (WF, n=20). The diet was designed according to the INRAE recommendations for the growth and maintenance needs of adult, non-pregnant ewes [75]. It consisted in varying the quantity of a wheat-based food supplement (Agneau-échange, AXERÉAL Elevage, Saint Germain de Salles, France). The food supplement was distributed in the morning and the animals had free access to straw and water and minerals to lick. Ewes from the experiment groups were fed in order to reach the goal of a median BCS of 2 in restricted groups and of 4 in well-fed groups and the quantity was adjusted according to the mean of body weight of the group. Ewes in the restricted group were initially fed 50% of their maintenance energy requirements and, once the target BCS was reached, they were fed 80% in order to maintain the desired nutritional status. Ewes in the WF groups were fed 165% of their maintenance energy requirements until the end of the experiment. The BW (kg) and BCS (on a scale of 1 to 5, 1 corresponding to very skinny ewes and 5 to obese ewes [74]) of animals were monitored once a month. Within each group, two subgroups were defined according to BPS exposure (0–50 µg/kg/day) for at least 3 month, 5.4±0.1 months (range: 3.6–7.9 months. The BPS, purchased from Sigma Aldrich (Madrid, Spain), was added to the feed in the form of a powder mixed with the cereals. Thus, there were four groups: R0 and R50 for the restricted ewes, and WF0 and WF50 for the well-fed ewes. Between September and December, the oestrus cycle of the 40 ewes was synchronised with a vaginal sponge of progesterone (Chrono-Gest® 20 mg,

MSD, Beaucouze, France) for 11 days, followed by intramuscular administration of pregnant mare serum gonadotropin (PMSG, Synchro-Part® PMSG 400 IU, CEVA Santé Animale, Libourne, France). Two days after PMSG administration, at the presumed time of the pre-ovulatory period, the ewes were slaughtered, and follicular cells of the dominant follicles were collected by aspirating the follicular fluid containing GCs. GCs were centrifuged and washed twice with phosphate-buffered saline (PBS) and then stored dry at -80 °C until analyses. Blood samples (5 mL) were collected at the time of slaughterhouse bleeding in heparinised tubes (17 IU/mL sodium heparin, Vacutainer®; Becton Dickinson and Company, Le Pont de Claix, France), centrifuged (3,700 g for 30 min at 4 °C) and plasma samples were stored at -20 °C for further assay of glucose, NEFA, BPS and its metabolite BPS-glucuronide (BPS-g).

#### Plasma glucose, non-esterified fatty-acids BPS and BPS-glucuronide assays

Plasma glucose and NEFA were quantified individually ( $n=80$ ) on a 2 and 5  $\mu$ L undiluted plasma sample, respectively, by colorimetric enzymatic methods using a Konelab 20 analyzer (Thermo Scientific, Gometz le Châtel, France) and kits provided by Bio-Mérieux (Marcy-l'Etoile, France) and Thermo Scientific (Villebon sur Yvette, France). BPS and BPS-g concentration were quantified as previously described [35] using liquid chromatography mass spectrometry with an Acquity U-HPLC device coupled to a Xevo-TQ triple quadrupole mass spectrometer (Waters, SaintQuentin-en-Yvelines, France) operated with positive electrospray ionization and MRM mode. All samples were quantified on the same day. The limit of quantification (LOQ) was set at 0.5 ng/mL (2 nM) for BPS and 0.05 ng/mL (0.10 nM) for BPS-g.

#### Protein extraction and quantification

The GC pellet was resuspended on ice with 100  $\mu$ L of lysis buffer (10 mM Tris-HCl + 2% sodium dodecyl sulphate [SDS] + 1X protease inhibitor). Then, it was sonicated (2×20 s, five times for each sample) and centrifuged (30 min, 10000 g, 4 °C). The supernatant was transferred to a new tube kept on ice and stored at -20 °C. The protein concentration was quantified using the colorimetric BC assay Protein Quantification kit (Interchim, Montluçon, France), following the manufacturer's recommendations. The optical density at 550 nm was measured with a Thermo LabSystems plate reader at 550 nm absorbance and with Ascent software for Multiskan equipment.

#### Preparation of GC samples for comparative proteomic analyses

After protein extraction and quantification, 50  $\mu$ g of protein per sample was separated with 4–10% SDS-polyacrylamide gel electrophoresis (80 V, 10 min and 180 V, 50 min). After separation, the gel was stained with Coomassie blue. It was cut into four strips for each track and washed in water and acetonitrile (1:1 [v/v], 5 min) followed by 100% acetonitrile (10 min). Reduction and cysteine alkylation were performed by successive incubation with 10 mM dithiothreitol in 50 mM ammonium bicarbonate (30 min, 56 °C), then 55 mM iodoacetamide in 50 mM ammonium bicarbonate (20 min, room temperature, in the dark). The pieces were incubated with 50 mM ammonium bicarbonate with acetonitrile (1:1 [v/v], 10 min) followed by acetonitrile (15 min). Proteolytic digestion was carried out overnight using 25 mM ammonium bicarbonate containing 12.5 ng/ $\mu$ L trypsin (sequencing grade, Roche Diagnostics, Paris, France). The resultant peptides were extracted by incubation in 5% formic acid (with sonication). The supernatant was removed and incubated with acetonitrile and 1% formic acid (1:1 [v/v], 10 min). After a final incubation with acetonitrile (5 min), the supernatant was removed and saved. These two peptide extractions were pooled and dried using a SPD1010 SpeedVac system (Thermosavant, ThermoFisher Scientific, Bremen, Germany).

#### NanoLC-MS/MS

Peptide mixtures were analysed with on-line nanoLC-MS/MS as described previously [76]. All experiments were performed on a dual linear ion trap Fourier-transform mass spectrometer (FT-MS) LTQ Orbitrap Velos Pro (Thermo Fisher Scientific, Bremen, Germany) coupled to an Ultimate® 3000 RSLC Ultra High-Pressure Liquid Chromatographer (Thermo Fisher Scientific, Bremen, Germany) controlled by Chromeleon Software (version 6.80 SR13). The samples were desalting and concentrated for 10 min at 5  $\mu$ L/min on an LC Packings trap column (Acclaim PepMap 100 C18, 75  $\mu$ m inner diameter × 2 cm long, 3  $\mu$ m particles, 100 Å pores). The peptide separation was conducted using a LC Packings nano-column (Acclaim PepMap C18, 75  $\mu$ m inner diameter × 50 cm long, 2  $\mu$ m particles, 100 Å pores) at 300 nL/min by applying a gradient of 2–45% B over 90 min. The mobile phases consisted of 0.1% formic acid, 97.9% water and 2% acetonitrile (v/v/v; A), and 0.1% formic acid, 19.9% water, 80% acetonitrile (v/v/v; B). The data were acquired using Xcalibur version 3.0.63 software (Thermo Fisher Scientific, San Jose, CA), in positive data-dependent mode in the 300–1800 m/z mass range. The resolution in the Orbitrap was set at  $R=60,000$ . The 20 most intense peptide ions with charge states  $\geq 2$  were isolated sequentially (isolation width 2 m/z, 1 microscan)

and fragmented in the high-pressure linear ion trap using the collision induced dissociation (CID) mode (collision energy 35%, activation time 10 ms, Qz 0.25). Dynamic exclusion was activated for 30 s with a repeat count of 1. The lock mass was enabled for accurate mass measurements. The polydimethylcyclosiloxane ((Si(CH<sub>3</sub>)<sub>2</sub>O)<sub>6</sub>, m/z 445.120025) ion was used for internal recalibration of the mass spectra MS/MS.

#### Protein identification and data validation

Ion searches were performed using the Mascot search engine version 2.7.0.1 (Matrix Science, London, UK) via the Proteome Discoverer 2.5 software (ThermoFisher Scientific, Bremen, Germany) against the NCBI prot\_Mammals database (2021/07). The search parameters included trypsin as the protease with two allowed missed cleavages and carbamidomethyl cysteine, methionine oxidation and acetylation of the N-terminal protein as variable modifications. The tolerance of the ions was set to 5 ppm for parent and 0.8 Da for-fragment ion matches. The Mascot results obtained from the target and decoy databases searches were analysed with the Scaffold Q+S v5.1.1 and Scaffold Quant v5.0.3 softwares (Proteome Software, Portland, OR, USA) using the protein cluster analysis option (assemblage of proteins into clusters based on shared peptide evidence). Peptide and protein identifications were accepted if they could be established with a probability of >95%, in accordance with the Peptide Prophet and the Protein Prophet algorithms, respectively. Proteins were identified with a minimum of two unique peptides. Extracted ion chromatogram (XIC) is based on the normalised values of the intensities of the chromatographic peaks corresponding to the peptides of a protein. XIC data were log transformed (log<sub>10</sub> precursor intensity). The names of clusters, redundant proteins, and potential contaminants (keratin from *Homo sapiens* and trypsin) were excluded from the lists. In addition, only *Homo sapiens* and the followed herbivorous species were retained: *Ovis aries*, *Ammotragus lervia*, *Bison bison bison*, *Bos indicus*, *Bos indicus* × *Bos taurus*, *Bos javanicus*, *Bos mutus*, *Bos taurus*, *Bubalus bubalis*, *Camelus bactrianus*, *Camelus dromedarius*, *Camelus ferus*, *Capra hircus*, *Cervus elaphus*, *Cervus elaphus hippelaphus*, *Cervus hangul yarkandensis*, *Equus asinus*, *Equus caballus*, *Equus przewalskii*, *Muntiacus muntjac*, *Muntiacus reevesi*, *Muntiacus vaginalis*, *Odocoileus virginianus texanus*, *Odocoileus virginianus virginianus*, *Ovis canadensis nelson*, and *Vicugna pacos*.

#### Drawing up a list of differentially abundant proteins (DAPs)

Regarding the proteins detected in all conditions, DAPs were identified after analysis of variance (ANOVA) on protein abundance ( $p \leq 0.05$ ) and t-test ( $p \leq 0.05$ ), when the fold-change (FC) between the two conditions was

≥2 or ≤0.5. Regarding the proteins present in one condition but not in the other, DAPs were identified after the chi-square test on the protein detection rate ( $p \leq 0.05$ ). Briefly, proteins were considered to be present in a biological sample when they were detected at least once in one of the three technical replicates. Proteins that were not detected in any biological replicate for a condition were tested using the chi-square test for the bisphenol effect (proteins quantified for exposed and unexposed animals regardless of diet) and the effect of diet (proteins quantified for restricted and well-fed animals regardless of BPS exposure), but also for pairwise analyses (R0 vs. R50, WF0 vs. WF50, R0 vs. WF0, and R50 vs. WF50). This yielded 17 proteins with a  $p \leq 0.05$  (chi-square test) for at least one of the comparisons (dose, diet or pairwise) and an average abundance (log<sub>10</sub> precursor intensity) ranging from 5.94 to 7.58. For pairwise analyses, proteins with significant differences in the detection rate according to bisphenol exposure were added to the lists of DAPs for the R0 vs. R50 and WF0 vs. WF50 comparisons; likewise, proteins exhibiting significant differences in the detection rate according to diet effect were added to the lists of DAPs for the R0 vs. WF0 and R50 vs. WF50 comparisons. Proteins that responded only to the pairwise analysis (R0 vs. R50, WF0 vs. WF50, R0 vs. WF0, or R50 vs. WF50) were added to the corresponding DAPs lists.

Principal component analysis (PCA) was performed and a heatmap was generated by using the Rstudio software (version 2023.03.0+386). PCA on DAPs (both ANOVA and the chi-square test) were carried out using the FactoMineR and ggplot2 packages. The percentage on each axis (dimension) represents the total variance of data according to dimension 1 (horizontal axis) and dimension 2 (vertical axis). Heatmap and hierarchical clustering on DAPs (both ANOVA and chi-square test  $p < 0.05$ ) were performed using the gplots package. For DAPs from the ANOVA, missing values (in one replicate among detected values in other replicates of the condition) were treated with the missMDA package [77]. For DAPs from the chi-square test, missing values (in all replicates of a condition) were deliberately replaced by '1' because the XIC data were log-transformed (log<sub>10</sub> precursor intensity), indicating the absence of detection.

#### Functional analysis and prediction of biological processes of DAPs

The overlaps of DAPs between the different conditions was visualised using the online tool jvenn (<https://jvenn.toulouse.inrae.fr/app/example.html>) [78]. Gene enrichment analysis was performed separately for each pairwise comparison. Because the *O. aries* genome contains less information than the *H. sapiens* genome, the latter was used as preferential database for functional analyses.

Gene lists of DAPs were used as input into the Database for Annotation, Visualisation and Integrated Discovery (DAVID version 2021) for Gene Ontology (GO) analysis. GO terms associated with over-represented biological processes ( $p < 0.05$ ) were considered significant. The Metascape Enrichment analysis tool was used to study the potential roles of DAPs (<https://metascape.org/>) [79]. The Kyoto Encyclopedia of Genes and Genomes (KEGG) pathways associated with 958 quantified proteins and DAPs from the pairwise comparisons were investigated using the Proteomaps software (<http://bionic-vis.biologie.uni-greifswald.de/>) [80]. For each comparison, proteomaps were created from the highest log<sub>10</sub> precursor intensity values of the overabundant DAPs in each pairwise comparison with a minimum FC  $\geq 2$  or  $\leq 0.5$ . For the proteins quantified, proteomaps were generated by using the highest value from the four groups (R0, R50, WF0 and WF50).

#### Abbreviations

APOA1	Apolipoprotein A1
BCS	Body condition score
BMI	Body mass index
BPA	Bisphenol A
BPS	Bisphenol S
BPS-g	BPS glucuronide
BMI	Body mass index
BSA	Bovine serum albumin
BW	Body weight
DAPs	Differentially abundant proteins
DEHP	Di(2-ethylhexyl) phthalate
FC	Fold-change
FDFT1	Farnesyl-diphosphate farnesyltransferase 1
FHIT	Bis(5'-adenosyl)-triphosphatase
GCs	Granulosa cells
GPX7	Glutathione peroxidase 7
GO	Gene Ontology
GUSB	$\beta$ -glucuronidase
LBP	Lipopolysaccharide-binding protein
LPS	Lipopolysaccharide
NCSTN	NF-kappa B signalling pathway; nicastrin
NDUFA7	NADH dehydrogenase 1 alpha subcomplex subunit 7
NEFA	Non-esterified fatty acids
NF- $\kappa$ B	Nuclear factor kappa-light-chain-enhancer of activated B cells
PBS	Phosphate-buffered saline
PCA	Principal component analysis
PFAS	Per- and polyfluoroalkyl substances
PFOA	Perfluorooctanesulfonic acid
PFOS	Perfluorooctane sulfonate
PMSG	Pregnant mare serum gonadotropin
PPAR $\gamma$	Peroxisome proliferator-activated receptor gamma
R	Restricted
RAB5B	Ras-related protein Rab-5B
RAB5C	Ras-related protein Rab-5 C
SQS	Squalene synthase
TPR	Translocated promoter region
TST	Thiosulfate sulfurtransferase
WF	Well-fed
XIC	Extracted ion chromatogram

#### Supplementary Information

The online version contains supplementary material available at <https://doi.org/10.1186/s12864-024-11034-2>.

Supplementary Material 1

Supplementary Material 2

Supplementary Material 3

Supplementary Material 4

#### Acknowledgements

Not applicable.

#### Author contributions

S.E. conceptualised the project, acquired and administrated the funding, S.E. and M.S.D. designed the methodology, and A.B. and S.E. supervised the work. O.T., O.L., A.D., S.U., P.P., D.T., V.L., V.M. and M.S.D. carried out the investigation, M-E.L.D.L.R., C.M., D.T. and V.L. were involved in data curation, and the formal analysis was made by M-E.L.D.L.R., D.T. and V.L. After the software exploitation by M-E.L.D.L.R., M-E.L.D.L.R., C.M., D.T., V.L. and M.S.D. proceeded to validation. M-E.L.D.L.R. and S.E. wrote the original draft; all the authors read, edited and approved the manuscript.

#### Funding

This research was financed by INRAE, “Centre Val de Loire” Region (BEMOL project, APR IR 2017-001 17108; PERFECT project, APR IR 2021-00144784), the French National Research Agency (MAMBO, project ANR-18-CE340011-01). The high-resolution mass spectrometer was financed (SMHART project, 35069) by the European Regional Development Fund (ERDF), the Conseil Régional du Centre, the French National Institute for Agricultural Research (INRAE) and the French National Institute of Health and Medical Research (Inserm).

#### Data availability

Proteomic mass spectrometry data were submitted to the ProteomeXchange Consortium via the PRIDE partner repository [70] with the identifier PXD047107.

#### Declarations

##### Ethical approval and consent to participate

All experimental procedures were conducted in accordance with the European Directive 2010/63/EU on the protection of animals used for scientific purposes and approved by the French Ministry of Nation Education, Higher Education, Research and Innovation after ethical assessment by the local ethics committee *Comité d’Ethique en Expérimentation Animale Val de Loire* (CEEA VdL) and INRAE consented to use the animals in this experimental protocol (protocols registered under APAFIS numbers 13965-2018042008519239v2 and 14014-2018030717477406v2).

##### Consent for publication

Not applicable.

##### Competing interests

The authors declare no competing interests.

##### Author details

<sup>1</sup>INRAE, CNRS, Université de Tours, PRC, Nouzilly 37380, France

<sup>2</sup>INRAE, PAO, Nouzilly 37380, France

<sup>3</sup>PIXANIM, INRAE, Université de Tours, CHU de Tours, Nouzilly 37380, France

<sup>4</sup>Service de Chirurgie Pédiatrique, CHU Poitiers, Poitiers, France

<sup>5</sup>CNRS UMR7267, Ecologie et biologie des interactions, Université de Poitiers, Poitiers 86000, France

Received: 24 May 2024 / Accepted: 12 November 2024

Published online: 16 November 2024

#### References

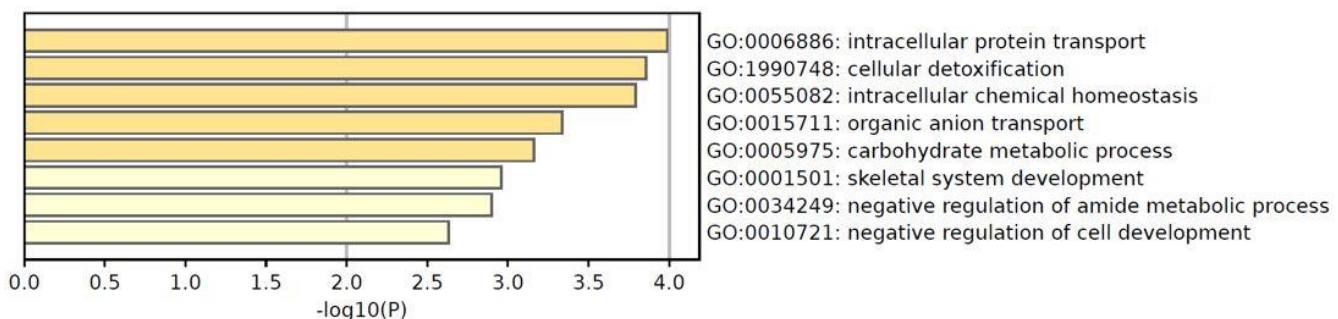
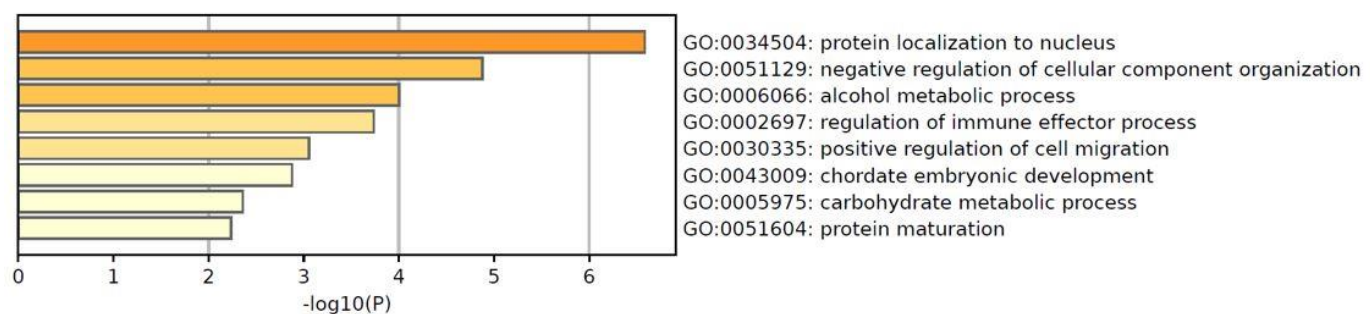
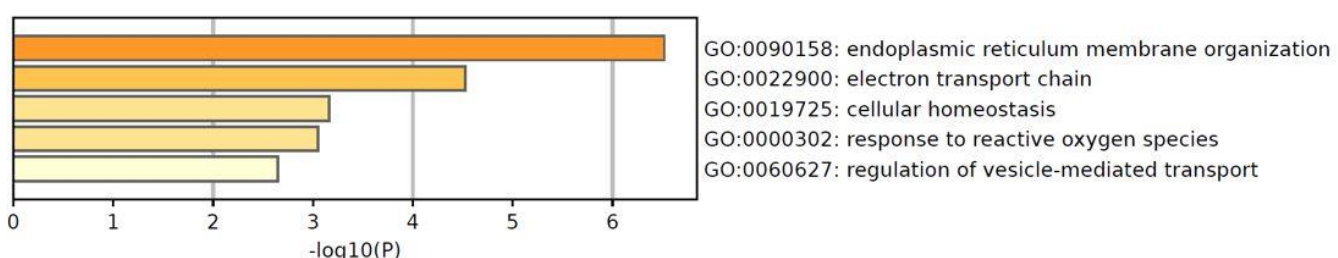
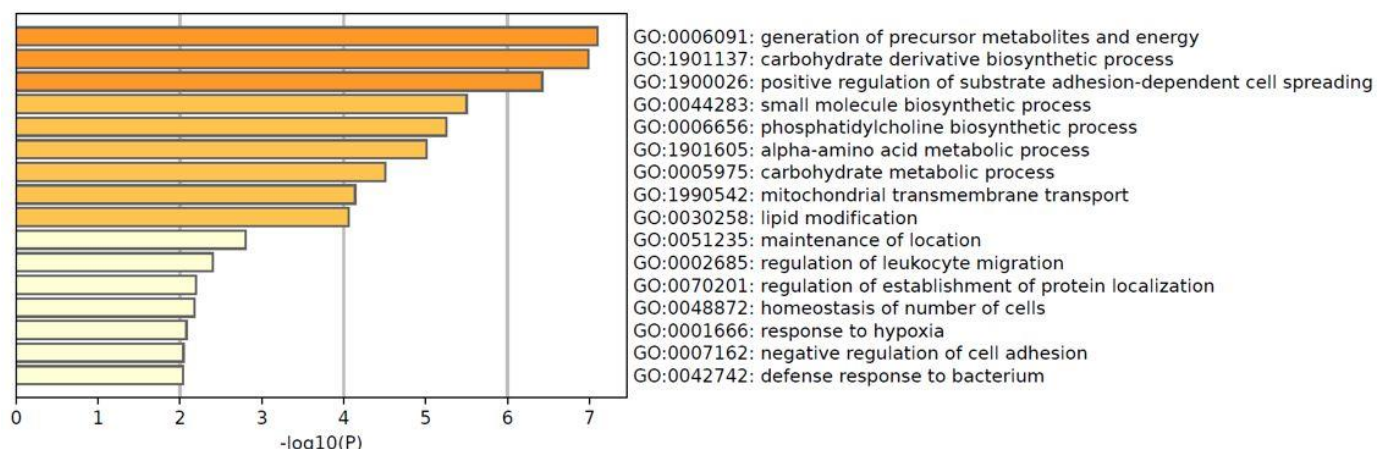
- Vandenberg LN, Hauser R, Marcus M, Olea N, Welshons WV. Human exposure to bisphenol A (BPA). *Reprod Toxicol*. 2007;24(2):139–77.

2. EFSA Panel on Food Contact Materials E, Flavourings, Aids P. Scientific opinion on the risks to public health related to the presence of bisphenol A (BPA) in foodstuffs. *EFSA J.* 2015;13(1):3978.
3. Kawa IA, Akbar M, Fatima Q, Mir SA, Jeelani H, Manzoor S, Rashid F. Endocrine disrupting chemical bisphenol A and its potential effects on female health. *Diabetes Metabolic Syndrome.* 2021;15(3):803–11.
4. Ma Y, Liu H, Wu J, Yuan L, Wang Y, Du X, Wang R, Marwa PW, Petlulu P, Chen X, et al. The adverse health effects of bisphenol A and related toxicity mechanisms. *Environ Res.* 2019;176:108575.
5. You HH, Song G. Review of endocrine disruptors on male and female reproductive systems. *Comp Biochem Physiol C Toxicol Pharmacol.* 2021;244:109002.
6. Skledar DG, Mašić LP. Bisphenol A and its analogs: do their metabolites have endocrine activity? *Environ Toxicol Pharmacol.* 2016;47:182–99.
7. Usman A, Ahmad M. From BPA to its analogues: is it a safe journey? *Chemosphere.* 2016;158:131–42.
8. Chen D, Kannan K, Tan H, Zheng Z, Feng Y-L, Wu Y, Widelka M. Bisphenol Analogues Other Than BPA: environmental occurrence, human exposure, and Toxicity—A review. *Environ Sci Technol.* 2016;50(11):5438–53.
9. Zhan W, Tang W, Shen X, Xu H, Zhang J. Exposure to bisphenol A and its analogs and polycystic ovarian syndrome in women of childbearing age: a multicenter case-control study. *Chemosphere.* 2023;313:137463.
10. Amar S, Binet A, Teteau O, Desmarchais A, Papillier P, Lacroix MZ, Maillard V, Guérif F, Elis S. Bisphenol S impaired human granulosa cell steroidogenesis in Vitro. *Int J Mol Sci.* 2020;21(5):1821.
11. de la Lebachelier ME, Wu L, Gayet M, Bousquet M, Buron C, Vignault C, Téteau O, Desmarchais A, Maillard V, Uzbekova S, et al. Cumulative and potential synergistic effects of seven different bisphenols on human granulosa cells in vitro? *Environ Pollut.* 2023;330:121818.
12. Paoli D, Pallotti F, Dima AP, Albani E, Alviggi C, Causio F, Dioguardi CC, Conforti A, Ciriminna R, Fabozzi G, et al. Phthalates and Bisphenol A: Presence in Blood serum and follicular fluid of Italian women undergoing assisted Reproduction techniques. *Toxics.* 2020; 8(4).
13. Gao C, He H, Qiu W, Zheng Y, Chen Y, Hu S, Zhao X. Oxidative stress, endocrine disturbance, and Immune Interference in humans showed relationships to serum bisphenol concentrations in a dense Industrial Area. *Environ Sci Technol.* 2021;55(3):1953–63.
14. Machtinger R, Orvieto R. Bisphenol A, oocyte maturation, implantation, and IVF outcome: review of animal and human data. *Reprod Biomed Online.* 2014;29(4):404–10.
15. Lloyd V, Morse M, Purakal B, Parker J, Benard P, Crone M, Pfiffner S, Szmyd M, Dinda S. Hormone-like effects of Bisphenol A on p53 and estrogen receptor alpha in breast Cancer cells. *BioResearch open Access.* 2019;8(1):169–84.
16. Rochester JR, Bolden AL. Bisphenol S and F: a systematic review and comparison of the hormonal activity of Bisphenol A substitutes. *Environ Health Perspect.* 2015;123(7):643–50.
17. Pelch KE, Li Y, Perera L, Thayer KA, Korach KS. Characterization of estrogenic and androgenic activities for Bisphenol A-like Chemicals (BPs): in Vitro Estrogen and Androgen receptors Transcriptional activation, Gene Regulation, and binding profiles. *Toxicol Sci.* 2019;172(1):23–37.
18. Monniaux D, Cadoret V, Clément F, Dalbies-Tran R, Elis S, Fabre S, Maillard V, Monget P, Uzbekova S. Folliculogenesis. In: Encyclopedia of Endocrine Diseases (Second Edition). Edited by Huhtaniemi I, Martini L. Oxford: Academic Press; 2019: 377–398.
19. Campen KA, Lavallée M, Combelles C. The impact of bisphenol S on bovine granulosa and theca cells. *Reprod Domest Anim.* 2018;53(2):450–7.
20. Berni M, Gigante P, Bussolati S, Grasselli F, Grolli S, Ramoni R, Basini G, Bisphenol S. A Bisphenol A alternative, impairs swine ovarian and adipose cell functions. *Domest Anim Endocrinol.* 2019;66:48–56.
21. Bujnakova Mlynarcikova A, Scsukova S. Bisphenol analogs AF, S and F: effects on functional characteristics of porcine granulosa cells. *Reprod Toxicol.* 2021;103:18–27.
22. Teteau O, Jaubert M, Desmarchais A, Papillier P, Binet A, Maillard V, Elis S. Bisphenol A and S Impaired ovine granulosa cell steroidogenesis. *Reproduction.* 2020;159(5):571–83.
23. Thoene M, Dziká E, Gonkowski S, Wojtkiewicz J. Bisphenol S in food causes hormonal and obesogenic effects comparable to or worse than bisphenol A: a literature review. *Nutrients.* 2020; 12(2).
24. Fontana R, Torre S. The deep correlation between Energy Metabolism and Reproduction: a view on the effects of Nutrition for women Fertility. *Nutrients.* 2016;8(2):87.
25. Seli E, Babayev E, Collins SC, Nemeth G, Horvath TL. Minireview: metabolism of female reproduction: regulatory mechanisms and clinical implications. *Mol Endocrinol.* 2014;28(6):790–804.
26. Sharma Y, Galvão AM. Maternal obesity and ovarian failure: is leptin the culprit? *Anim Reprod.* 2022;19(4):e20230007.
27. Talmor A, Dunphy B. Female obesity and infertility. *Best Pract Res Clin Obstet Gynaecol.* 2015;29(4):498–506.
28. Carwile JL, Michels KB. Urinary bisphenol A and obesity: NHANES 2003–2006. *Environ Res.* 2011;111(6):825–30.
29. Wells EM, Jackson LW, Koontz MB. Association between bisphenol A and waist-to-height ratio among children: National Health and Nutrition Examination Survey, 2003–2010. *Ann Epidemiol.* 2014;24(2):165–7.
30. Martínez M, Blanco J, Rovira J, Kumar V, Domingo JL, Schuhmacher M, Bisphenol A. Analogue (BPS and BPF) present a greater obesogenic capacity in 3T3-L1 cell line. *Food Chem Toxicol.* 2020;140:111298.
31. Tyner MDW, Maloney MO, Kelley BJ, Combelle CMH. Comparing the effects of bisphenol A, C, and F on bovine theca cells in vitro. *Reprod Toxicol.* 2022;111:27–33.
32. Samardzija D, Pogrmic-Majkic K, Fa S, Stanic B, Jasnic J, Andric N. Bisphenol A decreases progesterone synthesis by disrupting cholesterol homeostasis in rat granulosa cells. *Mol Cell Endocrinol.* 2018;461:55–63.
33. Desmarchais A, Téteau O, Papillier P, Jaubert M, Druart X, Binet A, Maillard V, Elis S. Bisphenol S impaired in vitro ovine early developmental oocyte competence. *Int J Mol Sci.* 2020;21(4):1238.
34. Téteau O, Liere P, Pianos A, Desmarchais A, Lasserre O, Papillier P, Vignault C, Lebachelier de la Rivière M-E, Maillard V, Binet A, et al. Bisphenol S alters the Steroidome in the Preovulatory follicle, Oviduct Fluid and plasma in Ewes with contrasted metabolic status. *Front Endocrinol.* 2022;13:892213.
35. Desmarchais A, Téteau O, Kasal-Hoc N, Cognié J, Lasserre O, Papillier P, Lacroix M, Vignault C, Jarrier-Gaillard P, Maillard V, et al. Chronic low BPS exposure through diet impairs in vitro embryo production parameters according to metabolic status in the ewe. *Ecotoxicol Environ Saf.* 2022;229:113096.
36. Mahé C, de la Lebachelier ME, Lasserre O, Tsikis G, Tomas D, Labas V, Elis S, Saint-Dizier M. Oral exposure to bisphenol S is associated with alterations in the oviduct proteome of an ovine model, with aggravated effects in overfed females. *BMC Genomics.* 2024;25(1):589.
37. Huang R, Li J, Liao M, Ma L, Laurent I, Lin X, Zhang Y, Gao R, Ding Y, Xiao X. Combinational exposure to Bisphenol A and a high-fat diet causes trans-generational malfunction of the female reproductive system in mice. *Mol Cell Endocrinol.* 2022;541:111507.
38. Tarapore P, Hennessy M, Song D, Ying J, Ouyang B, Govindarajah V, Leung YK, Ho SM. High butter-fat diet and bisphenol A additively impair male rat spermatogenesis. *Reprod Toxicol.* 2017;68:191–9.
39. Kannan A, Davila J, Gao L, Rattan S, Flaws JA, Bagchi MK, Bagchi IC. Maternal high-fat diet during pregnancy with concurrent phthalate exposure leads to abnormal placentation. *Sci Rep.* 2021;11(1):16602.
40. Zhang Y, Zhou L, Zhang Z, Xu Q, Han X, Zhao Y, Song X, Zhao T, Ye L. Effects of Di (2-ethylhexyl) phthalate and high-fat diet on lipid metabolism in rats by JAK2/STAT5. *Environ Sci Pollut Res.* 2020;27(4):3837–48.
41. Marques ES, Agudelo J, Kaye EM, Modaresi SMS, Pfohl M, Bečanová J, Wei W, Polunas M, Goedken M, Slitt AL. The role of maternal high fat diet on mouse pup metabolic endpoints following perinatal PFAS and PFAS mixture exposure. *Toxicology.* 2021;462:152921.
42. Curtiss LK, Valenta DT, Hime NJ, Rye K-A. What is so special about apolipoprotein AI in Reverse Cholesterol Transport? *Arterioscler Thromb Vasc Biol.* 2006;26(1):12–9.
43. Roberts LM, Buford TW. Lipopolysaccharide binding protein is associated with CVD risk in older adults. *Aging Clin Exp Res.* 2021;33(6):1651–8.
44. Meng L, Song Z, Liu A, Dahmen U, Yang X, Fang H. Effects of Lipopolysaccharide-binding protein (LBP) single nucleotide polymorphism (SNP) in infections, inflammatory diseases, metabolic disorders and cancers. *Front Immunol.* 2021;12:681810.
45. Morris G, Puri BK, Bortolasci CC, Carvalho A, Berk M, Walder K, Moreira EG, Maes M. The role of high-density lipoprotein cholesterol, apolipoprotein A and paraoxonase-1 in the pathophysiology of neuroprogressive disorders. *Neurosci Biobehav Rev.* 2021;125:244–63.
46. Aune SK, Helseth R, Kalstad AA, Laake K, Åkra S, Arnesen H, Solheim S, Seljeflot I. Links between adipose tissue gene expression of gut leakage markers, circulating levels, Anthropometrics, and Diet in patients with coronary artery disease. *Diabetes Metabolic Syndrome Obesity: Targets Therapy.* 2024;17:2177–90.

47. Jarvis S, Gethings LA, Samanta L, Pedroni SMA, Withers DJ, Gray N, Plumb RS, Winston RML, Williamson C, Bevan CL. High fat diet causes distinct aberrations in the testicular proteome. *Int J Obes (Lond)*. 2020;44(9):1958–69.
48. Ghanim H, Abuaysheh S, Sia CL, Korzeniewski K, Chaudhuri A, Fernandez-Real JM, Dandona P. Increase in plasma endotoxin concentrations and the expression of toll-like receptors and suppressor of cytokine signaling-3 in mononuclear cells after a high-fat, high-carbohydrate meal: implications for insulin resistance. *Diabetes Care*. 2009;32(12):2281–7.
49. Meng Y, Yannan Z, Ren L, Qi S, Wei W, Lihong J. Adverse reproductive function induced by maternal BPA exposure is associated with abnormal autophagy and activating inflammation via mTOR/TLR4/NF- $\kappa$ B signaling pathways in female offspring rats. *Reprod Toxicol*. 2020;96:185–94.
50. Morishima A, Ohkubo N, Maeda N, Miki T, Mitsuda N. NF $\kappa$ B regulates plasma apolipoprotein A-I and High Density Lipoprotein Cholesterol through inhibition of peroxisome proliferator-activated receptor  $\alpha^*$ . *J Biol Chem*. 2003;278(40):38188–93.
51. Pal S, Sahu A, Verma R, Haldar C. BPS-induced ovarian dysfunction: protective actions of melatonin via modulation of SIRT-1/Nrf2/NF $\kappa$ B and IR/PI3K/pAkt/GLUT-4 expressions in adult golden hamster. *J Pineal Res*. 2023;75(1):e12869.
52. Trusca VG, Dumitrescu M, Fenyo IM, Tudorache IF, Simionescu M, Gafencu AV. The mechanism of Bisphenol A Atherogenicity involves an apolipoprotein A-I downregulation through NF- $\kappa$ B activation. *Int J Mol Sci*. 2019;20(24):6281.
53. Tachmazidou I, Süveges D, Min JL, Ritchie GRS, Steinberg J, Walter K, Iotchkova V, Schwartzentruber J, Huang J, Memari Y, et al. Whole-genome sequencing coupled to Imputation Discovers Genetic Signals for anthropometric traits. *Am J Hum Genet*. 2017;100(6):865–84.
54. Warner ET, Jiang L, Adeji DN, Turman C, Gordon W, Wang L, Tamimi R, Kraft P, Lindström S. A Genome-Wide Association Study of Childhood Body Fatness. *Obes (Silver Spring)*. 2021;29(2):446–53.
55. Tansey TR, Shechter I. Structure and regulation of mammalian squalene synthase. *Biochim Biophys Acta*. 2000;1529(1–3):49–62.
56. Alharbi HF, Algonaiman R, Alduwayghiri R, Aljutaily T, Algheshairy RM, Almutairi AS, Alharbi RM, Alfurayh LA, Alshahwan AA, Alsadun AF, et al. Exposure to Bisphenol A substitutes, Bisphenol S and Bisphenol F, and its Association with developing obesity and diabetes Mellitus: a narrative review. *Int J Environ Res Public Health*. 2022, 19(23).
57. Boucher JG, Ahmed S, Atlas E. Bisphenol S induces adipogenesis in primary human preadipocytes from female donors. *Endocrinology*. 2016;157(4):1397–407.
58. Song Ba Y, Wang Ma F, Wei Ma Y, Chen Ba D, Deng Ba G. ATP5A1 participates in Transcriptional and Posttranscriptional Regulation of Cancer-Associated genes by modulating their expression and alternative splicing profiles in HeLa cells. *Technol Cancer Res Treat*. 2021;20:15330338211039126.
59. Maniam S, Coutts AS, Stratford MR, McGouran J, Kessler B, La Thangue NB. Cofactor strap regulates oxidative phosphorylation and mitochondrial p53 activity through ATP synthase. *Cell Death Differ*. 2015;22(1):156–63.
60. Hou S, Hao Q, Zhu Z, Xu D, Liu W, Lyu L, Li P. Unraveling proteome changes and potential regulatory proteins of bovine follicular granulosa cells by mass spectrometry and multi-omics analysis. *Proteome Sci*. 2019;17:4.
61. Elis S, Desmarchais A, Maillard V, Uzbekova S, Monget P, Dupont J. Cell proliferation and progesterone synthesis depend on lipid metabolism in bovine granulosa cells. *Theriogenology*. 2015;83(5):840–53.
62. McEvoy TG, Coull GD, Broadbent PJ, Hutchinson JS, Speake BK. Fatty acid composition of lipids in immature cattle, pig and sheep oocytes with intact zona pellucida. *J Reprod Fertil*. 2000;118(1):163–70.
63. Xue Y, Guo C, Hu F, Zhu W, Mao S. Undernutrition-induced lipid metabolism disorder triggers oxidative stress in maternal and fetal livers using a model of pregnant sheep. *FASEB J*. 2020;34(5):6508–20.
64. Mandrah K, Jain V, Ansari JA, Roy SK. Metabolomic perturbation precedes glycolytic dysfunction and procreates hyperglycemia in a rat model due to bisphenol S exposure. *Environ Toxicol Pharmacol*. 2020;77:103372.
65. Paigen K. Mammalian beta-glucuronidase: genetics, molecular biology, and cell biology. *Prog Nucleic Acid Res Mol Biol*. 1989;37:155–205.
66. Edlow AG, Chen M, Smith NA, Lu C, McElrath TF. Fetal bisphenol A exposure: concentration of conjugated and unconjugated bisphenol A in amniotic fluid in the second and third trimesters. *Reprod Toxicol*. 2012;34(1):1–7.
67. Skledar DG, Schmidt J, Fic A, Klopčič I, Trontelj J, Dolenc MS, Finel M, Mašič LP. Influence of metabolism on endocrine activities of bisphenol S. *Chemosphere*. 2016;157:152–9.
68. Pellerin É, Pellerin FA, Chabaud S, Pouliot F, Pelletier M, Bolduc S. Glucuronidated metabolites of Bisphenols A and S alter the properties of normal urothelial and bladder Cancer cells. *Int J Mol Sci* 2022, 23(21).
69. Peillix C, Kerever A, Lachhab A, Pelletier M. Bisphenol A, bisphenol S and their glucuronidated metabolites modulate glycolysis and functional responses of human neutrophils. *Environ Res*. 2021;196:110336.
70. Maruti SS, Li L, Chang JL, Prunty J, Schwarz Y, Li SS, King IB, Potter JD, Lampe JW. Dietary and demographic correlates of serum beta-glucuronidase activity. *Nutr Cancer*. 2010;62(2):208–19.
71. Gratz M, Kunert-Keil C, John U, Cascorbi I, Kroemer HK. Identification and functional analysis of genetic variants of the human  $\beta$ -glucuronidase in a German population sample. *Pharmacogen Genomics* 2005, 15(12).
72. Lombardo A, Bairati C, Goi G, Roggi C, Maccarini L, Bollini D, Burlina A. Plasma lysosomal glycohydrolases in a general population. *Clin Chim Acta*. 1996;247(1–2):39–49.
73. Funk JL, Wertheim BC, Frye JB, Blew RM, Nicholas JS, Chen Z, Bea JW. Association of  $\beta$ -glucuronidase activity with menopausal status, ethnicity, adiposity, and inflammation in women. *Menopause*. 2023;30(2):186–92.
74. Russel AJF, Doney JM, Gunn RG. Subjective assessment of body fat in live sheep. *J Agricultural Sci*. 1969;72(3):451–4.
75. Agabriel J. INRA Alimentation Des Bovines, Ovins et Caprins: Besoins Des Animaux – Valeurs Des Aliments. Tables INRA 2007, mise à jour 2010. Versailles, France: éditions Quae; 2013.
76. Labas V, Grasseau I, Cahier K, Gargaros A, Haricha G, Teixeira-Gomes A-P, Alves S, Bourin M, Gérard N, Blesbois E. Qualitative and quantitative peptidomic and proteomic approaches to phenotyping chicken semen. *J Proteom*. 2015;112:313–35.
77. Harris L, Fondrie WE, Oh S, Noble WS. Evaluating proteomics imputation methods with improved criteria. *bioRxiv* 2023:2023.2004.2007.535980.
78. Bardou P, Mariette J, Escudié F, Djemiel C, Klopp C. Jvenn: an interactive Venn diagram viewer. *BMC Bioinformatics*. 2014;15(1):293.
79. Zhou Y, Zhou B, Pache L, Chang M, Khodabakhshi AH, Tanaseichuk O, Benner C, Chanda SK. Metascape provides a biologist-oriented resource for the analysis of systems-level datasets. *Nat Commun*. 2019;10(1):1523.
80. Liebermeister W, Noor E, Flamholz A, Davidi D, Bernhardt J, Milo R. Visual account of protein investment in cellular functions. *Proc Natl Acad Sci U S A*. 2014;111(23):8488–93.

## Publisher's note

Springer Nature remains neutral with regard to jurisdictional claims in published maps and institutional affiliations.

**A** Functional enrichment analysis of differential proteins between R0 and R50**B** Functional enrichment analysis of differential proteins between WF0 and WF50**C** Functional enrichment analysis of differential proteins between R0 and WF0**D** Functional enrichment analysis of differential proteins between R50 and WF50

**Figure S1:** Functional enrichment analysis of differential proteins in ovine GCs between R0 and R50 (A), WF0 and WF50 (B), R0 and WF0 (C) and R50 and WF50 (D), performed using Metascape. (A) Bar graph of enriched biological processes in which GCs differential proteins in diet-restricted ewes, exposed or not to BPS, are involved. (B) Bar graph of enriched biological processes in which GCs differential proteins in well-fed ewes, exposed or not to BPS, are involved. (C) Bar graph of enriched biological processes in which GCs differential proteins in ewes not exposed to BPS with or without a restricted diet are involved. (D) Bar graph of enriched biological processes in which GCs differential proteins in ewes exposed to BPS with or without a restricted diet are involved.

Table S1

List of identified proteins in Granulosa Cell of Restricted (R) and Well-fed (WF) ewes exposed (50) or not (0) to bisphenol S

Protein Name	Species	Accession Number	Gene Name	Molecular Weight	Test	p-Value (ANOVA or Chi-square)	in R0 (detection rate %)	in R50 (detection rate %)	in WFO (detection rate %)	in WF50 (detection rate %)
aflatoxin B1 aldehyde reductase member 2	Ovis aries	XP_027821430.1	AKR7A2	41 kDa	Chi-square	0.007	6.76 (25%)	7.03 (100%)	N.D. (0%)	7.21 (100%)
cadherin-6 isoform X2	Bos taurus	XP_024837107.1	CDH6	80 kDa	Chi-square	0.012	N.D. (0%)	7.55 (25%)	7.43 (25%)	7.75 (75%)
dermcidin isoform 1 preprotein	Homo sapiens	NP_444513.1	DDC	11 kDa	Chi-square	0.046	5.47 (50%)	N.D. (0%)	5.94 (25%)	6.41 (75%)
squalene synthase isoform X2	Ovis aries	XP_000404500.1	FDFT1	48 kDa	Chi-square	0.012	6.56 (25%)	6.63 (100%)	N.D. (0%)	6.59 (50%)
bis(5'-adenosyl)-triphosphatase isoform X1	Ovis aries	XP_011954617.2	FHIT	17 kDa	Chi-square	0.012	N.D. (0%)	6.5 (50%)	5.76 (25%)	7.3 (100%)
beta-glucuronidase	Ovis aries	XP_027817734.1	GUSB	74 kDa	Chi-square	0.002	N.D. (0%)	6.88 (100%)	6.18 (50%)	6.6 (100%)
inactive hydroxysteroid dehydrogenase-like protein 1	Bos taurus	NP_001092341.1	HSOL1	37 kDa	Chi-square	0.003	6.17 (75%)	6.21 (100%)	N.D. (0%)	6.76 (75%)
complement factor H-related protein 2	Ovis aries	XP_004013976.1	LOC101123223	31 kDa	Chi-square	0.028	6.45 (50%)	N.D. (0%)	6.05 (25%)	7.15 (75%)
sulfhydryl oxidase 2 isoform X1	Capra hircus	XP_019115731.3	LOC101285934	87 kDa	Chi-square	0.003	N.D. (0%)	7.21 (75%)	6.25 (25%)	6.34 (100%)
SLC35A4 upstream open reading frame protein	Bubalus bubalis	XP_025148374.1	LOC112568698	11 kDa	Chi-square	0.012	5.41 (25%)	6.44 (75%)	N.D. (0%)	6.76 (75%)
nicastrin isoform X2	Ovis aries	XP_01039753.2	NCSTN	67 kDa	Chi-square	0.028	6.58 (50%)	6.8 (75%)	6.68 (75%)	N.D. (0%)
prolyl 4-hydroxylase subunit alpha-2 isoform X1	Ovis aries	XP_004006868.2	P4HA2	61 kDa	Chi-square	0.005	7.09 (75%)	6.8 (100%)	N.D. (0%)	N.D. (0%)
reticulon-4 isoform X1	Capra hircus	XP_017910740.1	RTNA	130 kDa	Chi-square	0.028	N.D. (0%)	7.14 (75%)	7.05 (75%)	6.16 (50%)
splicing factor 3B subunit 5	Bos taurus	NP_001020521.1	SF3B5	10 kDa	Chi-square	0.028	N.D. (0%)	6.56 (75%)	6.62 (75%)	6.57 (75%)
transportin-2 isoform X4	Ovis aries	XP_027825368.1	TNP02	103 kDa	Chi-square	0.003	6.32 (25%)	6.44 (75%)	N.D. (0%)	6.82 (100%)
nucleoprotein TPR	Capra hircus	XP_005691036.2	TPR	275 kDa	Chi-square	0.012	6.39 (25%)	6.87 (75%)	N.D. (0%)	6.02 (75%)
thiosulfate sulfurtransferase	Ovis aries	XP_014950344.2	TST	33 kDa	Chi-square	0.003	6.69 (75%)	6.91 (100%)	5.87 (25%)	N.D. (0%)
vesicle-associated membrane protein-associated protein B/C	Capra hircus	XP_017913111.1	VAPB	27 kDa	ANOVA	0.00037	6.54	7.36	7.38	7.52
lipopolysaccharide-binding protein	Ovis aries	XP_004014615.1	LBP	53 kDa	ANOVA	0.0012	7.28	7.9	7.14	6.69
apolipoprotein A-I	Ovis aries	XP_011950887.2	APOA1	30 kDa	ANOVA	0.0019	9.1	9.11	9.13	9.53
transthyretin precursor	Ovis aries	NP_001009800.1	TTR	16 kDa	ANOVA	0.0028	8.27	8.44	8.39	8.8
pre-B cell leukemia transcription factor-interacting protein 1 isoform X1	Ovis aries	XP_027831619.1	PBX1P1	90 kDa	ANOVA	0.0056	6.24	6.74	7.13	7.13
ITH2, partial	Cervus elaphus hippelaphus	OWK03472.1	-	103 kDa	ANOVA	0.0057	7.15	7.31	7.9	7.88
long-chain fatty acid transport protein 1	Ovis aries	XP_027825247.1	SLC27A1	71 kDa	ANOVA	0.0066	6.6	7.16	6.59	6.52
ras-related protein Rab-5C	Bos taurus	NP_001029915.1	RAB5C	23 kDa	ANOVA	0.0076	6.42	6.89	6.99	6.99
complement C1q subcomponent subunit C	Ovis aries	XP_027820684.1	C1QC	94 kDa	ANOVA	0.0085	Missing Value	7.26	7.21	6.94
vitronectin isoform X1	Ovis aries	XP_027831040.1	VTN	54 kDa	ANOVA	0.011	7.92	8.17	8.06	8.22
vitronectin	Capra hircus	XP_005693309.1	VTN	54 kDa	ANOVA	0.011	7.91	8.15	8.05	8.17
TPA: inter-alpha globulin inhibitor H2 polypeptide	Bos taurus	DA2A3635.1	ITH2	106 kDa	ANOVA	0.011	7.48	7.58	8.08	8.05
ras-related protein Rab-5A isoform X1	Ovis aries	XP_019470708.1	RAB5A	24 kDa	ANOVA	0.012	6.37	6.71	6.87	6.81
ras-related protein Rab-5B	Bos taurus	NP_001193120.1	RAB5B	24 kDa	ANOVA	0.017	6.37	6.71	6.86	6.88
glutamine amidotransferase-like class 1 domain-containing protein 3A, mitochondrial	Ovis aries	NP_001156032.1	GATD3	29 kDa	ANOVA	0.017	6.27	6.82	6.75	6.91
palmitoyl-protein thioesterase 1	Ovis aries	XP_004001885.2	PPT1	34 kDa	ANOVA	0.018	6.46	6.95	6.9	6.8
receptor expression-enhancing protein 5	Ovis aries	XP_014952182.2	REEPS	21 kDa	ANOVA	0.019	6.2	6.97	6.99	7.19
inter-alpha-trypsin inhibitor heavy chain H2	Ovis aries	XP_004014227.2	ITH2	106 kDa	ANOVA	0.020	7.58	7.61	8.18	8.1
tetranectin precursor	Bos taurus	NP_001039677.1	CLEC3B	22 kDa	ANOVA	0.022	7.07	7.13	6.97	7.47
immunoglobulin heavy chain variable region, partial	Ovis aries	CA045049.1	CD40	12 kDa	ANOVA	0.022	7.35	7.64	7.36	6.92
glucosidase 2 subunit beta	Ovis aries	XP_027825495.1	PRKCSH	60 kDa	ANOVA	0.023	7.22	7.94	7.91	7.53
zona pellucida sperm-binding protein 4	Ovis aries	XP_027818021.1	ZP4	59 kDa	ANOVA	0.025	6.72	7.08	7.07	Missing Value
protein ERGIC-53 isoform X1	Ovis aries	XP_014952852.8	LMAN1	58 kDa	ANOVA	0.025	6.51	7.36	7.04	6.54
GDP-fucose protein O-fucosyltransferase 2 isoform X1	Ovis aries	XP_027816944.1	POFUT2	50 kDa	ANOVA	0.030	7.06	7.49	6.97	6.94
non-specific lipid-transfer protein isoform X2	Bos indicus	XP_027393023.1	SCP2	52 kDa	ANOVA	0.030	5.85	6.53	6.69	6.94
histidine-rich glycoprotein	Capra hircus	XP_004005109.3	HRG	62 kDa	ANOVA	0.031	7.45	7.7	7.12	7.63
protein AMBP isoform X2	Ovis aries	XP_027827301.1	IGGCC1	134 kDa	ANOVA	0.034	Missing Value	6.58	6.25	6.51
immunoglobulin superfamily DCC subclass member 4	Bos indicus	XP_019812000.1	LOC105555509	10 kDa	ANOVA	0.037	6.41	6.84	6.83	6.85
dynein light chain 1, cytoplasmic-like	Ovis aries	XP_004008614.1	NDUFAT7	13 kDa	ANOVA	0.037	5.49	6.16	6.19	6.59
NADH dehydrogenase 1 alpha subcomplex subunit 7	Ovis aries	XP_004003109.3	NDUFB1	16 kDa	ANOVA	0.038	6.82	7.51	7.5	7.36
NADPH-cytochrome P450 reductase isoform X1	Ovis aries	XP_027827072.1	LRPAP1	42 kDa	ANOVA	0.047	6.68	7.09	7.34	7.19
electron transfer flavoprotein subunit beta isoform X2	Bos taurus	NP_00103222.1	VTN	54 kDa	ANOVA	0.046	7.1	7.92	7.72	7.8
electron transfer flavoprotein subunit beta isoform X1	Ovis aries	XP_027827072.1	VTN	54 kDa	ANOVA	0.046	7.1	7.92	7.72	7.8
complement component C7	Ovis aries	XP_001098591.1	RAB8A	24 kDa	ANOVA	0.041	7.05	7.33	7.52	7.68
Ig m chain C region membrane-bound form, partial	Ovis aries	XP_004018030.1	GLRX5	17 kDa	ANOVA	0.046	6.54	7.05	6.95	7.25
ras-related protein Rab-8A	Ovis aries	XP_001098591.1	RAB8A	24 kDa	ANOVA	0.046	7.18	7.53	7.77	7.78
glutaredoxin-related protein 5, mitochondrial	Ovis aries	XP_027820593.1	ETFB	28 kDa	ANOVA	0.038	7.21	7.7	7.73	7.78
vitronectin precursor	Ovis aries	XP_004015435.1	ETFB	28 kDa	ANOVA	0.038	7.21	7.7	7.73	7.78
alpha-2-macroglobulin receptor-associated protein isoform X2	Ovis aries	XP_004017066.2	C7	93 kDa	ANOVA	0.039	7.65	7.78	7.31	7.55
40S ribosomal protein S16 isoform 1	Bos taurus	XP_02781309.1	LOC105555509	10 kDa	ANOVA	0.037	6.41	6.84	6.83	6.85
microsomal glutathione S-transferase 1	Ovis aries	XP_004006861.1	MGST1	18 kDa	ANOVA	0.049	5.58	6.71	6.57	7.04
C4b-binding protein alpha chain isoform X1	Ovis aries	XP_012042362.6	LOC101119740	69 kDa	ANOVA	0.050	7.86	7.9	7.6	7.44
hem oxygenase 2	Ovis aries	XP_027817868.1	HMOX2	38 kDa	ANOVA	0.051	6.54	6	6.86	6.95
mannose-P dolichol utilization defect 1 protein	Ovis aries	XP_004021724.1	MPDU1	27 kDa	ANOVA	0.051	6.4	6.87	6.97	7.27
endothelin-converting enzyme 1 isoform X1	Ovis aries	XP_004018030.1	ECE1	91 kDa	ANOVA	0.054	5.78	7.09	7.44	6.75
histone H1.3	Ovis aries	XP_011956523.2	LOC101110397	22 kDa	ANOVA	0.054	8.7	9.21	9.35	9.18
histone H1.2	Ovis aries	XP_004019136.2	H1-2	21 kDa	ANOVA	0.056	8.72	9.25	9.36	9.2
histone H1.5	Camelus dromedarius	XP_010973014.2	H1-5	23 kDa	ANOVA	0.058	8.51	9.14	9.18	9.08
peroxisomal bifunctional enzyme	Ovis aries	XP_027813339.1	EHHADH	80 kDa	ANOVA	0.059	6.58	6.95	6.61	5.97
matrix Gla protein	Homo sapiens	NP_0010111	RPS16	16 kDa	ANOVA	0.047	7.18	7.4	7.53	7.77
alpha-N-acetylgalactosaminidase	Ovis aries	XP_004006862.1	MGST1	18 kDa	ANOVA	0.067	8.44	8.49	8.25	8.33
zona pellucida sperm-binding protein 3	Ovis aries	XP_004008513.1	ILVBL	68 kDa	ANOVA	0.068	6.13	7.25	6.17	6.42
complement component C8 alpha chain	Ovis aries	XP_027819102.1	DHRSX	37 kDa	ANOVA	0.070	6.03	6.56	6.5	6.67
complement component C4A-like	Ovis aries	XP_004017112.2	AMACR	42 kDa	ANOVA	0.082	7.59	8.07	8.09	8.27
acetolactate synthase-like protein	Ovis aries	XP_004012714.1	MPDU1	42 kDa	ANOVA	0.084	6.68	7.38	6.89	6.53
dehydrogenase/reductase SDR family member on chromosome X	Ovis aries	XP_004018511.2	GPX1	23 kDa	ANOVA	0.075	Missing Value	6.48	6.41	6.11
lamin	Capra hircus	XP_017896889.1	GPX1	21 kDa	ANOVA	0.076	6.24	7.37	7.13	7.12
glutathione peroxidase 1	Ovis aries	XP_027820957.1	FN1	249 kDa	ANOVA	0.078	9.41	9.86	9.47	9.16
glutathione peroxidase 7	Ovis aries	NP_001159672.1	PRDX2	22 kDa	ANOVA	0.079	7.52	7.49	7.96	7.97
peroxiredoxin-2	Ovis aries	XP_027823406.1	ESYT1	125 kDa	ANOVA	0.082	Missing Value	6.55	6.45	6.51
extended syntaptotagmin-1 isoform X1	Ovis aries	XP_004017112.2	AMACR	42 kDa	ANOVA	0.082	7.59	8.07	8.09	8.27
alpha-methylacyl-CoA racemase	Ovis aries	XP_01494207.1	HP1BP1	61 kDa	ANOVA	0.084	6.68	7.38	6.89	6.53
heterochromatin protein 1-binding protein 3 isoform X1	Ovis aries	XP_017915670.1	MIA3	211 kDa	ANOVA	0.088	6.34	6.97	6.53	6.67
melanoma inhibitory activity protein 3 isoform X1	Bos taurus	P07584.0	FN1	272 kDa	ANOVA	0.088	9.37	9.83	9.44	9.14
Fibronectin	Ovis aries	XP_014951776.2	SCARB2	54 kDa	ANOVA	0.091	7.14	7.55	7.38	6.93
lysosome membrane protein 2	Ovis aries	XP_027823737.5	NPTN	43 kDa	ANOVA	0.094	Missing Value	6.61	6.68	6.42
neuroplastin, partial	Bos mutus	XP_014332763.1	RPL22	15 kDa	ANOVA	0.094	7.16	7.42	7.34	7.64
60S ribosomal protein L22 isoform X2	Ovis aries	XP_027821348.1	HSPG2	469 kDa	ANOVA	0.095	7.6	8.19	7.6	7.54
basement membrane-specific heparan sulfate proteoglycan core protein	Ovis aries	XP_004004415.2	ERMP1	100 kDa	ANOVA	0.096	Missing Value	6.45	6.12	6.04
endoplasmic reticulum metallopeptidase 1	Ovis aries	XP_014958092.2	LOC101102019	15 kDa	ANOVA	0.099	8.82	9.25	9.33	9.21
histone H4-like, partial	Vicugna pacos	XP_031547614.1	IDH3A	40 kDa	ANOVA	0.10	7.32	7.66	7.39	7.73
isocitrate dehydrogenase subunit alpha, mitochondrial	Bos indicus	XP_019842670.1	LOC105557103	83 kDa	ANOVA	0.10	7.15	7.46	7.49	7.67
pentatricopeptide repeat-containing protein 1, mitochondrial-like	Capra hircus	XP_017906071.1	ADPGK	54 kDa	ANOVA	0.10	6.58	7.24	6.71	6.27
ADP-dependent glucokinase isoform X1	Capra hircus	XP_017906071.1	LOC1086363							

protein disulfide-isomerase A6	Xp_019824917.1	LOC109565403	48 kDa	ANOVA	0.14	8.61	8.88	8.56	8.34
enoyl-CoA hydratase, mitochondrial	Xp_017895763.1	ECHS1	31 kDa	ANOVA	0.14	7.2	7.57	7.19	7.66
catenin alpha-1	Xp_004008890.1	CTNNA1	100 kDa	ANOVA	0.14	6.3	6.44	6.96	6.46
peroxisomal multifunctional enzyme type 2	Xp_004008734.2	HSD17B4	87 kDa	ANOVA	0.14	6.95	7.33	6.68	7.28
complement C1s subcomponent	Xp_004009661.6	C1S	78 kDa	ANOVA	0.14	6.44	6.4	6	6.07
membrane-associated progesterone receptor component 1	Xp_001295509.1	PGRMC1	22 kDa	ANOVA	0.14	7.75	7.95	7.98	8.23
2-iminobutanate/2-iminopropanoate deaminase	Xp_001272642.1	RIDA	14 kDa	ANOVA	0.14	5.81	6.32	6.19	6.72
cytochrome b5	Xp_001159663.1	CYBSA	15 kDa	ANOVA	0.14	7.33	7.6	7.35	7.72
mitochondrial-processing peptidase subunit alpha	Xp_027821975.3	MPMC1	58 kDa	ANOVA	0.15	6.14	6.13	6.3	6.21
dolichyl-diphosphooligosaccharide–protein glycosyltransferase subunit 1	Xp_027813657.1	RPN1	69 kDa	ANOVA	0.15	8.1	8.5	8.27	8.09
retinol dehydrogenase 11	Xp_012037274.1	RDH11	37 kDa	ANOVA	0.15	6.56	6.97	6.77	6.57
sarcoplasmic/endoplasmic reticulum calcium ATPase 2	Xp_011953174.1	ATP2A2	110 kDa	ANOVA	0.15	6.59	7.08	7.15	7.29
apoptosis-inducing factor 1, mitochondrial isoform X2	Xp_004022430.1	AIFM1	66 kDa	ANOVA	0.15	7.11	7.37	7.08	6.98
thioredoxin-dependent peroxide reductase, mitochondrial	Xp_004020276.3	PRDX3	28 kDa	ANOVA	0.15	7.45	7.73	7.63	7.92
complement component C6	Xp_004017065.2	C6	105 kDa	ANOVA	0.15	7.28	7.55	7.21	7.23
cathepsin D	Xp_004008533.1	CALR	48 kDa	ANOVA	0.15	8.65	8.82	8.68	8.27
mannosyl-oligosaccharide glucosidase	Xp_004006147.4	M0G5	93 kDa	ANOVA	0.15	6.55	7.37	7.33	7.23
apolipoprotein E	Xp_027834259.1	APOE	36 kDa	ANOVA	0.16	6.72	7.52	6.8	6.91
lysosomal protective protein isoform X2	Xp_027830353.1	CTSA	54 kDa	ANOVA	0.16	6.43	6.57	6.53	6.91
dolichyl-diphosphooligosaccharide–protein glycosyltransferase subunit 2 isoform X1	Xp_027832978.1	RPN2	71 kDa	ANOVA	0.16	8.39	8.72	8.31	8.18
ATP-binding cassette subfamily B member 1 isoform X1	Xp_004022430.1	ABCD1	82 kDa	ANOVA	0.16	6.63	7.19	7.03	7.01
short-branched chain specific acyl-CoA dehydrogenase, mitochondrial	Xp_027816120.1	ACADS	47 kDa	ANOVA	0.16	6.89	7.05	6.35	6.63
cathepsin D	Xp_027815055.1	CTSD	45 kDa	ANOVA	0.16	6.97	7.54	7.78	7.21
40S ribosomal protein S27-like isoform X2	Xp_010831802.1	LOC104983941	16 kDa	ANOVA	0.16	6.37	6.74	6.78	6.84
ATP synthase subunit O, mitochondrial	Xp_005674722.1	ATP5PO	23 kDa	ANOVA	0.16	7.44	7.76	7.67	7.85
phosphatidylethanolamine-binding protein 1	Xp_004017427.1	PEPB1	21 kDa	ANOVA	0.16	7.01	7.04	7.04	7.42
histone H2B type 3-N	Xp_001075211.1	H2BC15	14 kDa	ANOVA	0.16	9.05	9.39	9.4	9.31
60S ribosomal protein L13a	Xp_004005173.1	-	37 kDa	ANOVA	0.16	6.72	7.03	7.25	7.28
histone H2A type 1-A	Xp_031544014.1	LOC102532758	14 kDa	ANOVA	0.17	8.73	9.12	9.21	9.08
short palate, lung and nasal epithelium carcinoma-associated protein 2A-like	Xp_027832882.1	LOC114117619	28 kDa	ANOVA	0.17	9.34	9.44	9.11	9.34
plasma membrane calcium-transporting ATPase 4	Xp_027831983.1	ATP2B4	133 kDa	ANOVA	0.17	6.8	7.09	7.09	7.01
procaglion galactosyltransferase 1	Xp_027825246.1	COLGALT1	72 kDa	ANOVA	0.17	7.71	7.9	7.89	7.63
complement C4 isoform X1	Xp_027814604.1	LOC101123672	192 kDa	ANOVA	0.17	8.9	9.01	8.77	8.9
histone H2A type 3-A-like, partial	Xp_010970234.1	LOC105082344	9 kDa	ANOVA	0.17	8.73	9.12	9.21	9.08
tissue alpha-L-fucosidase	Xp_004005173.2	FUCA1	54 kDa	ANOVA	0.17	6.87	7.24	6.97	6.84
pigment epithelium-derived factor isoform 1 precursor	Xp_001316832.1	SERPINF1	46 kDa	ANOVA	0.17	6.43	6.5	6.72	6.93
coiled-coil domain-containing protein 134 precursor	Xp_001192755.1	CCDC134	26 kDa	ANOVA	0.17	5.9	6.89	6.74	6.78
INHA	Xp_0040507.1	-	39 kDa	ANOVA	0.17	7.78	8.21	8	7.97
succinate dehydrogenase	Xp_027836013.1	SDHA	73 kDa	ANOVA	0.18	7.18	7.53	7.26	7.08
ER membrane protein complex subunit 1 isoform X2	Xp_027821434.1	EMC1	111 kDa	ANOVA	0.18	6.61	7.51	7.31	7.03
ATP-dependent 6-phosphofructokinase, liver type	Xp_027816583.1	PFKL	85 kDa	ANOVA	0.18	6.64	6.11	6.93	6.3
integrin beta-5 isoform X2	Xp_027812388.1	ITGB5	88 kDa	ANOVA	0.18	6.94	7.3	7.33	7.08
isobutyryl-CoA dehydrogenase, mitochondrial	Xp_017914891.1	ACAD8	45 kDa	ANOVA	0.18	6.88	6.99	6.84	7.02
vesicle-associated membrane protein-associated protein A isoform X1	Xp_014959144.1	VAPA	32 kDa	ANOVA	0.18	Missing Value	6.45	6.77	6.54
extracellular superoxide dismutase [Cu-Zn] isoform X1	Xp_014951904.2	SOD3	39 kDa	ANOVA	0.18	6.92	6.69	6.95	7.18
lamin-B1	Xp_004008711.1	LMNB1	66 kDa	ANOVA	0.18	7.71	7.41	Missing Value	7.79
tumor necrosis factor-inducible gene 6 protein	Xp_004004753.1	TNFAIP6	31 kDa	ANOVA	0.18	7.41	7.4	7.72	7.47
ferredoxin-1	Xp_029330.2	FDX1	14 kDa	ANOVA	0.18	6.16	5.89	6.85	7.07
aromatase	Xp_001116472.1	CYP19	58 kDa	ANOVA	0.18	6.9	7.43	6.85	7.23
PRA1 family protein 2	Xp_001039474.2	PRAF2	19 kDa	ANOVA	0.18	6.66	6.54	7.06	7.06
TPA; keratin 6A-like	Xp_004005228.1	DAA29993.1	63 kDa	ANOVA	0.18	7.78	7.81	7.81	8.13
protein disulfide-isomerase	Xp_027830078.1	P4HB	63 kDa	ANOVA	0.19	8.75	9.08	8.83	8.6
mitochondrial fission process protein 1 isoform X1	Xp_017916470.1	MTFP1	18 kDa	ANOVA	0.19	6.08	6.25	5.98	6.55
glutathione S-transferase P	Xp_017898539.1	LOC100861197	24 kDa	ANOVA	0.19	7.1	7.11	7.21	7.74
mitochondrial fission 1 protein isoform X2	Xp_002600001.1	BOSMUT	10 kDa	ANOVA	0.19	6.09	6.57	6.52	6.71
GPI transamidase component PIG-S	Xp_006042254.1	PIGS	62 kDa	ANOVA	0.19	6.75	7.14	6.74	6.54
glutathione S-transferase A1-like	Xp_004018947.1	LOC101106720	25 kDa	ANOVA	0.19	7.96	8.18	8.29	8.41
nucleoside diphosphate kinase A 1	Xp_004012798.1	LOC101102072	17 kDa	ANOVA	0.19	6.09	6.34	6.46	6.95
peptidyl-prolyl cis-trans isomerase B	Xp_004010585.1	PPIB	24 kDa	ANOVA	0.19	8.26	8.47	8.52	8.57
NADH dehydrogenase 1 alpha subcomplex subunit 2	Xp_004012798.1	NDUF11	11 kDa	ANOVA	0.19	6.51	6.84	6.64	6.99
ORM1-like protein 3	Xp_001069831.1	ORMDL3	17 kDa	ANOVA	0.19	5.58	6.25	5.95	6.02
ELAV (embryonic, lethal, abnormal vision, Drosophila)-like 1 isoform X2	Xp_004005135.1	Homo sapiens	EAW68950.1	-	50 kDa	ANOVA	0.19	6.8	7.07
mannan-binding lectin serine protease 2 isoform X2	Xp_027831448.1	MASP2	76 kDa	ANOVA	0.20	6.34	6.03	Missing Value	5.97
N-glycanase family member 1	Xp_005691363.1	SGSH	57 kDa	ANOVA	0.20	6.05	6.77	6.64	6.83
N-glycanase family member 2	Xp_006040259.1	ATPS51A	60 kDa	ANOVA	0.20	8.64	8.91	8.62	8.4
fibronectin beta chain	Xp_004017233.2	FB	57 kDa	ANOVA	0.20	10.6	10.4	10.1	10.1
5'-nucleotidase	Xp_004011351.1	NTSE	63 kDa	ANOVA	0.20	8.54	8.81	8.9	8.69
hepatitis A virus cellular receptor 1-like	Xp_004009061.1	LOC101111190	15 kDa	ANOVA	0.20	6.2	6.53	6.28	7.03
protein kinase-A precursor	Xp_001107983.1	TMEM176A	8 kDa	ANOVA	0.20	5.8	5.96	6.01	6.28
glutathione S-transferase A1 isoform X1	Xp_027814130.1	GST1	25 kDa	ANOVA	0.21	8.17	8.56	8.55	8.75
histone H2B type 3-N-like	Xp_027813837.1	RPL14	23 kDa	ANOVA	0.21	7.09	7.08	7.26	7.4
histone H2B type 2-like	Xp_019819308.1	LOC109516360	14 kDa	ANOVA	0.21	8.89	9.21	9.27	9.15
histone H2A type 3	Xp_011958166.1	ERLIN1	39 kDa	ANOVA	0.21	7.24	7.49	7.28	7.03
erlin-1	Xp_004012816.1	LRRC59	35 kDa	ANOVA	0.21	7.04	7.46	7.15	7.31
leucine-rich repeat-containing protein 59	Xp_004006628.2	LOC101107947	28 kDa	ANOVA	0.21	6.2	6.46	Missing Value	6.73
apolipoprotein F-like	Xp_004005173.2	Muntiac vaginalis	AAK12840.1	H2AX	11 kDa	ANOVA	0.21	8.86	9.17
H2A histone family member X, partial	Xp_004017402.1	HSP90B1	90 kDa	ANOVA	0.21	8.84	9.29	9.19	8.82
heat shock protein gp96 precursor, partial	Xp_004015407.1	AIAO54071	155 kDa	ANOVA	0.21	6.71	7.37	6.69	7.03
Aldehyde dehydrogenase 7 family, member A1	Xp_027829730.1	SERPINF1	44 kDa	ANOVA	0.22	7.26	7.01	7.21	7.41
pigment epithelium-derived factor isoform X1	Xp_004009611.1	LOC101111190	15 kDa	ANOVA	0.22	8.84	9.09	9.11	9.06
transferrin receptor protein 2 isoform X1	Xp_027817323.1	TFR2	88 kDa	ANOVA	0.22	8.54	8.84	8.55	8.69
histone H2B 1/2-like	Xp_019822332.1	LOC109564212	9 kDa	ANOVA	0.22	8.84	9.09	9.11	9.06
histone H2B type 3-N-like	Xp_019822179.1	LOC109562588	16 kDa	ANOVA	0.22	8.85	9.1	9.12	9.07
histone H2B type 2-like	Xp_019808662.1	LOC109553326	11 kDa	ANOVA	0.22	8.97	9.26	9.3	9.3
neutral alpha-glucosidase AB isoform X2	Xp_004011351.1	GNAAB	107 kDa	ANOVA	0.22	8.39	8.72	8.73	8.59
beta-2-glycoprotein 1 isoform X1	Xp_004009453.1	APOH	38 kDa	ANOVA	0.22	6.44	7.19	6.96	7.32
NADH dehydrogenase 1 alpha subcomplex subunit 11	Xp_004008632.1	NDUF11	15 kDa	ANOVA	0.22	6.59	6.8	6.7	7.19
cytochrome c oxidase subunit 7A-related protein, mitochondrial	Xp_004006504.1	LOC101115694	13 kDa	ANOVA	0.22	6.34	6.73	6.68	6.86
clusterin	Xp_004004480.1	LOC101113728	51 kDa	ANOVA	0.22	7.89	8.27	8	8.06
ATP synthase subunit alpha, mitochondrial precursor	Xp_004011709.1	ATP5F1A	60 kDa	ANOVA	0.22	8.6	8.87	8.59	8.39
protein disulfide-isomerase A3 precursor	Xp_001156517.1	PDIA3	57 kDa	ANOVA	0.22	8.86	9.21	9.06	8.7
vesicular integral-membrane protein VIP36 isoform X1	Xp_027825816.1	LMAN2	40 kDa	ANOVA	0.23	7.16	7.43	7.39	7.32
short-chain-specific acyl-CoA dehydrogenase, mitochondrial	Xp_027812426.1	ACADS	45 kDa	ANOVA	0.23	6.78	7.28	6.91	7.01
caprine hircus	Xp_017920331.1	NME2	17 kDa	ANOVA	0.23	6.06	6.22	6.6	6.91
Bos mutus	Xp_014334962.1	LOC102283318	48 kDa	ANOVA	0.23	6.14	6.53	6.36	6.83
ceruloplasmin isoform X1	Xp_004004842.2	ALDH1A1	92 kDa	ANOVA	0.23	8.9	9.31	9.24	8.89
ceruloplasmin isoform X1	Xp_027835594.1	SERPING1	52 kDa	ANOVA	0.24	8	8.07	7.91	8.09
ribosome-binding protein 1 isoform X3	Xp_027832521.1	RBP1	154 kDa	ANOVA	0.24	7.17	7.72	7.6	7.32
protein LYRIC isoform X1	Xp_027828995.1	MTDH	67 kDa	ANOVA	0.24	5.82	6.05	5.73	6.49
protein NipSNAP homolog 3A	Xp_027819363.1	NIPSNAP3A	29 kDa	ANOVA	0.24	5.59	6.58	Missing Value	6.27
paraspeckle component 1 isoform X1	Xp_027818838.1	PCP1	59 kDa	ANOVA	0.24	6.94	7.37	6.86	6.66
vitamin K-dependent protein C	Xp_004019479.2	PROC							

complement component C8 gamma chain isoform X1	Ovis aries	XP_027821902.1	C8G	30 kDa	ANOVA	0.27	7.3	7.31	6.95	7.27
ATP synthase subunit e, mitochondrial isoform X2	Bubalus bubalis	XP_025145348.1	ATPM5ME	12 kDa	ANOVA	0.27	6.93	7.34	7.12	7.4
alpha-2-HS-glycoprotein	Odocoileus virginianus texanus	XP_020734476.1	AHSG	38 kDa	ANOVA	0.27	7.89	8.23	8.1	7.91
late histone H2B.14-like	Bos indicus	XP_019822502.1	LOC109563569	14 kDa	ANOVA	0.27	8.42	8.86	8.89	8.98
hemoglobin subunit alpha-I/II	Bison bison bison	XP_010855734.1	LOC105001245	15 kDa	ANOVA	0.27	8.46	8.16	9.14	8.64
NAD(P) transhydrogenase, mitochondrial	Ovis aries	XP_004017056.2	NNT	114 kDa	ANOVA	0.27	7.48	7.98	7.87	7.61
gap junction alpha-1 protein	Ovis aries	XP_004011208.1	GJ1A1	43 kDa	ANOVA	0.27	7.45	8.06	7.87	7.96
NADH dehydrogenase 1 beta subcomplex subunit 4	Ovis aries	XP_004003003.2	NDUFB4	15 kDa	ANOVA	0.27	6.53	6.83	6.77	7.09
Hemoglobin subunit beta	Ovis aries	P02075.2	HBB	16 kDa	ANOVA	0.27	9.08	8.97	9.77	9.27
uroplakin-1b	Ovis aries	XP_011950373.1	UPK1B	30 kDa	ANOVA	0.28	6.72	6.67	6.27	Missing Value
procollagen-lysine-2-oxoglutarate 5-dioxygenase 1	Bubalus bubalis	XP_006076826.1	PLOD1	84 kDa	ANOVA	0.28	7.18	7.51	7.22	7.16
ribosome-binding protein 1	Bos mutus	XP_005904628.1	RRBP1	107 kDa	ANOVA	0.28	7.05	7.52	7.43	7.28
NADH dehydrogenase 1 beta subcomplex subunit 11, mitochondrial	Ovis aries	XP_004022189.1	NDUFB1	17 kDa	ANOVA	0.28	5.82	6.18	5.79	6.52
primary amino oxidase, lung isozyme	Ovis aries	XP_004013452.2	LOC101113086	87 kDa	ANOVA	0.28	7.6	7.6	7.32	7.69
MICOS complex subunit MCi60 isoform X1	Ovis aries	XP_004005935.3	IMMT	84 kDa	ANOVA	0.28	7.33	7.74	7.62	7.46
leukocyte cell-derived chemotaxin-2 precursor	Bos taurus	NP_776805.1	LECT2	16 kDa	ANOVA	0.28	5.83	5.93	5.96	6.4
mitochondrial 2-oxoglutarate/malate carrier protein	Ovis aries	NP_001207045.1	SLC25A11	34 kDa	ANOVA	0.28	7.04	7.35	7.46	7.6
ras-related protein Rab-12	Bos taurus	NP_001095762.1	RAB12	27 kDa	ANOVA	0.28	7.07	7.19	7.33	7.48
fumarate hydratase, mitochondrial	Bos taurus	NP_001069271.1	FH	55 kDa	ANOVA	0.28	7.79	7.93	7.74	7.61
carbonic anhydrase 2	Ovis aries	XP_027829052.1	CA2	29 kDa	ANOVA	0.29	6.91	6.88	7.63	6.96
SUN domain-containing protein 2 isoform X1	Ovis aries	XP_027823918.1	SUN2	88 kDa	ANOVA	0.29	7	7.59	7.51	6.88
monacylglycerol lipase ABHD6 isoform X1	Odocoileus virginianus texanus	XP_020743079.1	ABHD6	42 kDa	ANOVA	0.29	6.37	6.27	6.53	6.47
leucine-rich PPR motif-containing protein, mitochondrial	Ovis aries	XP_014948984.1	LRPPRC	158 kDa	ANOVA	0.29	5.63	6.39	Missing Value	6.22
glutamate dehydrogenase 1, mitochondrial	Bison bison bison	XP_010852694.1	GLUD1	62 kDa	ANOVA	0.29	6.28	7.02	6.45	6.12
cytochrome c oxidase assembly factor 3 homolog, mitochondrial	Capra hircus	XP_005693912.2	LOC102190454	12 kDa	ANOVA	0.29	5.94	6.33	Missing Value	6.53
estradiol 17-beta-dehydrogenase 11	Capra hircus	XP_005681936.2	HSDF17B11	33 kDa	ANOVA	0.29	6.87	6.48	7.06	7.11
L-lactate dehydrogenase B chain	Capra hircus	XP_005680842.2	LDHB	36 kDa	ANOVA	0.29	7.42	7.24	7.47	7.62
NADH dehydrogenase 1 subunit C2	Ovis aries	XP_004019479.1	NDUFV2	14 kDa	ANOVA	0.29	6.87	7.18	7.07	7.29
ras-related protein Rab-11B	Bos taurus	NP_001030468.1	RAB11B	24 kDa	ANOVA	0.29	7.23	7.38	7.44	7.53
galectin-3-binding protein isoform X1	Ovis aries	XP_027830011.1	LGALS2BP	62 kDa	ANOVA	0.30	7.23	7.5	7.42	7.43
Serpin A3-6	Capra hircus	XP_017921952.1	LOC102193611	46 kDa	ANOVA	0.30	8.42	8.49	8.16	8.46
U2 small nuclear ribonucleoprotein A'	Vicugna pacos	XP_006211551.1	SNRPA1	28 kDa	ANOVA	0.30	6.81	6.71	6.89	6.58
histone H3.1	Bos mutus	XP_005892274.1	LOC102280001	15 kDa	ANOVA	0.30	8.33	8.84	8.79	8.68
dehydrogenase/reductase SDR family member 1	Ovis aries	XP_004010348.1	DHRS1	34 kDa	ANOVA	0.30	6.03	6.42	Missing Value	6.37
starch-binding domain-containing protein 1	Ovis aries	XP_004009976.3	STBD1	36 kDa	ANOVA	0.30	6.96	6.88	7.03	7.18
cytochrome c oxidase subunit 5B, mitochondrial	Ovis aries	XP_004006204.1	LOC101110664	14 kDa	ANOVA	0.30	6.21	7.27	6.89	7.09
phosphoglycerate kinase 1	Ovis aries	XP_004003380.2	LOC10111279	78 kDa	ANOVA	0.30	7.28	7.3	7.43	7.69
translcocon-associated protein subunit gamma	Ovis aries	NP_001135988.1	PGK1	45 kDa	ANOVA	0.30	7.08	7	7.48	7.65
antithrombin-III precursor	Bos taurus	NP_001070512.1	SSR3	21 kDa	ANOVA	0.30	6.72	7.04	6.7	6.97
lg gamma-3 chain C region, partial	Ovis aries	NP_001009393.1	SERPINC1	52 kDa	ANOVA	0.30	8.19	8.17	8.06	8.13
histone H3	Bos mutus	ELR4850.1	-	33 kDa	ANOVA	0.30	8.67	8.35	9.22	8.85
H3L-like histone, partial	Homo sapiens	CABO2546.1	-	15 kDa	ANOVA	0.30	8.32	8.84	8.79	8.68
beta 2 glycoprotein I	Homo sapiens	AA096275.1	-	12 kDa	ANOVA	0.30	8.28	8.78	8.78	8.68
dolichyl-phosphoinosaccharide-protein glycosyltransferase subunit STT3B	Bos taurus	AAB20668.1	-	36 kDa	ANOVA	0.30	6.47	7.22	7.04	7.34
alpha-2-macroglobulin	Ovis aries	XP_027813742.1	STT3B	93 kDa	ANOVA	0.31	6.92	7.23	7.11	6.78
procollagen-2,2-exoglutarate 5-dioxygenase 2 isoform X1	Odocoileus virginianus texanus	XP_020760299.1	LOC101144654	155 kDa	ANOVA	0.31	8.23	8.21	8.06	8.02
fibulin-1 isoform X2	Capra hircus	XP_017904680.1	PLD05	88 kDa	ANOVA	0.31	7.15	7.15	6.9	6.9
pterin-4-alpha-carbinolamin dehydratase 2 isoform X2	Capra hircus	XP_017904389.1	FBNL1	75 kDa	ANOVA	0.31	7.02	6.66	7.08	6.98
carboxypeptidase N subunit 2	Ovis aries	XP_004023454.3	CPN2	60 kDa	ANOVA	0.31	6.3	Missing Value	6.23	6.47
cytoskeleton-associated protein 4	Ovis aries	XP_004006543.3	UGGT1	178 kDa	ANOVA	0.31	7.46	7.78	7.73	7.58
UDP-glucose/glycoprotein glucosyltransferase 1 isoform X1	Ovis aries	XP_004002060.2	DHCR24	60 kDa	ANOVA	0.31	7.25	7.71	7.42	7.42
delta(24)-sterol reductase	Cervus elaphus hippelaphus	OVWK09169.1	-	53 kDa	ANOVA	0.31	7.48	7.55	7.45	7.65
IDH3A	Bos taurus	NP_00106791.1	IER3IP1	9 kDa	ANOVA	0.31	6.06	6.3	6.21	6.58
immediate early response 3-interacting protein 1 precursor	Bos taurus	NP_00106789.1	ATP5M	6 kDa	ANOVA	0.31	6.28	6.75	6.53	6.71
ATP synthase membrane subunit DAPIT, mitochondrial	Ovis aries	NP_00106698.1	AHSG	39 kDa	ANOVA	0.31	8.33	8.6	8.43	8.31
alpha-2-HS-glycoprotein precursor	Bos taurus	ANNA46376.1	-	44 kDa	ANOVA	0.31	9.35	9.38	9.45	9.12
membrane-bound immunoglobulin gamma-1 heavy chain constant region, partial	Camelus dromedarius	XP_031302141.1	SLC25A5	33 kDa	ANOVA	0.32	8.28	8.48	8.47	8.38
annexin A6 isoform X2	Ovis aries	XP_027826224.1	ANXA6	75 kDa	ANOVA	0.32	7.03	7.65	7.71	7.52
integrin alpha-6 isoform X2	Capra hircus	XP_017920165.1	ITGA6	119 kDa	ANOVA	0.32	6.92	7.7	7.42	7.35
aspartyl/asparagine beta-hydroxylase isoform X1	Ovis aries	XP_012039134.2	ASPH	86 kDa	ANOVA	0.32	6.4	6.81	6.32	6.5
hypoxia up-regulated protein 1 isoform X1	Capra hircus	XP_011950949.2	HYOU1	111 kDa	ANOVA	0.32	7.91	8.25	8.33	8.17
pigment epithelium-derived factor	Ovis aries	XP_004017394.7	SERPINF1	46 kDa	ANOVA	0.32	7.15	7.02	7.15	7.37
diablo homolog, mitochondrial	Ovis aries	XP_004017389.1	DIABLO	31 kDa	ANOVA	0.32	5.85	6.26	6.43	6.57
annexin A6 isoform X1	Ovis aries	XP_004009036.1	ANXA6	76 kDa	ANOVA	0.32	7.03	7.65	7.71	7.52
isoamyl acetate-hydrolyzing esterase 1 homolog isoform X1	Ovis aries	XP_004005572.1	IAH1	28 kDa	ANOVA	0.32	6.23	6.15	5.83	6.53
hemoglobin subunit alpha	Ovis canadensis nelsoni	QI83449.1	HBA-T1	15 kDa	ANOVA	0.32	8.83	8.68	9.5	8.99
mitochondrial pyruvate carrier	Bos taurus	NP_001180050.1	MPC2	14 kDa	ANOVA	0.32	6.04	6.32	6.31	6.57
hemoglobin subunit beta-C	Ovis aries	NP_001066896.1	HBBC	16 kDa	ANOVA	0.32	8.78	8.68	9.43	8.94
D-dopachrome decarboxylase	Bos taurus	NP_001092620.1	DDT	13 kDa	ANOVA	0.32	5.67	5.76	5.71	6
alpha globin chain	Ovis aries	CAA49750.1	-	15 kDa	ANOVA	0.32	8.84	8.67	9.49	9
alpha globin	Homo sapiens	AA084749.1	-	14 kDa	ANOVA	0.32	7.23	7.51	8.17	7.76
similar to 60S ribosomal protein L7; similar to P18124 (PID:d13302)	Homo sapiens	AAD08846.1	-	29 kDa	ANOVA	0.32	6.95	7.33	7.21	7.41
DNA topoisomerase 1	Ovis aries	XP_027832995.1	TOP1	91 kDa	ANOVA	0.33	6.86	6.91	7.2	6.69
extracellular matrix protein 1 isoform X1	Ovis aries	XP_027830219.1	ECM1	61 kDa	ANOVA	0.33	7.57	8.12	7.8	7.64
mitochondrial proton/calcium exchanger protein isoform X1	Ovis aries	XP_027827113.1	LETM1	82 kDa	ANOVA	0.33	6.4	7.07	7.1	6.82
60S ribosomal protein L7a	Capra hircus	XP_017911629.1	RPL7A	30 kDa	ANOVA	0.33	7.59	7.76	7.73	7.86
alpha-2-antiplasmin isoform X1	Ovis aries	XP_012040849.3	SERPINF2	61 kDa	ANOVA	0.33	7.79	8.17	7.96	7.74
transmembrane 9 superfamily member 2	Ovis aries	XP_004012270.1	TMSMF9	76 kDa	ANOVA	0.33	6.31	6.46	6.51	6.51
cholesterol side-chain cleavage enzyme, mitochondrial precursor	Bos taurus	NP_001082758.1	CYP11A1	60 kDa	ANOVA	0.33	7.83	8.23	8.12	8.17
macrophage migration inhibitory factor	Bos taurus	NP_001028780.1	MIF	12 kDa	ANOVA	0.33	6.79	6.93	7.22	7.19
INH-B	Capra hircus	AE40509.1	-	48 kDa	ANOVA	0.33	6.88	7.2	6.77	6.97
mitochondrial malate dehydrogenase 2	Bos taurus	ABD72298.2	MDH2	30 kDa	ANOVA	0.33	8.42	8.67	8.51	8.62
cathepsin D (EC 3.4.23.5)	Bos taurus	AAB26186.1	-	38 kDa	ANOVA	0.33	6.61	7.19	7.47	6.96
major vault protein	Ovis aries	XP_027817904.1	MVP	99 kDa	ANOVA	0.34	6.52	7.09	7.08	5.55
lanosterol synthase	Ovis aries	XP_027817921.1	LSS	83 kDa	ANOVA	0.34	8.34	8.4	7.98	7.91
aldehyde dehydrogenase	Ovis aries	XP_027812202.1	BRI3BP	27 kDa	ANOVA	0.34	5.89	6.76	6.34	6.62
probable ATP-dependent RNA helicase DDX31 isoform X1	Ovis aries	XP_014959673.2	NIPSNAP2	34 kDa	ANOVA	0.34	5.96	6.7	6.45	6.52
heat shock protein beta-1	Ovis aries	XP_011956915.1	STG3A	42 kDa	ANOVA	0.34	6.17	6.89	5.81	Missing Value
protein Nip58n homolog 2 isoform X1	Ovis aries	XP_005685456.3	NDUF56	13 kDa	ANOVA	0.34	6.04	6.55	6.39	6.83
ribonuclease 4	Capra hircus	XP_004017458.1	ALDH2	57 kDa	ANOVA	0.34	8.19	8.4	7.98	7.74
aldehyde dehydrogenase, mitochondrial	Bison bison bison	XP_010842962.1	LOC104991931	42 kDa	ANOVA	0.34	7.21	7.68	7.46	7.33
immunoglobulin gamma 2 heavy chain constant region, partial	Bos taurus	NP_77230.1	UQCRC	10 kDa	ANOVA	0.34	9.35	9.4	9.38	9.07
immunoglobulin G heavy chain variable region, partial	Ovis aries	XP_027823689.1	LOC101104482	163 kDa	ANOVA	0.34	6.22	6.94	6.94	6.28
immunoglobulin lambda light chain constant region segment 1, partial	Ovis aries	XP_027820373.1	DDX31	81 kDa	ANOVA	0.34	6.76	6.95	6.04	6.73
complement factor H	Ovis aries	XP_027817273.1	HSPB1	22 kDa	ANOVA	0.34	7.91	7.74	8.04	8.23

haptoglobin precursor	Bubalus bubalis	NP_001277908.1	HP	45 kDa	ANOVA	0.38	8.38	6.76	6.84	6.03
cholesterol side-chain cleavage enzyme, mitochondrial	Capra hircus	NP_001274503.1	CYP1A1	60 kDa	ANOVA	0.38	7.91	8.27	8.06	8.14
immunoglobulin kappa-2 light chain variable region, partial	Ovis aries	AAB94900.1	-	13 kDa	ANOVA	0.38	7.18	6.94	7.46	7.04
serotransferrin	Ovis aries	XP_027816111.1	TF	77 kDa	ANOVA	0.39	9.24	9.26	9.45	9.33
fibronectin type III domain-containing protein 3B	Ovis aries	XP_014948026.2	FNDC3B	133 kDa	ANOVA	0.39	Missing Value	6.69	6.1	6.27
serpin A3-8	Ovis aries	XP_011954394.2	LOC101119509	47 kDa	ANOVA	0.39	8.36	8.34	8.3	8.12
calnexin	Capra hircus	XP_005682095.1	CANX	68 kDa	ANOVA	0.39	7.99	8.33	8.26	8.13
histone H2A type 1-B/E	Bos taurus	XP_005202300.1	LOC524236	14 kDa	ANOVA	0.39	9.31	9.54	9.48	9.51
pyruvate carboxylase, mitochondrial	Ovis aries	XP_027815692.1	PC	130 kDa	ANOVA	0.40	7.74	8.09	7.89	7.64
lamin-B2	Capra hircus	XP_017906266.1	LMB2	70 kDa	ANOVA	0.40	7.02	7.53	7.48	7.22
glutathione S-transferase Mu 1-like	Capra hircus	XP_017901368.1	LOC108633298	26 kDa	ANOVA	0.40	6.82	6.38	6.66	6.94
prolyl 4-hydroxylase subunit alpha-1 isoform X2	Ovis aries	XP_004021508.1	P4HA1	61 kDa	ANOVA	0.40	7.58	7.47	7.54	7.08
protein SEC13 homolog	Ovis aries	XP_004018574.1	SEC13	35 kDa	ANOVA	0.40	6.48	6.3	6.12	6.46
dihydroxyacetone-residue succinyltransferase component of 2-oxoglutarate dehydrogenase	Ovis aries	XP_004010842.2	DLST	49 kDa	ANOVA	0.40	6.07	7.1	6.82	6.61
Core histone macro-H2A.2	Camelus dromedarius	KAB1271219.1	-	53 kDa	ANOVA	0.40	7.38	7.49	7.54	7.44
lactadherin	Ovis aries	XP_027812864.1	MFGE8	48 kDa	ANOVA	0.41	8.63	8.51	8.83	8.56
nucleobindin-1	Capra hircus	XP_017918238.1	NUCB1	53 kDa	ANOVA	0.41	Missing Value	6.84	6.58	6.52
fructose-bisphosphate aldolase A	Vicugna pacos	XP_015092348.1	ALDOA	39 kDa	ANOVA	0.41	7.48	6.97	7.22	7.4
complement component C9	Ovis aries	XP_004017075.3	C9	62 kDa	ANOVA	0.41	7.92	8.19	7.95	7.91
60S ribosomal protein L18	Ovis aries	XP_004005402.1	RPL18	22 kDa	ANOVA	0.41	7.35	7.47	7.45	7.65
NADH dehydrogenase 1 beta subcomplex subunit 9 isoform X1	Ovis aries	XP_004011699.2	NDUFB9	22 kDa	ANOVA	0.41	6.87	7.09	7.02	7.18
ALDH2	Cervus elaphus hippelaphus	OWK15140.1	-	58 kDa	ANOVA	0.41	8.12	8.3	7.88	7.82
ATP-dependent RNA helicase A	Bos taurus	NP_776461.1	DHX9	142 kDa	ANOVA	0.41	7.44	7.75	7.68	7.68
gelsozin isoform X1	Ovis aries	XP_005202300.1	GSN	86 kDa	ANOVA	0.42	8.49	8.62	8.59	8.64
dihydroxyacetone-residue acetyltransferase component of pyruvate dehydrogenase complex	Capra hircus	XP_011950844.2	DLAT	69 kDa	ANOVA	0.42	6.45	6.79	6.65	6.53
complement factor I	Ovis aries	XP_004009671.1	CFI	69 kDa	ANOVA	0.42	7.25	6.93	7.08	7.31
Hexokinase-1	Bos taurus	P27595.1	HK1	103 kDa	ANOVA	0.42	6.57	7.2	6.9	6.98
histone H2A type 1-like	Ovis aries	XP_019841862.1	LOC109577385	14 kDa	ANOVA	0.43	9.39	9.6	9.54	9.54
cytochrome c oxidase subunit 4 isoform 1, mitochondrial	Capra hircus	XP_017917306.1	LOC102188434	20 kDa	ANOVA	0.43	6.51	7.18	6.25	7.41
HIG1 domain family member 1A, mitochondrial	Ovis aries	XP_011954842.1	HIGD1A	10 kDa	ANOVA	0.43	5.68	6.32	5.7	6.16
complement component C8 beta chain	Ovis aries	XP_004002065.2	C8B	66 kDa	ANOVA	0.43	7.23	7.51	7.22	7.29
Hemoglobin subunit beta-A	Bos indicus	XP_019841862.1	LOC109577385	14 kDa	ANOVA	0.43	9.39	9.6	9.54	9.54
Ion protease homolog, mitochondrial	Ovis aries	XP_02782561.1	LONP1	107 kDa	ANOVA	0.44	7.43	7.71	7.57	7.4
V-type proton ATPase subunit G 1	Ovis aries	XP_014948445.1	ATPV1G1	14 kDa	ANOVA	0.44	5.65	5.94	5.86	5.97
acetyl-CoA acetyltransferase, mitochondrial	Ovis aries	XP_027834968.1	ACAT1	45 kDa	ANOVA	0.45	7.78	7.94	7.74	7.91
scaffold attachment factor B1 isoform X2	Bos javanicus	P04346.1	-	16 kDa	ANOVA	0.43	8.66	8.53	9.21	8.7
delta-1-pyrroline-5-carboxylate dehydrogenase, mitochondrial	Ovis aries	XP_02782561.1	SAFB	180 kDa	ANOVA	0.45	6.59	7.38	7.24	6.69
very-long-chain 3-oxoacyl-CoA reductase	Ovis aries	XP_027821443.1	ALDH4A1	61 kDa	ANOVA	0.45	6.24	6.34	5.7	5.88
IDH3B protein, partial	Ovis aries	XP_004016470.1	HSID1B12	35 kDa	ANOVA	0.45	7.29	7.47	7.53	7.52
protein sel-1 homolog 1	Bos taurus	AAI04503.1	IDH3B	42 kDa	ANOVA	0.45	6.76	7.09	7	7.18
aconitase hydratase, mitochondrial	Ovis aries	XP_027827895.1	SEL1L	89 kDa	ANOVA	0.46	6.12	6.97	6.75	6.61
serpin A3-5	Ovis aries	XP_027823951.1	ACO2	85 kDa	ANOVA	0.46	7.77	8.2	7.96	7.84
serpin H1	Ovis aries	XP_027813163.1	LOC101115576	47 kDa	ANOVA	0.46	8.9	8.78	8.72	8.5
nodal modulator 1	Bos indicus	XP_01983080.1	SERPINH1	46 kDa	ANOVA	0.46	9.27	9.46	9.42	9.29
poly ADP-ribose] polymerase 1	Ovis aries	XP_014955983.2	LOC101111247	134 kDa	ANOVA	0.46	6.75	7.42	7.08	7.11
serpin A3-7-like	Ovis aries	XP_012042537.2	PARP1	113 kDa	ANOVA	0.46	5.84	7.12	6.45	5.4
serine/threonine-protein phosphatase PGAM5, mitochondrial isoform X1	Ovis aries	XP_011963749.2	LOC101115576	47 kDa	ANOVA	0.46	8.39	8.32	8.27	8.21
complement C5	Ovis aries	XP_004022113.1	HSID1B10	27 kDa	ANOVA	0.46	8.03	8.17	7.98	8.29
NADH dehydrogenase 1 alpha subcomplex subunit 12	Bos taurus	AAI04503.1	HSID1B2	35 kDa	ANOVA	0.46	7.29	7.47	7.53	7.52
mitochondrial carnitine/acylcarnitine carrier protein	Ovis aries	XP_004004015.2	ACO2	85 kDa	ANOVA	0.46	6.24	6.34	5.7	5.88
TOMM20	Ovis aries	XP_004008824.1	ATP5F1	18 kDa	ANOVA	0.46	6.89	7.08	7.17	7.32
40S ribosomal protein S3 isoform 2	Homo sapiens	NP_001247435.1	RP3	28 kDa	ANOVA	0.46	7.65	7.55	7.71	7.83
glyceraldehyde-3-phosphate dehydrogenase	Ovis aries	NP_00117739.1	GAPDH	36 kDa	ANOVA	0.46	8.39	7.99	8.43	8.49
SWI/SNF complex subunit SMARCC2	Camelus dromedarius	XP_031319512.3	SMARCC2	127 kDa	ANOVA	0.47	6.06	6.44	6.16	6.17
alpha-1B-glycoprotein	Ovis aries	XP_027834752.1	A1BG	54 kDa	ANOVA	0.47	8.36	8.51	8.39	8.43
persulfide dioxygenase ETHE1, mitochondrial isoform X1	Ovis aries	XP_027834207.1	ETHE1	22 kDa	ANOVA	0.47	7.4	7.6	7.46	7.58
ATPase family AAA domain-containing protein 3	Ovis aries	XP_027831593.1	LOC101105090	66 kDa	ANOVA	0.47	6.23	6.39	6.04	5.76
complement C5	Ovis aries	XP_004004015.2	LOC1011121825	189 kDa	ANOVA	0.47	8.14	8.06	8.13	8.22
NADH dehydrogenase 1 alpha subcomplex subunit 12	Bos taurus	AAI04503.1	NDUF1A2	17 kDa	ANOVA	0.47	6.24	6.47	6.39	6.57
mitochondrial amidoxime reducing component 2	Ovis aries	XP_001071404.1	SLC25A20	33 kDa	ANOVA	0.47	6.33	6.69	6.26	6.43
malate dehydrogenase, mitochondrial	EQUUS asinus	XP_014699026.1	HADHB	51 kDa	ANOVA	0.48	6.92	7.12	6.6	6.55
malate dehydrogenase, mitochondrial	Ovis aries	XP_012043312.3	MTACR2	37 kDa	ANOVA	0.48	6.34	6.38	6.62	6.91
delta(3,5)-Delta(2,4)-dienoyl-CoA isomerase, mitochondrial	Ovis aries	XP_004021309.2	MDH2	36 kDa	ANOVA	0.48	8.85	8.86	8.69	8.79
mitochondrial import receptor subunit TOMM20 homolog	Ovis aries	XP_004007043.2	TOMM22	15 kDa	ANOVA	0.48	6.51	6.72	6.22	6.93
sodium/potassium-transporting ATPase subunit alpha-1	Ovis aries	NP_001099360.1	ATP1A1	113 kDa	ANOVA	0.48	7.59	7.66	7.81	7.64
vesicle-associated membrane protein 3, partial	Bos mutus	ERLS8547.1	-	11 kDa	ANOVA	0.48	6.65	6.93	6.68	6.74
60S acidic ribosomal protein P2	Bos indicus	XP_019820217.1	RPLP2	13 kDa	ANOVA	0.49	6.79	6.92	6.83	7.11
Zinc transporter ZIP14 isoform X1	Ovis aries	XP_014948594.1	SLC39A14	54 kDa	ANOVA	0.49	6.78	6.12	Missing Value	Missing Value
immunoglobulin kappa light chain constant region, partial	Ovis aries	XP_027834753.1	C3	188 kDa	ANOVA	0.49	9.46	9.47	9.4	9.45
complement C3	Ovis aries	XP_027817731.1	EIF3B	89 kDa	ANOVA	0.49	Missing Value	6.6	Missing Value	6.36
eukaryotic translation initiation factor 3 subunit B	Ovis aries	XP_027821516.1	PGAMS	32 kDa	ANOVA	0.49	6.29	6.4	6.35	5.91
serine/threonine-protein phosphatase PGAM5, mitochondrial isoform X1	Ovis aries	XP_012034380.2	ERAP1	113 kDa	ANOVA	0.49	6.93	7.52	7.41	7.19
endoplasmic reticulum aminopeptidase 1 isoform X1	Ovis aries	XP_004015091.1	GOT2	48 kDa	ANOVA	0.49	8.01	8.23	8.05	8.08
aspartate aminotransferase, mitochondrial	Ovis aries	XP_004012087.1	PSMD12	53 kDa	ANOVA	0.49	Missing Value	5.98	Missing Value	6.03
26S proteasome non-ATPase regulatory subunit 12	Ovis aries	XP_004011893.1	DECRI	35 kDa	ANOVA	0.49	Missing Value	6.78	6.25	5.98
2,4-dienoyl-CoA reductase, mitochondrial	Ovis aries	XP_0040021309.2	DPBI	10 kDa	ANOVA	0.49	6.24	6.78	6.73	6.79
acyl-CoA-binding protein	Ovis aries	XP_004002719.1	COPA	130 kDa	ANOVA	0.49	6.92	6.52	6.95	6.9
coatomer subunit alpha isoform X1	Ovis aries	XP_004001742.1	COPIA	139 kDa	ANOVA	0.49	6.55	6.67	6.43	6.43
endoplasmic reticulum resident protein 29 precursor	Ovis aries	NP_001119826.1	ERP29	29 kDa	ANOVA	0.49	7.58	7.77	7.68	7.56
proteasome subunit alpha type-1	Bos taurus	NP_001070560.1	PPMA1	30 kDa	ANOVA	0.49	6.2	6.2	Missing Value	6.15
stearyl-CoA desaturase	Ovis aries	ACNS6166.1	SCD	42 kDa	ANOVA	0.49	6.2	6.11	Missing Value	Missing Value
Lipocalin/cytosolic fatty-acid binding domain-containing protein	Capra hircus	XP_017899918.1	LOC102183974	22 kDa	ANOVA	0.51	7.12	6.94	6.58	6.88
cytochrome b-c1 complex subunit 1, mitochondrial	Ovis aries	XP_011955483.2	LOC101110095	53 kDa	ANOVA	0.51	6.99	7.33	7.11	7.15
zona pellucida sperm-binding protein 2	Ovis aries	XP_004020876.3	ZP2	80 kDa	ANOVA	0.51	6.51	6.59	6.65	5.67
protein YIF1A isoform X2	Ovis aries	XP_004019740.1	YIF1A	32 kDa	ANOVA	0.51	5.39	6.32	6.32	6.37
60S ribosomal protein L6	Ovis aries	XP_004017428.1	LOC101109212	33 kDa	ANOVA	0.51	7.62	7.46	7.7	7.8
cathepsin B precursor	Ovis aries	NP_00295516.1	CTSB	37 kDa	ANOVA	0.51	6.61	6.48	6.5	6.95
inorganic pyrophosphatase 2, mitochondrial isoform X1	Bos taurus	XP_005207716.1	PPA2	39 kDa	ANOVA	0.52	6.67	6.64	6.69	6.86
inorganic pyrophosphatase 2, mitochondrial isoform X1	Ovis aries	XP_004018978.2	CFB	88 kDa	ANOVA	0.52	7.8	7.81	8.01	7.94
renin receptor	Ovis aries	XP_004008450.1	NDUF13	17 kDa	ANOVA	0.52	Missing Value	6.38	5.78	6.19
electron transfer flavoprotein subunit alpha, mitochondrial	Ovis aries	XP_004019791.1	NDUF13	43 kDa	ANOVA	0.54	6.54	Missing Value	Missing Value	6.41
26S proteasome non-ATPase regulatory subunit 13 isoform X2	Ovis aries	P20757.2	-	51 kDa	ANOVA	0.54	7.22	7.31	7.08	7.12
Angiotensinogen	Ovis aries	XP_027831878.1	MTX1	51 kDa	ANOVA	0.55	6.35	6.26	Missing Value	Missing Value
metaxin-1	Ovis aries	XP_027819014.1	AC54	79 kDa	ANOVA	0.55	6.18	6.49	6.49	6.57
long-chain-fatty-acid-CoA ligase 4 isoform X1	Ovis aries	XP_027834862.1	TOP2B	182 kDa	ANOVA	0.55	6.78	7.28	7.01	6.98

alpha-2-macroglobulin isoform X3	Ovis aries	XP_012030836.2	LOC101122940	164 kDa	ANOVA	0.59	8.5	8.45	8.39	8.28
4F2 cell-surface antigen heavy chain	Ovis aries	XP_004019669.2	SCL42	63 kDa	ANOVA	0.59	6.38	6.46	6.18	5.97
C3	Cervus elaphus hippelaphus	OWK124161.1	-	164 kDa	ANOVA	0.59	9.08	9.09	9.02	9.01
40S ribosomal protein S18	Camelus dromedarius	KAB1278269.1	-	8 kDa	ANOVA	0.59	6.11	6.21	6.2	6.46
RNA-binding protein 3 isoform X1	Odocoileus virginianus texanus	XP_020756899.1	RBM3	18 kDa	ANOVA	0.60	6.48	6.7	6.72	7.1
glia-derived nexin	Ovis aries	XP_004005018.1	SERPINE2	44 kDa	ANOVA	0.60	8.29	8.22	8.4	8.32
dnaI homolog subfamily C member 10	Ovis aries	XP_004004576.2	DNAJC10	91 kDa	ANOVA	0.60	5.72	6.8	6.48	5.88
transferrin receptor protein 1	Ovis aries	XP_004003050.1	TFRC	86 kDa	ANOVA	0.60	6.73	6.81	6.99	6.73
rab GDP dissociation inhibitor alpha	Ovis aries	NP_001155343.1	GDI1	51 kDa	ANOVA	0.60	6.47	6.58	6.1	6.46
isocitrate dehydrogenase 3 (NAD+)-gamma isoform a precursor	Bos taurus	AA46424.1	IDH3G	43 kDa	ANOVA	0.60	7.17	7.25	7.03	7.21
phospholysing phosphohistidine inorganic pyrophosphate phosphatase isoform X1	Ovis aries	XP_027816306.1	LHPP	29 kDa	ANOVA	0.61	5.55	5.35	Missing Value	5.54
serpin A3-1	Bos indicus	XP_019838879.1	LOC10957532	52 kDa	ANOVA	0.61	8.17	8.12	8.06	7.97
succinate-CoA ligase GDP-forming] subunit beta, mitochondrial	Ovis aries	XP_004018389.2	SUCLG2	47 kDa	ANOVA	0.61	7.16	7.3	7.14	7.35
protein transport protein Sec23A	Ovis aries	XP_004017955.1	SEC23A	86 kDa	ANOVA	0.61	Missing Value	6.84	6.41	6.46
serine protease HTRA2, mitochondrial	Ovis aries	XP_004006156.2	HTRA2	49 kDa	ANOVA	0.61	6.36	6.61	6.34	6.27
U2 small nuclear ribonucleoprotein B"	Bos taurus	NP_001179481.1	SNRPB2	25 kDa	ANOVA	0.61	6.33	6.44	6.69	6.73
ezrin	Ovis aries	XP_027828426.1	EZR	69 kDa	ANOVA	0.62	6.73	6.85	7.16	6.96
serpin A3-1	Ovis aries	XP_027813161.1	LOC101116892	46 kDa	ANOVA	0.62	8.87	8.89	8.75	8.65
insulin-like growth factor-binding protein complex acid labile subunit	Capra hircus	XP_017896378.1	IGFALS	66 kDa	ANOVA	0.62	6	6.57	Missing Value	6.49
COP-diacylglycerol-inositol 3-phosphatidyltransferase	Ovis aries	XP_004002094.2	CDPT	24 kDa	ANOVA	0.62	5.5	5.72	5.83	5.97
hydroxysteroid dehydrogenase-like protein 2	Ovis aries	XP_004004059.1	HSD2	45 kDa	ANOVA	0.62	6.86	6.84	6.79	6.86
estradiol 17-beta-dehydrogenase 1	Ovis aries	XP_027830302.1	HSD17B1	34 kDa	ANOVA	0.63	7.9	7.32	7.74	7.9
FUN14 domain-containing protein 2	Capra hircus	XP_017921255.1	LOC108638411	16 kDa	ANOVA	0.63	5.99	6.04	6.23	6.33
valacyclovir hydrolase isoform X2	Ovis aries	XP_004019198.3	BPH1	33 kDa	ANOVA	0.63	6.44	6.55	6.41	6.48
histone H1x	Ovis aries	XP_004018603.2	LOC101106288	22 kDa	ANOVA	0.63	7.65	7.9	7.85	7.72
F-actin-capping protein subunit alpha-1	Ovis aries	XP_004002380.1	CAPZA1	33 kDa	ANOVA	0.63	6.57	6.71	6.87	6.81
immunoglobulin lambda light chain F7-299	Capra hircus	AA4X5027.1	-	25 kDa	ANOVA	0.63	9.32	9.15	9.42	9.34
immunoglobulin light chain variable region, partial	Bos taurus	AAB6576.1	-	11 kDa	ANOVA	0.63	7.88	7.8	7.94	7.93
T-complex protein 1 subunit delta	Ovis aries	XP_019487682.2	LOC105608622	58 kDa	ANOVA	0.64	6.94	7.29	6.93	6.84
beta-2-glycoprotein 1	Ovis aries	XP_004013204.2	APOH	38 kDa	ANOVA	0.64	7.8	7.83	7.84	7.55
dihydrodiolipoyl dehydrogenase, mitochondrial	Ovis aries	XP_004007902.1	DLD	54 kDa	ANOVA	0.64	7	7.43	7.12	7.09
prostaglandin reductase 1	Ovis aries	XP_004004063.1	PTGR1	36 kDa	ANOVA	0.64	7.04	6.75	7.02	7.28
NADH dehydrogenase 1 beta subcomplex subunit 6	Ovis aries	NP_001172052.1	NDUFB6	16 kDa	ANOVA	0.64	6.45	6.77	6.63	6.59
immunoglobulin mu heavy chain variable region, partial	Capra hircus	ABX90001.1	-	16 kDa	ANOVA	0.64	6.33	6.41	5.96	Missing Value
fibrinogen gamma chain isoform X1	Ovis aries	XP_011952709.1	FGG	50 kDa	ANOVA	0.65	10.5	10.5	10.4	10.4
kininogen-1 isoform X2	Capra hircus	XP_005675214.1	KNG1	49 kDa	ANOVA	0.65	7.31	7.56	7.36	7.29
leucine-rich alpha-2-glycoprotein	Ovis aries	XP_004008643.2	LRG1	38 kDa	ANOVA	0.65	6.68	6.31	6.52	6.78
C-reactive protein	Ovis aries	XP_004002700.1	LOC101115145	25 kDa	ANOVA	0.65	7.65	7.49	7.58	7.83
serrate RNA effector molecule homolog isoform X1	Ovis aries	XP_027817707.1	SRRT	101 kDa	ANOVA	0.66	Missing Value	Missing Value	6.34	6.5
signal recognition particle receptor subunit beta	Ovis aries	XP_027816116.1	SRPRB	32 kDa	ANOVA	0.66	6.86	7.1	6.9	7.09
thioredoxin domain-containing protein 5	Ovis aries	XP_027814397.1	TXNDC5	54 kDa	ANOVA	0.66	7.5	7.7	7.6	7.45
T-complex protein 1 subunit alpha	Capra hircus	AA4X5027.1	-	25 kDa	ANOVA	0.66	6.59	6.94	6.96	6.9
vimentin	Ovis aries	ABPA48145.1	VIM	54 kDa	ANOVA	0.66	9.03	9.28	9.1	9
alpha-1,6-mannosylglycoprotein 6-beta-N-acetylgalactosaminyltransferase A	Ovis aries	XP_027820820.1	MGAT1	84 kDa	ANOVA	0.67	Missing Value	6.02	6.26	Missing Value
transmembrane protein 256	Ovis aries	XP_004012698.2	TMEM256	12 kDa	ANOVA	0.67	6.34	6.54	6.62	6.8
NADH dehydrogenase 1 alpha subcomplex subunit 5	Ovis aries	XP_004005221.1	LOC101114379	13 kDa	ANOVA	0.67	6.04	6.61	6.45	6.67
TPA: RNA binding motif protein 25	Bos taurus	DAZ5154.1	RBM25	115 kDa	ANOVA	0.67	5.8	6.02	6.24	5.95
bifunctional epoxide hydrolase 2	Ovis aries	XP_027820104.1	EPHX2	63 kDa	ANOVA	0.68	7.64	7.67	7.48	7.4
phosphate carrier protein, mitochondrial	Odocoileus virginianus texanus	XP_004002805.1	SLC25A3	40 kDa	ANOVA	0.68	7.63	7.82	7.38	7.78
78 kDa glucose-regulated protein	Ovis aries	XP_020730015.2	HSP45	72 kDa	ANOVA	0.68	9.28	9.48	9.37	9.34
transmembrane protein 56	Bos mutus	XP_005908781.1	LOC102271207	30 kDa	ANOVA	0.68	5.58	6.35	Missing Value	Missing Value
cytochrome b-c1 complex subunit 2, mitochondrial	Ovis aries	XP_004020879.1	LOC101120527	48 kDa	ANOVA	0.68	7.79	8	7.9	7.89
Putative ATP-dependent RNA helicase DDX17, partial	Bos mutus	ELR53727.1	-	80 kDa	ANOVA	0.68	6.74	7.06	7.12	7.11
alpha 1S casein	Bos taurus	ACGG63494.1	CSN1S1	24 kDa	ANOVA	0.68	5.76	5.69	5.98	5.86
Enoyl Coenzyme A hydratase, short chain, 1, mitochondrial	Bos taurus	AA09606.1	ECHS1	31 kDa	ANOVA	0.68	7.36	7.63	7.33	7.5
immunoglobulin lambda-6c light chain variable region, partial	Ovis aries	ABAB94913.1	-	12 kDa	ANOVA	0.68	6.94	6.95	6.58	7.15
alpha-2-macroglobulin-like	Vicugna pacos	XP_01256388.1	LOC10253880.8	165 kDa	ANOVA	0.69	7.78	7.79	7.7	7.57
C4b-binding protein alpha chain-like	Ovis aries	XP_02783030.1	KRT19	44 kDa	ANOVA	0.69	6.7	6.99	6.82	7.09
keratin, type I cytoskeletal 19	Bos indicus x Bos taurus	XP_02740887.1	LOC113899665	57 kDa	ANOVA	0.69	7.69	7.86	7.68	7.67
citrate synthase, mitochondrial-like	Capra hircus	XP_005690673.1	ATP1B1	35 kDa	ANOVA	0.69	Missing Value	6.98	6.68	6.62
sodium/potassium-transporting ATPase subunit beta-1	Ovis aries	XP_004005586.1	HSP45	72 kDa	ANOVA	0.69	9.3	9.5	9.39	9.37
endoplasmic reticulum chaperone Bip	Ovis aries	XP_004005056.2	A2K	26 kDa	ANOVA	0.69	7.41	7.48	7.58	7.38
adenylyl kinase 2, mitochondrial isoform x2	Ovis aries	XP_004004547.1	HIBCH	43 kDa	ANOVA	0.69	6.45	6.42	6.36	6.22
3-hydroxyisobutyryl-CoA hydrolase, mitochondrial isoform X1	Ovis aries	XP_004002896.2	PROS1	75 kDa	ANOVA	0.69	6.63	6.63	6.79	6.76
vitamin K-dependent protein S	Bos taurus	NP_001039663.1	PHB2	33 kDa	ANOVA	0.69	7.91	8.02	8.01	7.92
prothrombin	Bos taurus	CAAE1682.1	-	25 kDa	ANOVA	0.69	6.02	Missing Value	6.2	6.71
thrombospondin-1, partial	Cervus elaphus	ACT46910.1	HSP45	67 kDa	ANOVA	0.69	9.22	9.42	9.25	9.25
heat shock 70kDa protein 5 isoform 1	Homo sapiens	AAFI3605.1	HSP45	71 kDa	ANOVA	0.69	9.25	9.44	9.34	9.32
HSP90	Odocoileus virginianus texanus	XP_020768044.1	GBA1	60 kDa	ANOVA	0.70	6.32	6.88	5.96	6.25
glucosylceramidase	Capra hircus	XP_017898439.1	NAP1L4	44 kDa	ANOVA	0.70	6.2	6.12	6	5.74
nucleosome assembly protein 1-like 4 isoform X1	Ovis aries	XP_012033970.1	SIL1	55 kDa	ANOVA	0.70	5.96	6.15	6.15	Missing Value
nucleotide exchange factor SIL1 isoform X1	Bos taurus	NP_001029825.1	PPP1CB	27 kDa	ANOVA	0.70	6.62	6.39	6.46	6.67
serine/threonine-protein phosphatase PP1-beta catalytic subunit	Homo sapiens	BAA82664.1	PPP1CC	34 kDa	ANOVA	0.70	6.69	6.39	6.46	6.67
serine/threonine phosphatase 1 gamma, partial	Camelus dromedarius	XP_031319240.1	LOC105095187	29 kDa	ANOVA	0.71	6.6	6.75	6.67	6.67
NADH-cytochrome b5 reductase 3 isoform X2	Ovis aries	XP_027818905.1	EMD	30 kDa	ANOVA	0.71	5.99	6.05	5.52	5.8
emerin	Capra hircus	XP_017902886.1	PON2	39 kDa	ANOVA	0.71	6.63	6.83	6.76	6.69
serum paraoxonase/arylesterase 2	Ovis aries	XP_014958975.2	OAT	48 kDa	ANOVA	0.71	7.43	7.23	7.46	7.44
ornithine aminotransferase, mitochondrial	Ovis aries	XP_014956963.2	MSM01	35 kDa	ANOVA	0.71	6.87	6.83	6.76	7.09
methylsterol monooxygenase 1	Bos mutus	XP_014336459.1	NOPS8	62 kDa	ANOVA	0.71	6.09	6.46	6.35	6.1
nuclear protein 58 isoform X1	Bison bison	BISON1897.1	DPIAS	87 kDa	ANOVA	0.71	6.31	6.36	6.51	6.25
AP-2 complex subunit alpha-2, partial	Ovis aries	XP_005681801.1	ALB	69 kDa	ANOVA	0.71	10.4	10.6	10.4	10.4
serine/threonine-peptidase 1	Ovis aries	XP_004016255.1	TPP1	62 kDa	ANOVA	0.71	Missing Value	6.4	6.56	5.91
reticulocalbin-3	Ovis aries	XP_004015422.2	RCN3	38 kDa	ANOVA	0.71	6.68	6.84	6.59	6.44
cytochrome c oxidase subunit NDUF4A	Ovis aries	XP_004007802.1	NDUF4A	9 kDa	ANOVA	0.71	7.09	7.17	7.31	7.3
secretory carrier-associated membrane protein 3	Ovis aries	XP_004002634.2	SCAMP3	38 kDa	ANOVA	0.71	6.41	6.71	6.6	6.55
secretin receptor-associated membrane protein 3	Ovis aries	NP_001156518.1	PDIAS	60 kDa	ANOVA	0.71	6.48	6.68	6.43	Missing Value
protein disulfide-isomerase AS precursor	Ovis aries	NP_00115985.1	DKC1	57 kDa	ANOVA	0.71	6.95	6.67	Missing Value	Missing Value
N/H4A ribonucleoprotein complex subunit DCK1	Ovis aries	NP_001218692.1	ME1	64 kDa	ANOVA	0.71	Missing Value	6.55	Missing Value	6.46
NADP-dependent malic enzyme	Ovis aries	XP_027818801.1	DPP7	54 kDa	ANOVA	0.72	Missing Value	6.51	Missing Value	5.9
dipeptidyl peptidase 2	Ovis aries	XP_00401852.1	CTQBP	30 kDa	ANOVA	0.72	7.16	7.24	7.27	7.01
complement component 1 Q subcomponent-binding protein, mitochondrial	Ovis aries	XP_004006762.2	LOC101119895	21 kDa	ANOVA	0.72	7.11	7.01	7.01	7.29
TIMP-1 protein, partial	Bos taurus	AAD303.1	-	19 kDa	ANOVA	0.72	6.63	Missing Value	6.73	6.6
immunoglobulin alpha heavy chain, partial	Ovis aries	AAC4980.1	-	50 kDa	ANOVA	0.72	6.69	6.82	6.28	6.53
CAMP-dependent protein kinase type II-beta regulatory subunit	Ovis aries	XP_027824390.1	PRKAR2B	46 kDa	ANOVA	0.73	6.73	6.96	6.73	6.94
NAD-dependent protein deacetylase sirtuin-5, mitochondrial	Capra hircus	XP_017894704.1	SIRT3	34 kDa	ANOVA	0.73	6.19	6.36	6.06	6.3
alpha-1,1-tritypsin transcript variant 1	Ovis aries	XP_004001852.1	THRAP3	109 kDa	ANOVA					

torsin-1A-interacting protein 2	XP_004013887.2	LOC101122123	52 kDa	ANOVA	0.78	6.03	6.34	6.25	6.17	
proteasome subunit beta type-5	XP_004010385.1	PSMB5	29 kDa	ANOVA	0.78	Missing Value	6.08	5.72	6.35	
NADH dehydrogenase [ubiquinone] 1 alpha subcomplex subunit 10, mitochondrial isoform X1	XP_004018082.0	NDUF10	40 kDa	ANOVA	0.78	7.3	7.16	7.11	7.02	
catechol O-methyltransferase	XP_027812737.1	COMT	30 kDa	ANOVA	0.79	6.74	6.72	6.5	6.74	
serpin A3-S isoform X1	XP_017921950.1	LOC102174166	52 kDa	ANOVA	0.79	8.53	8.52	8.38	8.44	
medium-chain specific acyl-CoA dehydrogenase, mitochondrial	XP_017901046.1	LOC102190925	37 kDa	ANOVA	0.79	6.27	6.43	6.23	6.38	
hexokinase-2	XP_014949962.2	HK2	102 kDa	ANOVA	0.79	Missing Value	6.47	Missing Value	Missing Value	
proteasome activator complex subunit 2 isoform X2	XP_005685286.1	PSME2	27 kDa	ANOVA	0.79	6.61	5.63	6.13	6.48	
isocitrate dehydrogenase	XP_004018103.4	IDH2	51 kDa	ANOVA	0.79	7.38	7.46	7.2	7.43	
GPI-anchor transamidase	XP_004002140.1	PIGK	45 kDa	ANOVA	0.79	6.49	6.56	6.51	6.36	
ER membrane protein complex subunit 4	NP_001029719.1	EMC4	20 kDa	ANOVA	0.79	Missing Value	5.91	Missing Value	5.93	
immunoglobulin lambda 1 light chain, partial	ABU90640.1		23 kDa	ANOVA	0.79	9.01	9.09	9.14	8.93	
cell cycle and apoptosis regulator protein 2 isoform X4	XP_027820136.1	CCAR2	102 kDa	ANOVA	0.80	6.24	Missing Value	6.34	6.23	
T-complex protein 1 subunit epsilon isoform X2	XP_014334869.1	CCT5	56 kDa	ANOVA	0.80	6.9	6.84	6.85	6.53	
NSFL1 cofactor p47 isoform X1	XP_004014502.1	NSFL1C	41 kDa	ANOVA	0.80	6.21	6.5	Missing Value	6.24	
prothrombin precursor	NP_001159667.1	F2	70 kDa	ANOVA	0.80	7.8	7.74	7.76	7.9	
stathmin 1	BAG70133.1	STMN1	17 kDa	ANOVA	0.80	5.99	6.22	6.31	6.37	
peroxiredoxin-5	AGA19346.1	PRDX5	17 kDa	ANOVA	0.80	Missing Value	6.2	Missing Value	6.09	
dehydrogenase/reductase SDR family member 7B isoform X1	XP_027830550.1	DHRS7B	39 kDa	ANOVA	0.81	5.78	6.09	6.4	6.08	
primary amine oxidase, liver isozyme	XP_027830273.1	LOC101112834	91 kDa	ANOVA	0.81	7.74	7.7	7.77	7.85	
haloacid dehalogenase-like hydrolase domain-containing 5 isoform X1	XP_027823864.1	HDHD5	44 kDa	ANOVA	0.81	6.34	6.42	6.14	6.31	
cytoplasmic dynein 1 heavy chain 1	XP_027813216.1	DYNC1H1	532 kDa	ANOVA	0.81	Missing Value	Missing Value	Missing Value	5.9	
interleukin enhancer-binding factor 3 isoform X1	Capra hircus	XP_010831132.1	RUVBL1	50 kDa	ANOVA	0.81	Missing Value	6.81	Missing Value	6.24
rub-B-like	Bison bison bison	XP_005682280.1	PGLYRP2	64 kDa	ANOVA	0.81	6.26	Missing Value	6.17	Missing Value
N-acetylmuramoyl-L-alanine amidase	Capra hircus	XP_017906557.1	ILF3	96 kDa	ANOVA	0.81	6.52	6.59	6.82	6.48
complement C1q subcomponent subunit A isoform X1	Ovis aries	XP_004005192.1	C1QA	34 kDa	ANOVA	0.81	7.25	7.23	7.39	6.97
U6 snRNA-associated Sm-like protein LSM3	Bos taurus	NP_001032564.1	LSM3	12 kDa	ANOVA	0.81	5.79	5.75	5.82	5.84
malate dehydrogenase, cytoplasmic isoform MDH1	Bos taurus	NP_001029800.1	MDH1	36 kDa	ANOVA	0.81	6.74	6.55	6.48	6.82
guanine nucleotide-binding protein subunit alpha-13	Ovis aries	XP_014954475.2	GNA13	44 kDa	ANOVA	0.82	6.64	6.83	6.77	6.76
catalase isoform X1	Ovis aries	XP_004016445.1	CAT	60 kDa	ANOVA	0.82	7.3	7.48	7.22	7.19
rho GDP-dissociation inhibitor 1	Bos taurus	NP_788823.1	ARHGDI	23 kDa	ANOVA	0.82	6.6	6.75	6.56	6.8
nuclear mitotic apparatus protein 1 isoform X1	Ovis aries	XP_027835270.1	NUMA1	237 kDa	ANOVA	0.83	Missing Value	6.5	Missing Value	Missing Value
small integral membrane protein 1	Ovis aries	XP_027831530.1	SMM1	9 kDa	ANOVA	0.83	Missing Value	6.18	5.61	6.09
complement C3-like	Equus caballus	XP_025003563.1	LOC1000650505	186 kDa	ANOVA	0.83	8.51	8.46	8.54	8.5
nucleolin	Bos mutus	XP_014336327.1	LOC102278736	113 kDa	ANOVA	0.83	6.85	7.04	7.06	6.68
annexin A5	Ovis aries	XP_012034784.2	ANXA5	36 kDa	ANOVA	0.83	7.34	7.28	7.38	7.45
plasma serine protease inhibitor	Ovis aries	XP_004018025.1	SERPINAS	45 kDa	ANOVA	0.83	6.69	6.92	6.81	6.86
heat shock 70kDa protein 5 (glucose-regulated protein, 78kDa), isoform CRA_b	Homo sapiens	EWAS7621.1	-	51 kDa	ANOVA	0.83	9.08	9.24	9.05	9.1
CD14 antigen	Ovis aries	AIB95799.1	-	40 kDa	ANOVA	0.83	6.1	6.64	6.05	Missing Value
glutathione peroxidase 3	Ovis aries	XP_014951639.1	GPK3	26 kDa	ANOVA	0.84	6.91	7.03	7.03	6.49
MICOS complex subunit MIC13 isoform X1	Ovis aries	XP_012033429.2	MICOS13	15 kDa	ANOVA	0.84	5.66	Missing Value	5.83	6.46
multifunctional methyltransferase subunit TRM12-like protein	Ovis aries	XP_00419703.2	TRMT12	14 kDa	ANOVA	0.84	6.21	6.23	6.07	6.15
OCIA domain-containing protein 1 isoform X1	Ovis aries	XP_004008961.9	OCA1D	28 kDa	ANOVA	0.84	Missing Value	6.27	Missing Value	Missing Value
endoplasmic reticulum resident protein 44	Ovis aries	XP_004004270.1	ERP44	47 kDa	ANOVA	0.84	7.69	7.8	7.82	7.63
regulator complex protein LAMTOR3	Bos taurus	NP_001069450.1	LAMTOR3	14 kDa	ANOVA	0.84	5.87	6.14	6.09	6.1
RNA-binding protein 128	Ovis aries	XP_027829033.1	RBM12B	116 kDa	ANOVA	0.85	Missing Value	6.42	Missing Value	Missing Value
coatomer subunit gamma-1	Ovis aries	XP_027813655.1	COPG1	97 kDa	ANOVA	0.85	6.79	6.73	6.99	6.9
ADP-ribose pyrophosphatase, mitochondrial	Capra hircus	XP_005681938.1	NUDT9	39 kDa	ANOVA	0.85	Missing Value	5.93	6.33	6.14
hemopexin	Ovis aries	XP_004016259.1	HPX	52 kDa	ANOVA	0.85	8.56	8.31	8.53	8.42
Parathymosin	Bos taurus	P08814.2	PTMS	11 kDa	ANOVA	0.85	5.48	Missing Value	Missing Value	5.77
serpin A3-6 precursor	Bos taurus	NP_00139774.1	SERPINA3-6	46 kDa	ANOVA	0.85	8.3	8.18	8.3	8.15
beta-2-microglobulin	Ovis aries	ABP27878.1	-	14 kDa	ANOVA	0.85	6.65	6.77	Missing Value	6.99
transaldolase	Ovis aries	XP_027815783.1	TALDO1	38 kDa	ANOVA	0.86	6.06	6.3	6.36	6.53
heat shock protein 75 kDa, mitochondrial	Ovis aries	XP_014959382.1	TRAP1	79 kDa	ANOVA	0.86	7.54	7.77	7.68	7.54
deoxyribonuclease-1-like 1, partial	Ovis aries	XP_004227020.1	DNASE1L	36 kDa	ANOVA	0.86	6.08	6.16	Missing Value	Missing Value
cytochrome b-c1 complex subunit Rieske, mitochondrial	Ovis aries	XP_004194543.1	LOC101113001	30 kDa	ANOVA	0.86	Missing Value	6.46	Missing Value	6.23
adipocyte plasma membrane-associated protein	Ovis aries	XP_004143562.2	APPMAP	46 kDa	ANOVA	0.86	7.82	7.95	7.76	7.73
cytochrome c oxidase assembly factor 1 homolog	Bos taurus	NP_001029428.1	COA1	15 kDa	ANOVA	0.86	Missing Value	5.88	Missing Value	6.32
succinate-CoA ligase [ADP-forming] subunit beta, mitochondrial	Ovis aries	XP_027829360.1	SUCL2A1	51 kDa	ANOVA	0.87	Missing Value	6.72	6.1	6.23
nicalin isoform X1	Ovis aries	XP_027825701.1	NCLN	63 kDa	ANOVA	0.87	6.46	6.67	6.41	6.18
3-ketoacyl-CoA thiolase, mitochondrial isoform X2	Ovis aries	XP_027816604.1	ACAA2	42 kDa	ANOVA	0.87	7.36	7.33	7.14	7.22
phosphoglucomutase-2 isoform X1	Ovis aries	XP_014951922.2	PGM2	69 kDa	ANOVA	0.87	6.17	6.49	Missing Value	6.53
coiled-coil domain-containing protein 167	Capra hircus	XP_005696338.3	CCDC167	13 kDa	ANOVA	0.87	4.89	5.52	5.31	5.52
glucose-6-phosphate isomerase	Ovis aries	XP_004015200.2	GPI	63 kDa	ANOVA	0.87	6.54	6.8	6.24	6.61
elongation factor 1-t	Ovis aries	XP_004006563.3	TSFM	37 kDa	ANOVA	0.87	6.41	6.12	5.73	6.11
elongation factor 2, mitochondrial	Bos taurus	NP_001069561.1	CNRP1	19 kDa	ANOVA	0.87	Missing Value	5.83	Missing Value	6.08
CB1 cannabinoid receptor-interacting protein 1	Bos taurus	NP_001029544.1	ABHD11	34 kDa	ANOVA	0.87	6.7	6.67	6.47	6.49
protein ABHD11	Bos indicus	XP_019812404.1	ATP5PB	29 kDa	ANOVA	0.88	7.2	7.1	7.01	7.38
ATP synthase F(0) complex subunit B1, mitochondrial	Capra hircus	XP_017909833.1	RTRAF	28 kDa	ANOVA	0.88	6.49	Missing Value	Missing Value	6.18
UFOS56 protein C1orf166 homolog	Ovis aries	XP_004003349.1	COPB2	102 kDa	ANOVA	0.88	6.5	6.7	6.93	6.8
coatomer subunit beta'	Bos taurus	NP_001075916.1	SEPTIN11	49 kDa	ANOVA	0.88	Missing Value	6.37	Missing Value	5.78
septin-11	Ovis aries	NP_001009449.1	EFF1D	31 kDa	ANOVA	0.88	7.35	7.38	7.43	7.42
elongation factor 1-delta	Bos mutus	XP_005809618.1	SAMM50	58 kDa	ANOVA	0.89	Missing Value	6.37	Missing Value	Missing Value
sorting and assembly machinery component 50 homolog	Ovis aries	XP_005699833.1	CNRP1	14 kDa	ANOVA	0.89	6.98	7.19	7.09	7.15
elongation factor 1-gamma	Ovis aries	XP_027825701.1	NCLN	63 kDa	ANOVA	0.89	6.59	6.95	6.67	6.15
serine hydroxymethyltransferase, mitochondrial isoform X1	Ovis aries	XP_004017038.1	GPK8	24 kDa	ANOVA	0.89	5.76	6.15	5.9	Missing Value
probable glutathione peroxidase 8 isoform X1	Ovis aries	XP_004101460.2	MTHFD1L	105 kDa	ANOVA	0.89	5.86	6.2	6.06	Missing Value
monofunctional C1-tetrahydrofolate synthase, mitochondrial	Ovis aries	XP_004009686.1	HADH	34 kDa	ANOVA	0.89	6.68	6.71	6.69	6.54
hydroxycyclin-coenzyme A dehydrogenase, mitochondrial	Ovis aries	AAB49491.1	ABHD8	12 kDa	ANOVA	0.89	6.84	6.56	6.94	6.65
immunoglobulin lambda-6a light chain variable region, partial	Ovis aries	XP_027826972.1	WFS1	100 kDa	ANOVA	0.90	Missing Value	6.35	Missing Value	Missing Value
wolframin	Capra hircus	XP_017905340.1	MFSD10	62 kDa	ANOVA	0.90	Missing Value	5.72	5.9	5.76
major facilitator superfamily domain-containing protein 10 isoform X1	Ovis aries	XP_001196180.1	APOO	23 kDa	ANOVA	0.91	6.1	6.17	6.14	6.25
B-cell receptor-associated protein 31	Capra hircus	XP_017908268.1	BCAP31	28 kDa	ANOVA	0.91	Missing Value	6.07	5.59	6.23
aldose reductase	Ovis aries	XP_004008126.1	AKR1B1	36 kDa	ANOVA	0.91	6.81	6.46	6.71	6.91
eukaryotic translation initiation factor 3 subunit L isoform X1	Ovis aries	XP_004007031.1	EIF3L	67 kDa	ANOVA	0.91	Missing Value	6.1	Missing Value	6.03
Aldo-keto reductase family 1 member B1	Bos taurus	P16116	36 kDa	ANOVA	0.91	6.94	6.61	6.51	6.58	
solute carrier family 12 member 7 isoform X1	Ovis aries	XP_02782112.1	NCL	79 kDa	ANOVA	0.91	7.33	7.16	7.57	7.41
serine/threonine-protein phosphatase 2A 65 kDa regulatory subunit A alpha isoform-like	Bos indicus x Bos taurus	XP_027369917.1	LOC1011375586	65 kDa	ANOVA	0.91	6.5	6.54	6.36	6.31
cytochrome b-type B isoform X2	Ovis aries	XP_014956033.1	LOC101121621	16 kDa	ANOVA	0.91	7.44	7.39	7.44	7.6
MICOS complex subunit MIC26 isoform X1	Ovis aries	XP_001196180.1	APOO	23 kDa	ANOVA	0.91	6.1	6.17	6.14	6.25
NADH dehydrogenase 1 alpha subcomplex subunit 9, mitochondrial	Capra hircus	XP_005681037.1	NDUFQ9	43 kDa	ANOVA	0.91	7.16	7.07	7.02	7.1
transketolase	Ovis aries	XP_004018343.1	TKT	68 kDa	ANOVA	0.91	6.82	6.8	6.6	6.77
TPA: Ikeract protein (serine-arginine rich) 1-like	Bos taurus	DAAI8755.1	FUSIP1	31 kDa	ANOVA	0.91	6.68	6.9	6.95	6.95
ras related v-ras simian leukemia viral oncogene homolog A, partial	Ovis aries	ABF5737.1	RALA	21 kDa	ANOVA	0.91	Missing Value	6.22	6.01	5.89
immunoglobulin heavy chain precursor, partial	Bos taurus	AAD52601.1	RAHDH	13 kDa	ANOVA	0.91	6.83	6.29	6.6	6.63
solute carrier family 12 member 7 isoform X1	Ovis aries	XP_027835994.1	SCLC1A7	119 kDa	ANOVA	0.92	Missing Value	6.28	Missing Value	Missing Value
dolichol-phosphate mannosyltransferase subunit 1	Ovis aries	XP_027833130.1	DPM1	30 kDa	ANOVA	0.92	6.98	6.88	7.01	6.93
zinc-alpha-2-glycoprotein	Ovis aries	XP_011960249.3	ME2	65 kDa	ANOVA					

annexin A4	XP_004005861.1	ANXA4	36 kDa	ANOVA	0.95	7.65	7.49	7.62	7.43
2-amino-3-ketobutyrate coenzyme A ligase, mitochondrial	EPY88370.1	-	62 kDa	ANOVA	0.95	6.56	6.57	6.55	6.61
7-dehydrocholesterol reductase	XP_027815288.1	DHC7R	54 kDa	ANOVA	0.96	7.06	7	6.94	6.89
serpin A3-1 isoform X1	XP_019838877.1	LOC109575331	51 kDa	ANOVA	0.96	8.27	8.2	8.28	8.15
protein ABHD11 isoform X2	XP_004021304.1	ABHD11	33 kDa	ANOVA	0.96	7.31	7.26	7.29	7.31
enoyl-CoA delta isomerase 1, mitochondrial isoform X2	XP_004020766.1	EC11	33 kDa	ANOVA	0.96	6.45	6.01	5.76	6.09
glutamine-tRNA ligase	XP_004018519.2	QARS1	87 kDa	ANOVA	0.96	Missing Value	6.55	5.84	Missing Value
inositol-3-phosphate synthase 1	NP_001039497.1	ISYNAA1	61 kDa	ANOVA	0.96	5.99	5.96	Missing Value	5.1
complement component C3d, partial	ABR24137.1	-	34 kDa	ANOVA	0.96	8.82	8.78	8.87	8.75
manganese-transporting ATPase 13A1	XP_014338681.1	ATP13A1	140 kDa	ANOVA	0.97	6.07	6.13	5.72	5.95
plasminogen isoform X1	XP_012038601.1	PLG	90 kDa	ANOVA	0.97	8	8.13	8.1	8.02
2-methoxy-6-propenyl-1,4-benzoquinol methylase, mitochondrial	XP_005891545.1	CQQS	38 kDa	ANOVA	0.97	Missing Value	6.1	Missing Value	Missing Value
MICOS complex subunit MIC27	XP_004022778.1	APOOL	29 kDa	ANOVA	0.97	Missing Value	Missing Value	6.13	5.67
eukaryotic translation initiation factor 3 subunit C	XP_004020914.1	EIF3C	105 kDa	ANOVA	0.97	6.33	6.33	6.02	5.76
sarcoplasmic membrane-associated protein isoform X2	XP_004018415.1	SLMAP	97 kDa	ANOVA	0.97	Missing Value	Missing Value	Missing Value	6.21
heme-binding protein 1	XP_004006893.1	HEBP1	21 kDa	ANOVA	0.97	5.87	5.7	5.8	6.41
26S proteasome non-ATPase regulatory subunit 5	XP_0040004072.2	PMSD5	56 kDa	ANOVA	0.97	Missing Value	5.93	Missing Value	5.36
beta-1,3-glucosyltransferase	XP_027829425.1	B3GLCT	56 kDa	ANOVA	0.98	6.01	5.83	Missing Value	Missing Value
syntaxin-18 isoform X2	XP_027826981.1	STX18	30 kDa	ANOVA	0.98	6.09	5.52	5.9	5.47
long-chain-fatty-acid-CoA ligase 3	XP_027821040.1	ACSL3	80 kDa	ANOVA	0.98	6.33	Missing Value	Missing Value	5.74
chitinase domain-containing protein 1	XP_027815774.1	CHID1	46 kDa	ANOVA	0.98	6.85	7.03	6.91	7.08
heterogeneous nuclear ribonucleoprotein H-like	XP_020756619.1	LOC101141932	48 kDa	ANOVA	0.98	Missing Value	6.08	6.15	6.04
tubulin alpha-1C chain	XP_017903331.1	LOC102178426	50 kDa	ANOVA	0.98	8.06	7.92	7.95	7.8
craniofacial development protein 2	XP_012044952.1	LOC101127269	66 kDa	ANOVA	0.98	Missing Value	Missing Value	Missing Value	6.81
enoyl-[acyl-carrier-protein] reductase, mitochondrial isoform X2	XP_012005634.3	MECR	40 kDa	ANOVA	0.98	6.1	6.1	Missing Value	Missing Value
annexin A7	XP_011960675.2	ANXA7	50 kDa	ANOVA	0.98	Missing Value	6.44	Missing Value	5.92
translocase-associated protein subunit delta isoform X1	XP_004010328.1	PKM	58 kDa	ANOVA	0.98	7.28	7.11	7.42	7.13
pyruvate kinase PKM isoform X2	XP_004007077.1	POLDIP3	46 kDa	ANOVA	0.98	6.06	6.12	Missing Value	Missing Value
polymerase delta-interacting protein 3 isoform X1	XP_004005800.1	PREB	46 kDa	ANOVA	0.98	Missing Value	5.92	5.73	
prolactin regulatory element-binding protein isoform X1	XP_004002637.2	FDPS	40 kDa	ANOVA	0.98	Missing Value	6.56	6.02	Missing Value
farnesyl pyrophosphate synthase	NP_001138656.1	SLIRP	12 kDa	ANOVA	0.98	5.46	5.68	5.62	Missing Value
SRA stem-loop-interacting RNA-binding protein, mitochondrial	AAD33073.1	ENO1	47 kDa	ANOVA	0.98	7.99	7.68	7.84	7.69
alpha enolase	XP_027826816.1	ENOS	93 kDa	ANOVA	0.99	5.94	6	Missing Value	Missing Value
mulfunctional protein ADE2 isoform X2	XP_027813542.1	SACM1L	61 kDa	ANOVA	0.99	6.05	6.24	Missing Value	6.16
phosphatidylinositol phosphatase SAC1 isoform X2	XP_020727988.1	IVD	53 kDa	ANOVA	0.99	Missing Value	Missing Value	6.67	
isovaleryl-CoA dehydrogenase, mitochondrial isoform X2	XP_019831842.1	PRDX6	25 kDa	ANOVA	0.99	6.71	6.42	6.48	6.52
peroxiredoxin-6	XP_004022354.1	F9	52 kDa	ANOVA	0.99	6.21	6.54	6.36	5.94
coagulation factor IX	XP_004022186.1	UBA1	118 kDa	ANOVA	1.00	Missing Value	6.75	6.34	6.28
band 3 anion transport protein	XP_004018542.2	LOC101112427	19 kDa	ANOVA	1.00	Missing Value	5.72	Missing Value	
lumican	XP_004006300.1	LUM	39 kDa	ANOVA	0.99	7.17	7.04	6.97	6.94
NADH dehydrogenase 1 beta subcomplex subunit 5, mitochondrial isoform X1	XP_005227728.1	SSR4	19 kDa	ANOVA	0.98	7.65	7.63	7.54	7.62
nuclearular helicase 2	XP_004010328.1	PKM	58 kDa	ANOVA	0.98	7.28	7.11	7.42	7.13
beta-hexosaminidase subunit alpha precursor	XP_027815342.1	ACLY	121 kDa	ANOVA	0.99	6.11	6.13	Missing Value	Missing Value
ATP-citrate synthase	XP_001033711.1	ACLY	121 kDa	ANOVA	0.99	6.3	5.99	6.35	6.4
glutamine-fructose-6-phosphate aminotransferase [isomerizing] 2	XP_004018642.1	PTGRN	53 kDa	ANOVA	0.99	Missing Value	Missing Value	6.67	
alpha-tubulin, partial	XP_004022352.1	PTGRN	53 kDa	ANOVA	0.99	6.71	6.42	6.48	6.52
ubiquitin-like modifier-activating enzyme 1	XP_004022186.1	UBA1	118 kDa	ANOVA	1.00	Missing Value	6.75	6.34	6.28
cathelicidin-7	XP_004015361.3	TOMM40	38 kDa	ANOVA	1.00	Missing Value	5.72	Missing Value	
mitochondrial import receptor subunit TOM40 homolog	XP_004013942.1	COLGALT2	73 kDa	ANOVA	1.00	Missing Value	6.54	6.13	6.35
procollagen galactosyltransferase 2	XP_004013652.2	PTPR1	170 kDa	ANOVA	1.00	5.92	Missing Value	Missing Value	6.2
bifunctional glutamate/proline-tRNA ligase	XP_004003269.2	PTX3	42 kDa	ANOVA	1.00	Missing Value	6.49	6.2	
penetrin-related protein PTX3	XP_004003269.2	PTX3	42 kDa	ANOVA	1.00	6	Missing Value	Missing Value	6.07
tapasin precursor	XP_027835128.1	OAF	31 kDa	ANOVA	--	Missing Value	Missing Value	Missing Value	
out at first protein homolog	XP_027833512.1	OAF	31 kDa	ANOVA	--	Missing Value	Missing Value	Missing Value	
liver carboxylesterase-like	XP_027833512.1	OAF	31 kDa	ANOVA	--	Missing Value	Missing Value	Missing Value	
presequence protease, mitochondrial	XP_027832607.1	PITRM1	116 kDa	ANOVA	--	Missing Value	Missing Value	Missing Value	
torsin-1A-interacting protein 1 isoform X1	XP_027831718.1	TOR1AIP1	69 kDa	ANOVA	--	Missing Value	Missing Value	Missing Value	
von Willebrand factor A domain-containing protein 1	XP_027831601.1	VWA1	44 kDa	ANOVA	--	Missing Value	6.67	Missing Value	
prostaglandin F2 receptor negative regulator	XP_027831367.1	PTGRN	100 kDa	ANOVA	--	Missing Value	Missing Value	Missing Value	
ceramide synthase 2	XP_027830326.1	CERS2	45 kDa	ANOVA	--	Missing Value	6.53	Missing Value	
fatty acid synthase	XP_027830105.1	FASN	274 kDa	ANOVA	--	Missing Value	Missing Value	Missing Value	
lysosomal alpha-glucosidase	XP_027830043.1	GAA	105 kDa	ANOVA	--	Missing Value	Missing Value	Missing Value	6.51
D-3-phosphoglycerate dehydrogenase	XP_027829492.1	PGDH	56 kDa	ANOVA	--	Missing Value	Missing Value	Missing Value	
DNA replication licensing factor MCM4	XP_027828737.1	MCM4	94 kDa	ANOVA	--	Missing Value	Missing Value	Missing Value	
platelet glycoprotein 4	XP_027824393.1	LOC1011151515	53 kDa	ANOVA	--	Missing Value	Missing Value	Missing Value	
ribosomal RNA small subunit methyltransferase NEP1 isoform X1	XP_027823724.1	EMG1	29 kDa	ANOVA	--	5.73	Missing Value	Missing Value	
trans-Golgi network integral membrane protein 2	XP_027823511.1	TGNOLN2	36 kDa	ANOVA	--	Missing Value	Missing Value	Missing Value	
carnitine O-acetyltransferase isoform X2	XP_027822120.3	CRAT	71 kDa	ANOVA	--	Missing Value	Missing Value	Missing Value	
protein transport protein Sec16A isoform X1	XP_027821966.1	SEC16A	250 kDa	ANOVA	--	Missing Value	Missing Value	Missing Value	
high mobility group protein B3	XP_027819221.1	HMG83	23 kDa	ANOVA	--	Missing Value	Missing Value	Missing Value	
acid ceramidase	XP_027818540.1	ASAH1	45 kDa	ANOVA	--	Missing Value	5.8	Missing Value	
DNA replication licensing factor MCM7 isoform X1	XP_027818515.1	MCM7	81 kDa	ANOVA	--	Missing Value	Missing Value	Missing Value	
bifunctional 2'-phosphoadenosine 5'-phosphosulfate synthase 2	XP_027818165.1	PAPS2	70 kDa	ANOVA	--	Missing Value	Missing Value	Missing Value	
ribonuclease inhibitor isoform X1	XP_027815764.1	RNH1	52 kDa	ANOVA	--	Missing Value	Missing Value	Missing Value	
serum amyloid A protein-like	XP_027815397.1	LOC105604171	15 kDa	ANOVA	--	Missing Value	Missing Value	Missing Value	
BOLA class I histocompatibility antigen, alpha chain BL3-7-like isoform X4	XP_027814691.1	SLC16A9	143 kDa	ANOVA	--	Missing Value	6.07	Missing Value	
cytosol 10-gene tetrameric protein	XP_027813689.1	ALDH11	99 kDa	ANOVA	--	Missing Value	Missing Value	Missing Value	
laminin subunit beta-2 isoform X1	XP_027813448.1	LOC101106719	196 kDa	ANOVA	--	Missing Value	Missing Value	Missing Value	
semaphorin-7A	XP_027812996.3	SEMA7	75 kDa	ANOVA	--	Missing Value	Missing Value	Missing Value	6.24
glutathione S-transferase theta-3 isoform X3	XP_027812644.1	LOC101118990	27 kDa	ANOVA	--	Missing Value	Missing Value	Missing Value	
seleoprotein M	XP_027812608.1	SELENO1	16 kDa	ANOVA	--	Missing Value	Missing Value	Missing Value	
protein NipSnap homolog 1 isoform X1	XP_027812531.1	NIPSNAP1	33 kDa	ANOVA	--	Missing Value	6.68	Missing Value	
squamous cell carcinoma antigen recognized by T-cells 3 isoform X2	XP_027812531.1	SART3	109 kDa	ANOVA	--	Missing Value	Missing Value	Missing Value	
extended synaptotagmin-2	XP_027812464.1	SYNT2	107 kDa	ANOVA	--	Missing Value	Missing Value	Missing Value	
Bubalus bubalis	XP_025134345.1	SNRNPA0	43 kDa	ANOVA	--	Missing Value	5.88	Missing Value	
Bos taurus	XP_024848786.1	-	25 kDa	ANOVA	--	Missing Value	Missing Value	Missing Value	
annexin A1	XP_02077194.1	ANXA1	39 kDa	ANOVA	--	Missing Value	6.23	Missing Value	
histone H3.3C-like	XP_020757183.1	LOC101142384	20 kDa	ANOVA	--	Missing Value	Missing Value	Missing Value	
protein disulfide-isomerase TMX3	XP_019841967.1	TMX3	65 kDa	ANOVA	--	Missing Value	Missing Value	6.31	Missing Value
lysine-tRNA ligase isoform X1	XP_019843247.1	KARS1	71 kDa	ANOVA	--	Missing Value	Missing Value	Missing Value	
mitochondrial import inner membrane translocase subunit Tim8	XP_019811827.1	TIMM8A	11 kDa	ANOVA	--	Missing Value	Missing Value	Missing Value	
chromoblast protein homolog 1 isoform X1	XP_019728922.1	B2GALT6	37 kDa	ANOVA	--	Missing Value	Missing Value	Missing Value	
flavin reductase (NADPH)	XP_019728922.1	FLVRB	22 kDa	ANOVA	--	Missing Value	Missing Value	Missing Value	
prolyl 3-hydroxylase 3	XP_019704043.1	P3H3	80 kDa	ANOVA	--	Missing Value	Missing Value	Missing Value	
keratin, type II cuticular Hb1	XP_019704043.1	PTPR1	14 kDa	ANOVA	--	Missing Value	Missing Value	Missing Value	
phosphohistidine phosphatase	XP_019704043.1	PTPR1	14 kDa	ANOVA	--	5.87	Missing Value	Missing Value	
septin-2	XP_019704043.1	SEPTIN2	41 kDa	ANOVA	--	Missing Value	Missing Value	5.87	
transmembrane protein	XP_019704043.1	SEPTIN2	41 kDa	ANOVA	--	Missing Value	Missing Value	5.72	
transmembrane protein isoform X1	XP_019704043.1	SEPTIN2	41 kDa	ANOVA	--	Missing Value	Missing Value	5.72	
peroxisomal acyl-coenzyme A oxidase 1 isoform X1	XP_019694428.2	AOCX1	75 kDa	ANOVA	--	Missing Value	Missing Value	Missing Value	
carboxypeptidase D	XP_019694042.2	CPD	153 kDa	ANOVA	--	Missing Value	Missing Value	Missing Value	
unconventional myosin-Id isoform X2	XP_019693912.1	MYO1D	116 kDa	ANOVA	--	Missing Value	Missing Value	Missing Value	
hspn3-2	XP_019692596.2	SYNE2	799 kDa	ANOVA	--	Missing Value	Missing Value	Missing Value	
kinectin isoform X1	XP_019692570.2	KTN1	157 kDa	ANOVA	--	Missing Value	Missing Value	5.9	
protein transport protein Sec31A isoform X1	XP_019692070.2	SE31A	134 kDa	ANOVA	--	Missing Value	Missing Value	6.22	
E3 SUMO-protein ligase RanBP2 isoform X1	XP_019694854.1	RANBP2	340 kDa	ANOVA	--	Missing Value	Missing Value	Missing Value	
serpin peptidase inhibitor, clade A (alpha-1 antiproteinase, antitrypsin), member 14 isoform ?	XP_019694043.1	SERPINA14	50 kDa	ANOVA	--	Missing Value	Missing Value	Missing Value	
cystatin-C	XP_019694043.1	LOC102184534	16 kDa	ANOVA	--	Missing Value	Missing Value	Missing Value	6.08
N-acetylgalactosamine-6-sulfatase isoform X3	XP_019693328.1	AGK3	50 kDa	ANOVA	--	Missing Value	Missing Value	Missing Value	
E3 ubiquitin-protein ligase RNF213 isoform X1	XP_019693328.1	RNF213	591 kDa	ANOVA	--	Missing Value	Missing Value	Missing Value	
general vesicular transport factor p115 isoform X1	XP_019693328.1	USO1	109 kDa	ANOVA	--	Missing Value	Missing Value	6.22</td	

SUMO-activating enzyme subunit 1 isoform X1	Ovis aries	XP_004015383.1	SAE1	38 kDa	ANOVA	--	Missing Value	Missing Value	Missing Value	Missing Value
DDRGK domain-containing protein 1	Ovis aries	XP_004014421.1	DDRGK1	36 kDa	ANOVA	--	Missing Value	5.73	Missing Value	Missing Value
acyl-CoA synthetase family member 2, mitochondrial	Ovis aries	XP_004012812.2	ACSF2	68 kDa	ANOVA	--	Missing Value	Missing Value	5.92	Missing Value
peroxin isoform X1	Ovis aries	XP_004012160.2	POSTN	93 kDa	ANOVA	--	Missing Value	Missing Value	Missing Value	Missing Value
NHL repeat-containing protein 3	Ovis aries	XP_004012147.1	NHLRC3	39 kDa	ANOVA	--	Missing Value	6.35	Missing Value	Missing Value
protein PRKC1	Ovis aries	XP_004008706.1	PRKC1	46 kDa	ANOVA	--	Missing Value	Missing Value	Missing Value	Missing Value
ATP-dependent Clp protease proteolytic subunit, mitochondrial	Ovis aries	XP_004008625.1	CLPP	30 kDa	ANOVA	--	Missing Value	6.43	Missing Value	Missing Value
biliverdin reductase A	Ovis aries	XP_004008040.1	BLVRA	34 kDa	ANOVA	--	Missing Value	6.15	Missing Value	Missing Value
ATP-dependent 6-phosphofructokinase, muscle type	Ovis aries	XP_004006455.2	PFKM	94 kDa	ANOVA	--	Missing Value	Missing Value	Missing Value	Missing Value
peroxycysteine oxidase 1	Ovis aries	XP_004005853.2	PCVOX1	57 kDa	ANOVA	--	Missing Value	Missing Value	Missing Value	Missing Value
disintegrin and metalloproteinase domain-containing protein 17	Ovis aries	XP_004005725.1	ADAM17	93 kDa	ANOVA	--	Missing Value	Missing Value	Missing Value	Missing Value
protein lifeguard 3	Ovis aries	XP_004004971.1	TMBIM1	34 kDa	ANOVA	--	Missing Value	Missing Value	Missing Value	Missing Value
aldehyde oxidase	Ovis aries	XP_004004859.1	AOX1	148 kDa	ANOVA	--	Missing Value	Missing Value	Missing Value	Missing Value
nucleoporin NUP35	Ovis aries	XP_004004571.1	NUP35	35 kDa	ANOVA	--	Missing Value	5.91	Missing Value	Missing Value
fructose-1,6-bisphosphatase 1	Ovis aries	XP_004004141.1	FBP1	37 kDa	ANOVA	--	Missing Value	Missing Value	Missing Value	6.02
apolipoprotein A-II	Ovis aries	XP_004002742.1	APOA2	11 kDa	ANOVA	--	Missing Value	Missing Value	Missing Value	6.35
MHC class I molecule, partial	Ovis aries	SPC0556.1	-	40 kDa	ANOVA	--	Missing Value	Missing Value	Missing Value	Missing Value
anti-SARS-CoV-2 immunoglobulin light chain variable region, partial	Homo sapiens	QKK35531.1	-	12 kDa	ANOVA	--	Missing Value	Missing Value	Missing Value	Missing Value
Cytochrome P450c17	Ovis aries	Q29497.2	CYP17A1	57 kDa	ANOVA	--	Missing Value	5.67	Missing Value	Missing Value
Serum amyloid A protein	Ovis aries	P42819.1	SAA	13 kDa	ANOVA	--	Missing Value	Missing Value	Missing Value	Missing Value
Follicle-stimulating hormone receptor	Homo sapiens	P23945.3	FSHR	78 kDa	ANOVA	--	Missing Value	Missing Value	Missing Value	Missing Value
Superoxide dismutase [Cu-Zn]	Ovis aries	P09670.2	SOD1	16 kDa	ANOVA	--	Missing Value	Missing Value	Missing Value	Missing Value
Hemoglobin subunit beta-C(NA)	Ammotragus lervia	P02080.1	-	12 kDa	ANOVA	--	4.83	Missing Value	Missing Value	Missing Value
TRAP1, partial	Cervus elaphus hippelaphus	OWK11054.1	-	31 kDa	ANOVA	--	Missing Value	Missing Value	Missing Value	Missing Value
proteolipid protein 2	Bos taurus	NP_976239.1	PLP2	17 kDa	ANOVA	--	Missing Value	Missing Value	Missing Value	Missing Value
prefoldin subunit 5	Bos taurus	NP_777157.1	PFdns	17 kDa	ANOVA	--	Missing Value	Missing Value	Missing Value	5.74
adiponectin precursor	Ovis aries	NP_001295494.1	ADIPQ	26 kDa	ANOVA	--	Missing Value	Missing Value	Missing Value	Missing Value
IgG receptor FcRn large subunit p51 precursor	Ovis aries	NP_001116875.1	FCGR1	39 kDa	ANOVA	--	Missing Value	Missing Value	Missing Value	Missing Value
mitochondrial import receptor subunit TOM6 homolog	Bos taurus	NP_00107190.1	TOMM6	8 kDa	ANOVA	--	Missing Value	Missing Value	Missing Value	Missing Value
delta(14)-sterol reductase LBR	Bos taurus	NP_001093799.1	LBR	71 kDa	ANOVA	--	Missing Value	5.8	Missing Value	Missing Value
prefoldin subunit 1	Bos taurus	NP_001071530.1	PFDN1	14 kDa	ANOVA	--	Missing Value	Missing Value	Missing Value	5.81
syntaxis-7	Bos taurus	NP_001071332.1	STX7	30 kDa	ANOVA	--	Missing Value	6.16	Missing Value	Missing Value
protein FMC1 homolog	Bos taurus	NP_001070465.1	FMC1	13 kDa	ANOVA	--	Missing Value	5.82	Missing Value	Missing Value
calcineurin B homologous protein 1	Bos taurus	NP_001069044.1	CHP1	22 kDa	ANOVA	--	Missing Value	Missing Value	Missing Value	Missing Value
glycogen phosphorylase, liver form	Bos taurus	NP_001068671.1	PYGL	97 kDa	ANOVA	--	Missing Value	Missing Value	Missing Value	Missing Value
mitochondrial import inner membrane translocase subunit Tim17-B	Bos taurus	NP_001039953.1	TIMM17B	18 kDa	ANOVA	--	Missing Value	Missing Value	Missing Value	6
minor histocompatibility antigen H13	Bos taurus	NP_001039589.2	HM13	42 kDa	ANOVA	--	5.97	5.95	Missing Value	Missing Value
regulator complex protein LAMTOR2	Bos taurus	NP_001029963.1	LAMTOR2	14 kDa	ANOVA	--	5.63	Missing Value	Missing Value	Missing Value
signal peptidase complex subunit 1	Bos taurus	NP_001029576.1	SPCS1	12 kDa	ANOVA	--	Missing Value	Missing Value	6.16	Missing Value
nuclear envelope phosphatase-regulatory subunit 1	Bos taurus	NP_001029475.1	CNEP1R1	14 kDa	ANOVA	--	Missing Value	Missing Value	Missing Value	Missing Value
lipid droplet-regulating VLDL assembly factor AUP1	Bos taurus	NP_001015555.1	AUP1	46 kDa	ANOVA	--	Missing Value	Missing Value	Missing Value	Missing Value
DNA replication licensing factor MCM3	Bos taurus	NP_001013604.2	MCM3	91 kDa	ANOVA	--	Missing Value	Missing Value	Missing Value	Missing Value
DNA replication licensing factor MCM6	Camelus ferus	EPY87703.1	-	136 kDa	ANOVA	--	Missing Value	Missing Value	Missing Value	Missing Value
Ig kappa chain V-I region RPMI 6410 precursor-like protein	Camelus ferus	EPY82054.1	-	40 kDa	ANOVA	--	Missing Value	Missing Value	6.21	Missing Value
tRNA-splicing ligase RtcB-like protein	Camelus ferus	EPY77446.1	-	98 kDa	ANOVA	--	5.76	Missing Value	Missing Value	Missing Value
Aspartate aminotransferase, cytoplasmic, partial	Bos mutus	ELRS9015.1	-	47 kDa	ANOVA	--	Missing Value	Missing Value	Missing Value	Missing Value
TPA: CAP1 protein-like	Bos taurus	DAA23999.1	-	51 kDa	ANOVA	--	Missing Value	Missing Value	6.19	Missing Value
TPA: CAP1 protein-like	Bos taurus	DAA17006.1	PB1	185 kDa	ANOVA	--	Missing Value	Missing Value	Missing Value	Missing Value
TPA: ER lumen protein retaining receptor 2	Bos taurus	DAA15085.1	KDELR2	24 kDa	ANOVA	--	Missing Value	Missing Value	Missing Value	Missing Value
solute carrier family 27 member 2, partial	Bos taurus	AKG52548.1	SLC27A2	63 kDa	ANOVA	--	Missing Value	Missing Value	Missing Value	Missing Value
DnaJ (Hsp40) homolog, subfamily C, member 3	Bos taurus	AAI26581.1	DNAJC3	58 kDa	ANOVA	--	Missing Value	Missing Value	Missing Value	Missing Value
Derlin	Bos taurus	AII02072.1	DERL2	13 kDa	ANOVA	--	Missing Value	Missing Value	Missing Value	6.28
immunoglobulin kappa-1 light chain variable region, partial	Ovis aries	AAB94899.1	-	13 kDa	ANOVA	--	Missing Value	Missing Value	Missing Value	Missing Value

Table S2

**List of differentially abundant proteins according to the diet and the dose of bisphenol S after global ANOVA analysis and chi square test**

Heatmap Cluster	Protein Name	Species	Accession Number	Gene Name	Molecular Weight	Test	p-Value (ANOVA or Chi-square)	in R0 (detection rate %)	in R50 (detection rate %)	in WFO (detection rate %)	in WF50 (detection rate %)
C1	cadherin-6 isoform X2	Bos taurus	XP_024837107.1	CDH6	80 kDa	Chi-square	0.012	N.D. (0%)	7.55 (25%)	7.43 (25%)	7.75 (75%)
C1	bis(5'-adenosyl)-triphosphatase isoform X1	Ovis aries	XP_011954617.2	FHIT	17 kDa	Chi-square	0.012	N.D. (0%)	6.5 (50%)	5.76 (25%)	7.3 (100%)
C1	beta-glucuronidase	Ovis aries	XP_027817734.1	GUSB	74 kDa	Chi-square	0.002	N.D. (0%)	6.88 (100%)	6.18 (50%)	6.6 (100%)
C1	sulphydryl oxidase 2 isoform X1	Capra hircus	XP_017911573.1	LOC102189594	87 kDa	Chi-square	0.003	N.D. (0%)	7.21 (75%)	6.25 (25%)	6.34 (100%)
C1	splicing factor 3B subunit 5	Bos taurus	NP_001020521.1	SF3B5	10 kDa	Chi-square	0.028	N.D. (0%)	6.56 (75%)	6.62 (75%)	6.57 (75%)
C1	vesicle-associated membrane protein-associated protein B/C	Capra hircus	XP_017913111.1	VAPB	27 kDa	ANOVA	0.00037	6.54	7.36	7.38	7.52
C1	transthyretin precursor	Ovis aries	NP_001009800.1	TTR	16 kDa	ANOVA	0.0028	8.27	8.44	8.39	8.8
C1	pre-B-cell leukemia transcription factor-interacting protein 1 isoform X1	Ovis aries	XP_027831619.1	PBXIP1	90 kDa	ANOVA	0.0056	6.24	6.74	7.13	7.13
C1	ITIH2, partial	elaphus hippo	OWK03472.1	-	103 kDa	ANOVA	0.0057	7.15	7.31	7.9	7.88
C1	ras-related protein Rab-5C	Bos taurus	NP_001029915.1	RAB5C	23 kDa	ANOVA	0.0076	6.42	6.89	6.99	6.99
C1	complement C1q subcomponent subunit C	Ovis aries	XP_027820684.1	C1QC	94 kDa	ANOVA	0.0085	Missing Value	7.26	7.21	6.94
C1	vitronectin isoform X1	Ovis aries	XP_027831040.1	VTN	54 kDa	ANOVA	0.011		7.92	8.17	8.06
C1	vitronectin	Capra hircus	XP_005693309.1	VTN	54 kDa	ANOVA	0.011	7.91	8.15	8.05	8.17
C1	TPA: inter-alpha globulin inhibitor H2 polypeptide	Bos taurus	DAA23635.1	ITIH2	106 kDa	ANOVA	0.011	7.48	7.58	8.08	8.05
C1	ras-related protein Rab-5A isoform X1	Ovis aries	XP_014947086.1	RAB5A	24 kDa	ANOVA	0.012	6.37	6.71	6.87	6.81
C1	ras-related protein Rab-5B	Bos taurus	NP_001193120.1	RAB5B	24 kDa	ANOVA	0.017	6.37	6.71	6.86	6.88
C1	glutamine amidotransferase-like class 1 domain-containing protein 3A, mitochondrial	Ovis aries	NP_001156032.1	GATD3	29 kDa	ANOVA	0.017	6.27	6.82	6.75	6.91
C1	palmitoyl-protein thioesterase 1	Ovis aries	XP_004001885.2	PPT1	34 kDa	ANOVA	0.018	6.46	6.95	6.9	6.8
C1	receptor expression-enhancing protein 5	Ovis aries	XP_014952182.2	REEP5	21 kDa	ANOVA	0.019	6.2	6.97	6.99	7.19
C1	inter-alpha-trypsin inhibitor heavy chain H2	Ovis aries	XP_004014227.2	ITIH2	106 kDa	ANOVA	0.020	7.58	7.61	8.18	8.1
C1	non-specific lipid-transfer protein isoform X2	ndicus x Bos t2	XP_027393023.1	SCP2	52 kDa	ANOVA	0.030	5.85	6.53	6.69	6.94
C1	histidine-rich glycoprotein	Ovis aries	XP_004003109.3	HRG	62 kDa	ANOVA	0.031	7.45	7.7	7.12	7.63
C1	immunoglobulin superfamily DCC subclass member 4	Ovis aries	XP_027827301.1	IGDCC4	134 kDa	ANOVA	0.034	Missing Value	6.58	6.25	6.51
C1	dynein light chain 1, cytoplasmic-like	Bos indicus	XP_019812000.1	LOC109555509	10 kDa	ANOVA	0.037		6.41	6.84	6.85
C1	NADH dehydrogenase 1 alpha subcomplex subunit 7	Ovis aries	XP_004008614.1	NDUFA7	13 kDa	ANOVA	0.037	5.49	6.16	6.19	6.59
C1	NADPH-cytochrome P450 reductase isoform X1	Ovis aries	XP_027817441.1	LOC101115252	87 kDa	ANOVA	0.038	6.82	7.51	7.5	7.36
C1	electron transfer flavoprotein subunit beta isoform X2	Ovis virginianus	XP_020755939.1	ETFB	28 kDa	ANOVA	0.038	7.21	7.7	7.73	7.78
C1	electron transfer flavoprotein subunit beta isoform X1	Ovis aries	XP_004015435.3	ETFB	28 kDa	ANOVA	0.038	7.21	7.7	7.73	7.78
C1	ras-related protein Rab-8A	Bos taurus	NP_001098951.1	RAB8A	24 kDa	ANOVA	0.041	7.09	7.33	7.52	7.68
C1	glutaredoxin-related protein 5, mitochondrial	Ovis aries	XP_004018030.1	GLRX5	17 kDa	ANOVA	0.046	6.54	7.05	6.95	7.25
C1	vitronectin precursor	Bos taurus	NP_001030222.1	VTN	54 kDa	ANOVA	0.046	7.71	7.92	7.72	7.8
C1	alpha-2-macroglobulin receptor-associated protein isoform X2	Ovis aries	XP_027827072.1	LRPAP1	42 kDa	ANOVA	0.047	6.68	7.09	7.34	7.19
C1	40S ribosomal protein S16 isoform 1	Homo sapiens	NP_0010111	RP516	16 kDa	ANOVA	0.047	7.18	7.4	7.53	7.77
C1	microsomal glutathione S-transferase 1	Ovis aries	XP_004006867.1	MGST1	18 kDa	ANOVA	0.049	5.58	6.71	6.57	7.04
C2	aflatoxin B1 aldehyde reductase member 2	Ovis aries	XP_027821430.1	AKR7A2	41 kDa	Chi-square	0.007	6.76 (25%)	7.03 (100%)	N.D. (0%)	7.21 (100%)
C2	squalene synthase isoform X2	Ovis aries	XP_004004500.1	FDFT1	48 kDa	Chi-square	0.012	6.56 (25%)	6.63 (100%)	N.D. (0%)	6.59 (50%)
C2	inactive hydroxysteroid dehydrogenase-like protein 1	Bos taurus	NP_001092341.1	HSDL1	37 kDa	Chi-square	0.003	6.17 (75%)	6.21 (100%)	N.D. (0%)	6.76 (75%)
C2	SLC35A4 upstream open reading frame protein	3ubalus bubali	XP_025148374.1	LOC112586898	11 kDa	Chi-square	0.012	5.41 (25%)	6.44 (75%)	N.D. (0%)	6.76 (75%)
C2	transportin-2 isoform X4	Ovis aries	XP_027825368.1	TNPO2	103 kDa	Chi-square	0.003	6.32 (25%)	6.44 (75%)	N.D. (0%)	6.82 (100%)
C2	nucleoprotein TPR	Capra hircus	XP_005691036.2	TPR	275 kDa	Chi-square	0.012	6.39 (25%)	6.87 (75%)	N.D. (0%)	6.02 (75%)
C3	dermcidin isoform 1 preproprotein	Homo sapiens	NP_444513.1	DCD	11 kDa	Chi-square	0.046	5.47 (50%)	N.D. (0%)	5.94 (25%)	6.41 (75%)
C3	complement factor H-related protein 2	Ovis aries	XP_004013976.1	LOC101123223	31 kDa	Chi-square	0.028	6.45 (50%)	N.D. (0%)	6.05 (25%)	7.15 (75%)
C3	apolipoprotein A-I	Ovis aries	XP_011950887.2	APOA1	30 kDa	ANOVA	0.0019	9.1	9.11	9.13	9.53
C3	tetranectin precursor	Bos taurus	NP_001039677.1	CLEC3B	22 kDa	ANOVA	0.022	7.07	7.13	6.97	7.47
C3	protein AMBP isoform X2	Capra hircus	XP_005684398.1	AMBP	39 kDa	ANOVA	0.033	6.97	7.07	7.14	7.53
C4	nicastin isoform X2	Ovis aries	XP_012039753.2	NCSTN	67 kDa	Chi-square	0.028	6.58 (50%)	6.8 (75%)	6.68 (75%)	N.D. (0%)
C4	prolyl 4-hydroxylase subunit alpha-2 isoform X1	Ovis aries	XP_004008688.1	P4HA2	61 kDa	Chi-square	0.005	7.09 (75%)	6.8 (100%)	7.13 (100%)	N.D. (0%)
C4	reticulon-4 isoform X1	Capra hircus	XP_017910740.1	RTN4	130 kDa	Chi-square	0.028	N.D. (0%)	7.14 (75%)	7.05 (75%)	6.16 (50%)
C4	thiosulfate sulfurtransferase	Ovis aries	XP_014950344.2	TST	33 kDa	Chi-square	0.003	6.99 (75%)	6.91 (100%)	5.87 (25%)	N.D. (0%)
C4	lipopolysaccharide-binding protein	Ovis aries	XP_004014615.1	LBP	53 kDa	ANOVA	0.0012	7.28	7.9	7.14	6.69
C4	long-chain fatty acid transport protein 1	Ovis aries	XP_027825247.1	SLC27A1	71 kDa	ANOVA	0.0066	6.6	7.16	6.59	6.52
C4	immunoglobulin heavy chain variable region, partial	Ovis aries	CAD45049.1	12 kDa	ANOVA	0.022	7.35	7.64	7.36	6.92	
C4	glucosidase 2 subunit beta	Ovis aries	XP_027825495.1	PRKCSH	60 kDa	ANOVA	0.023	7.22	7.94	7.91	7.53
C4	zona pellucida sperm-binding protein 4	Ovis aries	XP_027818021.1	ZP4	59 kDa	ANOVA	0.025	6.72	7.08	7.07	Missing Value
C4	protein ERGIC-53 isoform X1	Ovis aries	XP_014959285.2	LMAN1	58 kDa	ANOVA	0.025	6.51	7.36	7.04	
C4	GDP-fucose protein O-fucosyltransferase 2 isoform X1	Ovis aries	XP_027816944.1	POFUT2	50 kDa	ANOVA	0.030	7.06	7.49	6.97	6.94
C4	complement component C7	Ovis aries	XP_004017066.2	C7	93 kDa	ANOVA	0.039	7.65	7.78	7.31	7.55
C4	Ig mu chain C region membrane-bound form, partial	Ovis aries	XP_027813089.1	LOC101113211	54 kDa</						

Table S2

**List of differentially abundant proteins between 0 and 50 µg/kg/day of BP in restricted (R) ewes**

Protein Name	Species	Accession Number	Gene Symbol	Molecular Weight	ANOVA		Corrected fold-change R50:R0	Corrected fold-change R0:R50	Chi-square	Average	
					p-value	Log2 Fold change corrected R50:R0				R0 (detection rate %)	R50 (detection rate %)
aflatoxin B1 aldehyde reductase member 2	Ovis aries	XP_027821430.1	AKR7A2	41 kDa	-	-	-	-	0.007	6.76 (25%)	7.03 (100%)
beta-glucuronidase	Ovis aries	XP_027817734.1	GUSB	74 kDa	-	-	-	-	0.00194577	N.D. (0%)	6.88 (100%)
inactive hydroxysteroid dehydrogenase-like protein 1	Bos taurus	NP_001092341.1	HSDL1	37 kDa	-	-	-	-	0.003	6.17 (75%)	6.21 (100%)
complement factor H-related protein 2	Ovis aries	XP_004013976.1	LOC101123223	31 kDa	-	-	-	-	0.028	6.45 (50%)	N.D. (0%)
sulphydryl oxidase 2 isoform X1	Capra hircus	XP_017911573.1	LOC102189594	87 kDa	-	-	-	-	0.003	N.D. (0%)	7.21 (75%)
SLC35A4 upstream open reading frame protein	Bubalus bubalis	XP_025148374.1	LOC112586898	11 kDa	-	-	-	-	0.012	5.41 (25%)	6.44 (75%)
reticulon-4 isoform X1	Capra hircus	XP_017910740.1	RTN4	130 kDa	-	-	-	-	0.028	N.D. (0%)	7.14 (75%)
splicing factor 3B subunit 5	Bos taurus	NP_001020521.1	SF3B5	10 kDa	-	-	-	-	0.028	N.D. (0%)	6.56 (75%)
transportin-2 isoform X4	Ovis aries	XP_027825368.1	TNPO2	103 kDa	-	-	-	-	0.003	6.32 (25%)	6.44 (75%)
nucleoprotein TPR	Capra hircus	XP_005691036.2	TPR	275 kDa	-	-	-	-	0.012	6.39 (25%)	6.87 (75%)
complement C1q subcomponent subunit C	Ovis aries	XP_027820684.1	C1QC	94 kDa	0.012	Reference Missing	-	-	-	6.44	7.32
gap junction alpha-1 protein	Ovis aries	XP_004011208.1	GJA1	43 kDa	0.041	2.06	4.17	0.24	-	7.60	8.10
glutaredoxin-related protein 5, mitochondrial	Ovis aries	XP_004018030.1	GLRX5	17 kDa	0.034	1.84	3.58	0.28	-	6.48	7.12
PREDICTED: glutathione peroxidase 7	Capra hircus	XP_017899689.1	GPX7	21 kDa	0.031	3.96	15.56	0.06	-	6.49	7.28
acetolactate synthase-like protein	Ovis aries	XP_004008513.1	ILVBL	68 kDa	0.044	3.95	15.45	0.06	-	6.36	7.11
Inhibin alpha chain	Capra hircus	AEP40507.1	INHA	39 kDa	0.0089	1.43	2.69	0.37	-	7.90	8.25
clusterin	Ovis aries	XP_004004480.1	LOC101113728	51 kDa	0.047	1.33	2.51	0.40	-	8.00	8.32
NADPH-cytochrome P450 reductase isoform X1	Ovis aries	XP_027817441.1	LOC101115252	87 kDa	0.028	2.33	5.03	0.20	-	6.99	7.64
PREDICTED: LOW QUALITY PROTEIN: ADP-ribosylation factor 4-like, partial	Bos mutus	XP_014337480.1	LOC102268931	29 kDa	0.03	2.91	7.52	0.13	-	5.53	6.39
matrix Gla protein	Ovis aries	XP_004006882.1	MGP	12 kDa	0.018	1.58	2.99	0.33	-	6.81	7.24
microsomal glutathione S-transferase 1	Ovis aries	XP_004006867.1	MGST1	18 kDa	0.025	4.06	16.68	0.06	-	5.84	6.71
mannose-P-dolichol utilization defect 1 protein	Ovis aries	XP_004012714.2	MPDU1	27 kDa	0.015	1.8	3.48	0.29	-	6.33	6.94
ORM1-like protein 3	Bos taurus	NP_001069835.1	ORMDL3	17 kDa	0.02	2.43	5.39	0.19	-	5.54	6.10
GDP-fucose protein O-fucosyltransferase 2 isoform X1	Ovis aries	XP_027816944.1	POFUT2	50 kDa	0.045	1.51	2.85	0.35	-	7.02	7.49
palmitoyl-protein thioesterase 1	Ovis aries	XP_004001885.2	PPT1	34 kDa	0.019	1.69	3.23	0.31	-	6.60	6.94
PRA1 family protein 2	Bos taurus	NP_001039474.1	PRAF2	19 kDa	0.023	2.04	4.11	0.24	-	6.13	6.76
ras-related protein Rab-5A isoform X1	Ovis aries	XP_014947086.1	RAB5A	24 kDa	0.026	1.29	2.45	0.41	-	6.47	6.81
ras-related protein Rab-5B	Bos taurus	NP_001193120.1	RAB5B	24 kDa	0.027	1.29	2.45	0.41	-	6.48	6.81
ras-related protein Rab-5C	Bos taurus	NP_001029915.1	RAB5C	23 kDa	0.029	1.63	3.10	0.32	-	6.53	6.95
retinol dehydrogenase 11	Ovis aries	XP_012037274.1	RDH11	37 kDa	0.019	1.37	2.58	0.39	-	6.54	6.97
LOW QUALITY PROTEIN: long-chain fatty acid transport protein 1	Ovis aries	XP_027825247.1	SLC27A1	71 kDa	0.026	1.92	3.78	0.26	-	6.52	7.17
thioredoxin-related transmembrane protein 1	Ovis aries	XP_004010572.2	TMX1	32 kDa	0.026	1.21	2.31	0.43	-	6.48	6.93
PREDICTED: vesicle-associated membrane protein-associated protein B/C	Capra hircus	XP_017913111.1	VAPB	27 kDa	0.0093	3	8.00	0.13	-	6.69	7.37
PREDICTED: vitamin K epoxide reductase complex subunit 1 isoform X1	Capra hircus	XP_017895520.1	VKORC1	18 kDa	0.04	1.42	2.68	0.37	-	6.04	6.47

Table S2

**List of differentially abundant proteins between 0 and 50 µg/kg/day of BP in well-fed (WF) ewes**

Protein Name	Species	Accession Number	Gene Symbol	Molecular Weight	p-value	ANOVA		Corrected fold-change WF50:WF0	Corrected fold-change WF0:WF50	p-value	Chi-square	Average
						Log2 Fold change corrected WF50:WF0	Corrected fold-change WF0:WF50				WF0 (detection rate %)	WF50 (detection rate %)
aflatoxin B1 aldehyde reductase member 2	Ovis aries	XP_027821430.1	AKR7A2	41 kDa	-	-	-	-	-	0.007	N.D. (0%)	7.21 (100%)
beta-glucuronidase	Ovis aries	XP_027817734.1	GUSB	74 kDa	-	-	-	-	-	0.002	6.18 (50%)	6.6 (100%)
inactive hydroxysteroid dehydrogenase-like protein 1	Bos taurus	NP_001092341.1	HSDL1	37 kDa	-	-	-	-	-	0.003	N.D. (0%)	6.76 (75%)
sulphydryl oxidase 2 isoform X1	Capra hircus	XP_017911573.1	LOC102189594	87 kDa	-	-	-	-	-	0.003	6.25 (25%)	6.34 (100%)
SLC35A4 upstream open reading frame protein	Bubalus bubalis	XP_025148374.1	LOC112586898	11 kDa	-	-	-	-	-	0.012	N.D. (0%)	6.76 (75%)
nicastrin isoform X2	Ovis aries	XP_012039753.2	NCSTN	67 kDa	-	-	-	-	-	0.028	6.68 (75%)	N.D. (0%)
prolyl 4-hydroxylase subunit alpha-2 isoform X1	Ovis aries	XP_004008688.1	P4HA2	61 kDa	-	-	-	-	-	0.005	7.13 (100%)	N.D. (0%)
transportin-2 isoform X4	Ovis aries	XP_027825368.1	TNP02	103 kDa	-	-	-	-	-	0.003	N.D. (0%)	6.82 (100%)
nucleoprotein TPR	Capra hircus	XP_005691036.2	TPR	275 kDa	-	-	-	-	-	0.012	N.D. (0%)	6.02 (75%)
DNA-(apurinic or apyrimidinic site) lyase	Ovis aries	XP_004010439.2	APEX1	36 kDa	0.021	1	2.00	0.5	-	6.20	6.55	
apolipoprotein A-I	Ovis aries	XP_011950887.2	APOA1	30 kDa	0.021	1.23	2.35	0.43	-	9.07	9.47	
apolipoprotein A-IV	Ovis aries	XP_004016096.1	APOA4	43 kDa	0.045	1.85	3.61	0.28	-	7.84	8.35	
branched-chain-amino-acid aminotransferase, mitochondrial isoform X1	Ovis aries	XP_027834382.1	BCAT2	45 kDa	0.024	1.74	3.34	0.30	-	7.35	7.74	
ttranectin precursor	Bos taurus	NP_001039677.1	CLEC3B	22 kDa	0.025	1.63	3.10	0.32	-	6.90	7.40	
endothelin-converting enzyme 1 isoform X1	Ovis aries	XP_027821363.1	ECE1	91 kDa	0.049	-2.37	0.19	5.17	-	7.43	6.94	
histidine-rich glycoprotein	Ovis aries	XP_004003109.3	HRG	62 kDa	0.022	1.7	3.25	0.31	-	7.16	7.63	
lipopolysaccharide-binding protein	Ovis aries	XP_004014615.1	LBP	53 kDa	0.029	-1.55	0.34	2.93	-	7.17	6.59	
lamin	Ovis aries	XP_027832136.1	LMNA	74 kDa	0.0094	-2.82	0.14	7.06	-	7.32	6.62	
lamin-B1	Ovis aries	XP_004008711.1	LMNB1	66 kDa	0.049	-1.57	0.34	2.97	-	7.84	7.45	
glutathione S-transferase P	Capra hircus	XP_017898539.1	LOC100861197	24 kDa	0.022	1.73	3.32	0.30	-	7.23	7.61	
protein disulfide-isomerase A4	Ovis aries	XP_027824715.1	PDIA4	73 kDa	0.043	-1.32	0.40	2.50	-	8.25	7.91	
TPA: profilin 1-like	Bos taurus	DAA33226.1	PFN1	15 kDa	0.038	1.88	3.68	0.27	-	6.21	6.87	
retinol-binding protein 4	Ovis aries	XP_027815955.1	RBP4	23 kDa	0.035	2.75	6.73	0.15	-	6.87	7.47	
SUN domain-containing protein 2 isoform X1	Ovis aries	XP_027823918.1	SUN2	88 kDa	0.046	-2.15	0.23	4.44	-	7.44	6.94	
transthyretin precursor	Ovis aries	NP_001009800.1	TTR	16 kDa	0.04	1.3	2.46	0.41	-	8.36	8.78	
zona pellucida sperm-binding protein 3	Ovis aries	XP_004021030.2	ZP3	47 kDa	0.021	-3.43	0.09	10.78	-	7.20	6.69	

Table S2

**List of differentially abundant proteins between restricted (R) and well-fed (WF) ewes exposed to 0 µg/kg/day of BP in well-fed ewes (overabundant in R0 than WF0)**

Protein Name	Species	Accession Number	Gene Symbol	Molecular Weight	R0 vs SO		Corrected fold-change WF0:R0	Corrected fold-change R0:WF0	Chi-square	Average	
					p-value	Log2 Fold change WF0:R0				R0 (detection rate %)	WF0 (detection rate %)
aflatoxin B1 aldehyde reductase member 2	Ovis aries	XP_027821430.1	AKR7A2	41 kDa	-	-	-	-	0.007	6.76 (25%)	N.D. (0%)
cadherin-6 isoform X2	Bos taurus	XP_024837107.1	CDH6	80 kDa	-	-	-	-	0.012	N.D. (0%)	7.43 (25%)
dermcidin isoform 1 preproprotein	Homo sapiens	NP_444513.1	DCD	11 kDa	-	-	-	-	0.046	5.47 (50%)	5.94 (25%)
squalene synthase isoform X2	Ovis aries	XP_004004500.1	FDFT1	48 kDa	-	-	-	-	0.012	6.56 (25%)	N.D. (0%)
bis(5'-adenosyl)-triphosphatase isoform X1	Ovis aries	XP_011954617.2	FHIT	17 kDa	-	-	-	-	0.012	N.D. (0%)	5.76 (25%)
reticulon-4 isoform X1	Capra hircus	XP_017910740.1	RTN4	130 kDa	-	-	-	-	0.028	N.D. (0%)	7.05 (75%)
splicing factor 3B subunit 5	Bos taurus	NP_001020521.1	SF3B5	10 kDa	-	-	-	-	0.028	N.D. (0%)	6.62 (75%)
thiosulfate sulfurtransferase	Ovis aries	XP_014950344.2	TST	33 kDa	-	-	-	-	0.003	6.99 (75%)	5.87 (25%)
alpha globin chain	Ovis aries	CAA49750.1	-	15 kDa	0.033	2.25	4.76	0.21	-	8.87	9.62
alpha globin	Homo sapiens	CAA23749.1	-	14 kDa	0.029	2.9	7.46	0.13	-	7.42	7.95
ITIH2, partial	Cervus elaphus hippelaphus	OWK03472.1	-	103 kDa	0.015	2.54	5.82	0.17	-	7.35	7.95
apolipoprotein D	Ovis aries	XP_004003075.1	APOD	24 kDa	0.027	-1	0.50	2.00	-	6.86	6.73
electron transfer flavoprotein subunit beta isoform X1	Ovis aries	XP_004015435.3	ETFB	28 kDa	0.047	1.73	3.32	0.30	-	7.27	7.79
Adrenodoxin	Ovis aries	P29330.2	FDX1	14 kDa	0.017	2.41	5.31	0.19	-	6.20	6.93
glutaredoxin-related protein 5, mitochondrial	Ovis aries	XP_004018030.1	GLRX5	17 kDa	0.029	1.4	2.64	0.38	-	6.51	7.04
histone H1.2	Ovis aries	XP_004019136.2	H1-2	21 kDa	0.045	2.19	4.56	0.22	-	8.74	9.46
histone H1.5	Camelus dromedarius	XP_010973014.2	H1-5	23 kDa	0.048	2.27	4.82	0.21	-	8.56	9.30
hemoglobin subunit alpha	Ovis canadensis nelsoni	QJ83449.1	HBA-T1	15 kDa	0.03	2.32	4.99	0.20	-	8.87	9.62
Hemoglobin subunit beta	Ovis aries	P02075.2	HBB	16 kDa	0.023	2.39	5.24	0.19	-	9.11	9.89
inter-alpha-trypsin inhibitor heavy chain H2	Ovis aries	XP_004014227.2	ITIH2	106 kDa	0.017	2.01	4.03	0.25	-	7.70	8.19
Kininogen-1	Bos taurus	P01044.1	KNG1	69 kDa	0.019	1.01	2.01	0.50	-	6.99	7.33
histone H1.3	Ovis aries	XP_011956523.2	LOC101109397	22 kDa	0.042	2.19	4.56	0.22	-	8.72	9.44
alpha-2-macroglobulin receptor-associated protein isoform X2	Ovis aries	XP_027827072.1	LRPAP1	42 kDa	0.014	2.2	4.59	0.22	-	6.71	7.41
matrix Gla protein	Ovis aries	XP_004006882.1	MGP	12 kDa	0.0031	1.47	2.77	0.36	-	6.80	7.09
mannose-P-dolichol utilization defect 1 protein	Ovis aries	XP_004012714.2	MPDU1	27 kDa	0.026	2.02	4.06	0.25	-	6.38	6.93
NADH dehydrogenase [ubiquinone] 1 alpha subcomplex subunit 7	Ovis aries	XP_004008614.1	NDUFA7	13 kDa	0.028	2.48	5.58	0.18	-	5.76	6.29
pre-B-cell leukemia transcription factor-interacting protein 1 isoform X1	Ovis aries	XP_027831619.1	PBX1P1	90 kDa	0.019	3.04	8.22	0.12	-	6.30	7.10
palmitoyl-protein thioesterase 1	Ovis aries	XP_004001885.2	PPT1	34 kDa	0.022	1.51	2.85	0.35	-	6.61	6.95
peroxiredoxin-2	Ovis aries	NP_001159672.1	PRDX2	22 kDa	0.0076	1.46	2.75	0.36	-	7.50	8.02
glucosidase 2 subunit beta	Ovis aries	XP_027825495.1	PRKCSH	60 kDa	0.028	2.37	5.17	0.19	-	7.37	8.02
ras-related protein Rab-5B	Bos taurus	NP_001193120.1	RAB5B	24 kDa	0.0045	1.69	3.23	0.31	-	6.49	6.93
ras-related protein Rab-5C	Bos taurus	NP_001029915.1	RAB5C	23 kDa	0.0091	1.94	3.84	0.26	-	6.54	7.07
receptor expression-enhancing protein 5	Ovis aries	XP_014952182.2	REEP5	21 kDa	0.023	2.73	6.63	0.15	-	6.23	7.02
transmembrane protein 256	Ovis aries	XP_004012698.2	TMEM256	12 kDa	0.039	1.01	2.01	0.50	-	6.25	6.67
vesicle-associated membrane protein-associated protein B/C	Capra hircus	XP_017913111.1	VAPB	27 kDa	0.0057	2.92	7.57	0.13	-	6.71	7.46
zona pellucida sperm-binding protein 3	Ovis aries	XP_004021030.2	ZP3	47 kDa	0.011	2.5	5.66	0.18	-	6.75	7.27
Hemoglobin subunit beta-A	Bos javanicus	P04346.1	-	16 kDa	0.029	1.89	3.71	0.27	-	8.74	9.35

Table S2

**List of differentially abundant proteins between restricted (R) and well-fed (WF) ewes exposed to 50 µg/kg/day of BP in well-fed ewes (overabundant in R50 than WF50)**

Protein Name	Species	Accession Number	Gene Symbol	Molecular Weight	p-value	R50 vs WF50		Corrected fold-change WF50:R50	Corrected fold-change R50:WF50	p-value	Chi-square	Average	
						Log2 Fold change WF50:R50	Corrected fold-change WF50:R50					R50 (detection rate %)	WF50 (detection rate %)
cadherin-6 isoform X2	Bos taurus	XP_024837107.1	CDH6	80 kDa	-	-	-	-	-	0.012	7.55 (25%)	7.75 (75%)	
dermcidin isoform 1 preproprotein	Homo sapiens	NP_444513.1	DCD	11 kDa	-	-	-	-	-	0.046	N.D. (0%)	6.41 (75%)	
squalene synthase isoform X2	Ovis aries	XP_004004500.1	FDFT1	48 kDa	-	-	-	-	-	0.012	6.63 (100%)	6.59 (50%)	
bis(5'-adenosyl)-triphosphatase isoform X1	Ovis aries	XP_011954617.2	FHT	17 kDa	-	-	-	-	-	0.012	6.5 (50%)	7.3 (100%)	
complement factor H-related protein 2	Ovis aries	XP_004013976.1	LOC101123223	31 kDa	-	-	-	-	-	0.028	N.D. (0%)	7.15 (75%)	
nicastrin isoform X2	Ovis aries	XP_012039753.2	NCSTN	67 kDa	-	-	-	-	-	0.028	6.8 (75%)	N.D. (0%)	
prolyl 4-hydroxylase subunit alpha-2 isoform X1	Ovis aries	XP_004008688.1	P4HA2	61 kDa	-	-	-	-	-	0.005	6.8 (100%)	N.D. (0%)	
thiosulfate sulfurtransferase	Ovis aries	XP_014950344.2	TST	33 kDa	-	-	-	-	-	0.003	6.91 (100%)	N.D. (0%)	
PREDICTED: ADP-dependent glucokinase isoform X1	Capra hircus	XP_017910167.1	ADPGK	54 kDa	0.0057	-3.27	0.10	9.65	-	7.04	6.30		
aldehyde dehydrogenase, mitochondrial	Ovis aries	XP_004017458.1	ALDH2	57 kDa	0.043	-1.53	0.35	2.89	-	8.24	7.87		
apolipoprotein A-I	Ovis aries	XP_011950887.2	APOA1	30 kDa	0.0075	1.31	2.48	0.40	-	8.93	9.38		
ATP synthase subunit alpha, mitochondrial	Ovis aries	XP_004020569.1	ATPSF1A	60 kDa	0.022	-1.59	0.33	3.01	-	8.75	8.36		
ATP synthase subunit beta, mitochondrial	Ovis aries	XP_004006621.1	ATPSF1B	56 kDa	0.016	-1.45	0.37	2.73	-	8.96	8.55		
branched-chain-amino-acid aminotransferase, mitochondrial isoform X1	Ovis aries	XP_027834382.1	BCAT2	45 kDa	0.042	1.99	3.97	0.25	-	7.11	7.67		
complement C1s subcomponent	Ovis aries	XP_004006966.1	C1S	78 kDa	0.017	-1.12	0.46	2.17	-	6.32	6.00		
calreticulin	Ovis aries	XP_004008533.1	CALR	48 kDa	0.026	-1.79	0.29	3.46	-	8.65	8.10		
dolichyl-diphosphooligosaccharide--protein glycosyltransferase 48 kDa subunit	Ovis aries	XP_004005208.2	DDOST	49 kDa	0.0058	-1.25	0.42	2.38	-	8.17	7.79		
peroxisomal bifunctional enzyme	Ovis aries	XP_027813339.1	EHHADH	80 kDa	0.023	-3.28	0.10	9.71	-	6.81	6.21		
NADPH:adrenodoxin oxidoreductase, mitochondrial	Ovis aries	XP_027829849.1	FDXR	54 kDa	0.05	-1.34	0.40	2.53	-	7.57	7.08		
fibrinogen beta chain	Ovis aries	XP_004017233.2	FGB	57 kDa	0.013	-1.18	0.44	2.27	-	10.29	9.95		
fumarate hydratase, mitochondrial	Bos taurus	NP_001069271.1	FH	55 kDa	0.031	-1.04	0.49	2.06	-	7.74	7.53		
fibronectin isoform X11	Ovis aries	XP_027820957.1	FN1	249 kDa	0.014	-2.22	0.21	4.66	-	9.65	9.14		
heterochromatin protein 1-binding protein 3 isoform X1	Ovis aries	XP_014949207.1	HP1BP3	61 kDa	0.0043	-2.83	0.14	7.11	-	7.14	6.60		
basement membrane-specific heparan sulfate proteoglycan core protein	Ovis aries	XP_027821348.1	HSPG2	469 kDa	0.014	-2.18	0.22	4.53	-	8.10	7.45		
acetolactate synthase-like protein	Ovis aries	XP_004008513.1	ILVBL	68 kDa	0.037	-2.79	0.14	6.92	-	6.97	6.40		
lipopolysaccharide-binding protein	Ovis aries	XP_004014615.1	LBP	53 kDa	0.00095	-4.02	0.06	16.22	-	7.79	6.54		
protein ERGIC-53 isoform X1	Ovis aries	XP_014959285.2	LMAN1	58 kDa	0.018	-2.76	0.15	6.77	-	7.26	6.49		
lamin-B1	Ovis aries	XP_004008711.1	LMNB1	66 kDa	0.022	-1.83	0.28	3.56	-	7.89	7.38		
Ig mu chain C region membrane-bound form, partial	Ovis aries	XP_027813089.1	LOC101113211	54 kDa	0.043	-1.23	0.43	2.35	-	7.68	7.38		
inhibitor of carbonic anhydrase-like isoform X2	Ovis aries	XP_004003380.2	LOC101117129	78 kDa	0.034	1.28	2.43	0.41	-	7.18	7.59		
PREDICTED: protein disulfide-isomerase A6	Bos indicus	XP_019824917.1	LOC109565403	48 kDa	0.015	-1.66	0.32	3.16	-	8.63	8.23		
lysophospholipid acyltransferase 5	Ovis aries	XP_027823723.1	LPCAT3	56 kDa	0.035	-1.85	0.28	3.61	-	6.33	6.13		
protein NipSnap homolog 3A	Ovis aries	XP_027819963.1	NIPSNAP3A	29 kDa	0.0043	-1.07	0.48	2.10	-	6.52	6.21		
protein disulfide-isomerase	Ovis aries	XP_027830078.1	P4HB	63 kDa	0.035	-1.54	0.34	2.91	-	8.88	8.48		
GPI transamidase component PIG-T isoform X1	Ovis aries	XP_027833042.1	PIGT	74 kDa	0.036	-1.96	0.26	3.89	-	6.68	5.96		
GDP-fucose protein O-fucosyltransferase 2 isoform X1	Ovis aries	XP_027816944.1	POFUT2	50 kDa	0.016	-1.84	0.28	3.58	-	7.33	6.89		
retinol-binding protein 4	Ovis aries	XP_027815955.1	RBP4	23 kDa	0.045	1.55	2.93	0.34	-	6.96	7.40		
PREDICTED: reticulocalbin-2 isoform X2	Capra hircus	XP_017921860.1	RCN2	36 kDa	0.00022	-2.95	0.13	7.73	-	7.09	6.30		
dolichyl-diphosphooligosaccharide--protein glycosyltransferase subunit 1	Ovis aries	XP_027813657.1	RPN1	69 kDa	0.038	-1.36	0.39	2.57	-	8.33	8.05		
dolichyl-diphosphooligosaccharide--protein glycosyltransferase subunit 2 isoform X1	Ovis aries	XP_027832978.1	RPN2	71 kDa	0.0099	-1.73	0.30	3.32	-	8.49	8.04		
calcium-binding mitochondrial carrier protein Aralar2 isoform X1	Ovis aries	XP_004007792.1	SLC25A13	74 kDa	0.04	-2.14	0.23	4.41	-	6.90	6.31		
long-chain fatty acid transport protein 1	Ovis aries	XP_027825247.1	SLC27A1	71 kDa	0.0026	-2.18	0.22	4.53	-	7.04	6.48		
CMP-N-acetyleneuraminate-beta-galactosamide-alpha-2,3-sialyltransferase 4 isoform X1	Ovis aries	XP_011956915.1	ST3GAL4	42 kDa	0.025	Missing Value	-	-	-	6.81	5.77		
SUN domain-containing protein 2 isoform X1	Ovis aries	XP_027823918.1	SUN2	88 kDa	0.025	-2.39	0.19	5.24	-	7.55	6.88		
mitochondrial import receptor subunit TOM70	Ovis aries	XP_004002928.1	TOMM70	68 kDa	0.024	-2.32	0.20	4.99	-	6.67	6.20		
transthyretin precursor	Ovis aries	NP_001009800.1	TTR	16 kDa	0.043	1.13	2.19	0.46	-	8.33	8.69		
immunoglobulin lambda light chain constant region 2 allotypic variant IGLC2c, partial	Bos taurus	AEM05840.1	-	11 kDa	0.017	1.34	2.53	0.40	-	7.85	8.21		
immunoglobulin heavy chain variable region, partial	Ovis aries	CAD45049.1	-	12 kDa	0.013	-2.28	0.21	4.86	-	7.41	6.97		

Table S3

**List of differentially abundant proteins according to the diet and the dose of bisphenol S after chi-square test**

Protein Name	Species	Accession Number	Gene Symbol	Molecular Weight	in R0 (detection rate %)	in R50 (detection rate %)	in WFO (detection rate %)	in WF50 (detection rate %)	Dose effect p-value (chi-square)	Diet effect p-value (chi-square)	R0 vs R50 p-value (chi-square)	WFO vs WF50 p-value (chi-square)	R0 vs WFO p-value (chi-square)	R50 vs WF50 p-value (chi-square)
aflatoxin B1 aldehyde reductase member 2	Ovis aries	XP_027821430.1	AKR7A2	41 kDa	6.76 (25%)	7.03 (100%)	N.D. (0%)	7.21 (100%)	<b>0.007</b>	0.106	0.285	<b>0.005</b>	<b>0.028</b>	-
cadherin-6 isoform X2	Bos taurus	XP_024837107.1	CDH6	80 kDa	N.D. (0%)	7.55 (25%)	7.43 (25%)	7.75 (75%)	0.614	<b>0.012</b>	0.285	1.000	<b>0.028</b>	0.157
dermcidin isoform 1 preproprotein	Homo sapiens	NP_444513.1	DCD	11 kDa	5.47 (50%)	N.D. (0%)	5.94 (25%)	6.41 (75%)	0.317	<b>0.046</b>	0.102	1.000	-	-
squalene synthase isoform X2	Ovis aries	XP_004004500.1	FDFT1	48 kDa	6.56 (25%)	6.63 (100%)	N.D. (0%)	6.59 (50%)	0.131	<b>0.012</b>	0.285	0.102	<b>0.028</b>	0.102
bis(5'-adenosyl)-triphosphatase isoform X1	Ovis aries	XP_011954617.2	FHIT	17 kDa	N.D. (0%)	6.5 (50%)	5.76 (25%)	7.3 (100%)	0.131	<b>0.012</b>	0.102	0.285	<b>0.028</b>	0.102
beta-glucuronidase	Ovis aries	XP_027817734.1	GUSB	74 kDa	N.D. (0%)	6.88 (100%)	6.18 (50%)	6.6 (100%)	<b>0.002</b>	0.302	<b>0.005</b>	0.102	0.102	-
inactive hydroxysteroid dehydrogenase-like protein 1	Bos taurus	NP_001092341.1	HSDL1	37 kDa	6.17 (75%)	6.21 (100%)	N.D. (0%)	6.76 (75%)	<b>0.003</b>	0.248	<b>0.028</b>	<b>0.028</b>	0.285	0.285
complement factor H-related protein 2	Ovis aries	XP_004013976.1	LOC101123223	31 kDa	6.45 (50%)	N.D. (0%)	6.05 (25%)	7.15 (75%)	0.614	0.614	<b>0.028</b>	0.157	-	-
sulphydryl oxidase 2 isoform X1	Capra hircus	XP_017911573.1	LOC102189594	87 kDa	N.D. (0%)	7.21 (75%)	6.25 (25%)	6.34 (100%)	<b>0.003</b>	0.317	<b>0.028</b>	<b>0.028</b>	<b>0.028</b>	0.285
SLC35A4 upstream open reading frame protein	Bubalus bubalis	XP_025148374.1	LOC112586898	11 kDa	5.41 (25%)	6.44 (75%)	N.D. (0%)	6.76 (75%)	<b>0.012</b>	0.614	0.157	<b>0.028</b>	-	-
nicastrin isoform X2	Ovis aries	XP_012039753.2	NCSTN	67 kDa	6.58 (50%)	6.8 (75%)	6.68 (75%)	N.D. (0%)	0.317	0.317	0.465	<b>0.028</b>	0.465	<b>0.028</b>
prolyl 4-hydroxylase subunit alpha-2 isoform X1	Ovis aries	XP_004008688.1	P4HA2	61 kDa	7.09 (75%)	6.8 (100%)	7.13 (100%)	N.D. (0%)	0.106	0.106	0.285	<b>0.005</b>	0.285	<b>0.005</b>
reticulon-4 isoform X1	Capra hircus	XP_017910740.1	RTN4	130 kDa	N.D. (0%)	7.14 (75%)	7.05 (75%)	6.16 (50%)	0.317	0.317	<b>0.028</b>	0.465	<b>0.028</b>	0.465
splicing factor 3B subunit 5	Bos taurus	NP_001020521.1	SF3B5	10 kDa	N.D. (0%)	6.56 (75%)	6.62 (75%)	6.57 (75%)	0.131	0.131	<b>0.028</b>	1.000	<b>0.028</b>	1.000
transportin-2 isoform X4	Ovis aries	XP_027825368.1	TNPO2	103 kDa	6.32 (25%)	6.44 (75%)	N.D. (0%)	6.82 (100%)	<b>0.003</b>	1.000	0.157	<b>0.005</b>	0.285	0.285
nucleoprotein TPR	Capra hircus	XP_005691036.2	TPR	275 kDa	6.39 (25%)	6.87 (75%)	N.D. (0%)	6.02 (75%)	<b>0.012</b>	0.614	0.157	<b>0.028</b>	0.285	1.000
thiosulfate sulfurtransferase	Ovis aries	XP_014950344.2	TST	33 kDa	6.99 (75%)	6.91 (100%)	5.87 (25%)	N.D. (0%)	1.000	<b>0.003</b>	0.285	0.285	0.157	<b>0.005</b>